

FINAL REPORT

on

PRODUCTION OF Pu-238 IN COMMERCIAL POWER REACTORS:
TARGET FABRICATION, POSTIRRADIATION EXAMINATION,
AND PLUTONIUM AND NEPTUNIUM RECOVERY

to

HEAT SOURCE BRANCH
SPACE NUCLEAR SYSTEMS DIVISION
U. S. ENERGY RESEARCH AND DEVELOPMENT ADMINISTRATION

January 31, 1975

by

M. Pobereskin, W. Langendorfer, L. Lowry,
D. Farmelo, V. Scotti, and O. Kruger

BATTELLE
Columbus Laboratories
505 King Avenue
Columbus, Ohio 43201

MASTER

NOTICE
This report was prepared as an account of work sponsored by the United States Government. Neither the United States nor the United States Energy Research and Development Administration, nor any of their employees, nor any of their contractors, subcontractors, or their employees, makes any warranty, express or implied, or assumes any legal liability or responsibility for the accuracy, completeness or usefulness of any information, apparatus, product or process disclosed, or represents that its use would not infringe privately owned rights.

DISCLAIMER

This report was prepared as an account of work sponsored by an agency of the United States Government. Neither the United States Government nor any agency Thereof, nor any of their employees, makes any warranty, express or implied, or assumes any legal liability or responsibility for the accuracy, completeness, or usefulness of any information, apparatus, product, or process disclosed, or represents that its use would not infringe privately owned rights. Reference herein to any specific commercial product, process, or service by trade name, trademark, manufacturer, or otherwise does not necessarily constitute or imply its endorsement, recommendation, or favoring by the United States Government or any agency thereof. The views and opinions of authors expressed herein do not necessarily state or reflect those of the United States Government or any agency thereof.

DISCLAIMER

Portions of this document may be illegible in electronic image products. Images are produced from the best available original document.

TABLE OF CONTENTS

	<u>Page</u>
SUMMARY	i
I. INTRODUCTION.	1
II. TARGET ROD FABRICATION DEVELOPMENT	3
Materials Selection.	3
Target Pellet Constituents.	3
Cladding Components	5
Pellet Preparation	14
Target Specifications	14
Target Fabrication.	16
Zirconia Pellet Fabrication	21
Pellet Characterization.	24
Chemistry	24
Metallographic Examination.	31
Autoradiography	31
Property Measurements.	35
Thermal Expansion	39
Thermal Cycling	39
Compatibility Testing.	43
Encapsulation and Quality Assurance.	47
Weld Qualification.	47
Encapsulation Procedures.	51
Cleaning and Inspection	52
Shipment and Assembly.	55
Fabrication Optimization Studies	55
Cladding Specification.	58
Pellet Specification.	59
Pellet Fabrication.	60
III. POSTIRRADIATION EXAMINATION	70
Stereo Visual Examination.	70
Gamma Scan	75

TABLE OF CONTENTS (Continued)

	<u>Page</u>
Cover Gas Analysis	77
Target Rod Disassembly	80
Metallographic Examination	83
Postirradiation Chemical Analyses.	91
Electron Microprobe Analysis	99
Dosimetry Results.	119
Conclusions.	126
IV. PROCESSING STUDIES	128
Dissolution.	128
Experimental Procedure.	130
Results	132
Recovery	135
Alternate Diluents	137
The Production Cycle	141
V. RECOMMENDATIONS	145
VI. REFERENCES	146
APPENDIX A - Battelle-Columbus Specification for Neptunia-Calcia-Stabilized Zirconia Target Pellets	
APPENDIX B - Specification for Type 304L Stainless Steel Tubing for Nuclear Application	
APPENDIX C - General Specifications for Neptunia Target Pellets	
APPENDIX D - Informal Reprocessing Proposal	

LIST OF TABLES

Table 1. Specified Neptunium Content of Various Target Rod Segments. . .	2
Table 2. Results of Chemical Analyses on NpO ₂ Powder Received from Savannah River	6
Table 3. Typical and Analyzed Impurities in the Calcia-Stabilized Zirconia Powder	7

LIST OF TABLES (Continued)

	<u>Page</u>
Table 4. Chemical Analysis Data for Type 304 Stainless Steel Target Tube Materials	10
Table 5. Chemical Analysis of Type 304 Stainless Steel Rod Used for Target End Components and Other Hardware.	13
Table 6. Results of Initial Sintering Studies of Various NpO ₂ Target Rod Pellets.	18
Table 7. Process Parameters and Densities of NpO ₂ Target Pellets	23
Table 8. Total Gas Release and Moisture Contents of Selected NpO ₂ Pellets.	26
Table 9. Results of Mass Spectrometric Analysis of Gas from 77 w/o NpO ₂ Pellet.	26
Table 10. Impurities Present in Selected Pellets from Various Batches of Material After Sintering	28
Table 11. Summary of Major Oxide Constituent Analyses for the Target Pellets.	29
Table 11A. Neptunium Content of Target Pellets	30
Table 12. Summary of Heat-Treatment Conditions for the Second Group of Test Capsules.	45
Table 13. NpO ₂ Target Segment Experimental and Design Data.	53
Table 14. Compilation of Green Density Data for Pellets Pressed at Different Parameters from Ball Milled Powder.	62
Table 15. Summary of Data for Various Processing Parameters	64
Table 16. Average Sintered Density of Pellets Prepared from Powder Processed Under Different Conditions	68
Table 17. Neptunium Rod Diameters	74
Table 18. Gas Analysis.	79
Table 19. Xenon and Krypton Isotopic Analysis	79
Table 20. Results of BCL Chemical Analyses of Irradiated NpO ₂ Targets	98
Table 21. Results of Analysis for Pu ²³⁶ Content in the Pu ²³⁸	100
Table 22. Results of Plutonium Isotopic Analyses.	101
Table 23. Summary of Chemical Analysis of Neptunia Target Rods.	102
Table 24. Summary of Microprobe Analyses on Irradiated NpO ₂ Targets	120
Table 25. Thermal and Fast Dosimetry Results.	123
Table 26. Constants and Parameters Used in Flux Calculations.	123
Table 27. Analysis of ZrO ₂ (CaO)-NpO ₂ -PuO ₂ Sample Pellets.	129
Table 28. Results of Dissolution Experiments.	133
Table 29. Results of Anion Exchange Recovery Procedure.	136
Table 30. Alternate Materials for Target Diluent.	139

LIST OF FIGURES

	<u>Page</u>
Figure 1. Typical CaO-Stabilized ZrO ₂ Particle Configuration and Size Distribution	8
Figure 2. Unidentified Inclusions (Dark) in Matrix of Seamless Type 304 Stainless Steel Tubing	11
Figure 3. Typical Microstructure of Type 304 Stainless Steel Tubing Showing Grain Structure and Stringer Inclusions	12
Figure 4. Microstructure of Type 304 Stainless Steel Rod Stock.	15
Figure 5. Process Flow Diagram for Pellet Fabrication	22
Figure 6. Typical Microstructure of 14.65 w/o NpO ₂ Composition After Sintering at 1675 C for 2 hr (Pellet Batch 1)	32
Figure 7. Microstructure of Typical Pellet from Batch 2 Containing Nominal 15.18 w/o NpO ₂	32
Figure 8. Microstructure of Typical Pellet from Batch 3 Containing Nominal 15.18 w/o NpO ₂	33
Figure 9. Microstructure of 25.53 w/o NpO ₂ Composition Batch (Pellet Batch 6) After Sintering at 1675 C for 2 hr	33
Figure 10. Microstructure of 44.47 w/o NpO ₂ Composition (Pellet Batch 5) After Sintering at 1675 C for 2 hr.	34
Figure 11. Typical Microstructure of 71.69 w/o NpO ₂ Composition (Pellet Batch 4) After Sintering at 1600 C for 2 hr	34
Figure 12. Autoradiographs of Various Metallographic Specimens	36-38
Figure 13. Thermal Expansion Curve of the 14.65 w/o NpO ₂ Material.	40
Figure 14. Comparison of Calculated and Measured Temperature Cycles of Various NpO ₂ Target Compositions	42
Figure 15. Typical Appearance of Longitudinal Section from Type 304 Stainless Steel Capsule Which Contained Pellet After Heat Treatment at 500 C (932 F) for 1 Month.	44
Figure 16. View of Welding Fixture as Set Up in Glove Box.	48
Figure 17. Typical Microstructure of Weld Encompassing the Type 304 Stainless Steel Cladding-End Fitting Interface.	50
Figure 18. Neptunium Target Rods Assembled and Fastened to Bench	56
Figure 19. Change in Average Green Density of Pellets with Pressing Pressure	63
Figure 20. Variation of Pellet Sintered Density as a Function of Ball Milling Time and Sintering Temperature.	66
Figure 21. Variation of Pellet Sintered Density as a Function of Sintering Temperature for Constant Ball Milling Time.	67
Figure 22. Neptunium Fuel Assembly J-14 With Target Rod Assembly	71

LIST OF FIGURES (Continued)

	<u>Page</u>
Figure 23. Flow Diagram for Destructive Examination.	72
Figure 24. As-Received Neptunium Target Rods 1 and 2	73
Figure 25. Neptunium Target Rod Gamma Scan	76
Figure 26. Plot of Initial NpO ₂ Percent Concentration Versus Relative Gamma-Scan Intensity.	78
Figure 27. Neptunium Target Rod 2 - Sections A, B, and C (Slit Open for Visual Examination)	81
Figure 28. Neptunium Target Rod 2 - Sections D Top and D Bottom (Slit Open for Visual Examination).	82
Figure 29. Neptunium Rod Number Two Sectioning Schematic	84
Figure 30. Neptunium Target Rod 2 As-Polished Metallographic Sample 1 from Section D.	85
Figure 31. Neptunium Target Rod 2 As-Polished Metallographic Sample 3 from Section D.	86
Figure 32. Neptunium Target Rod 2 As-Polished Metallographic Sample 4 from Section D.	87
Figure 33. Neptunium Target Rod 2 As-Polished Metallographic Sample 6 from Section C.	88
Figure 34. Neptunium Target Rod 2 As-Polished Metallographic Sample 8 from Section B.	89
Figure 35. Neptunium Target Rod 2 As-Polished Metallographic Sample 11 from Section A.	90
Figure 36. Irradiated NpO ₂ Target Metallographic Sample D-1, Etched Condition.	92
Figure 37. Irradiated NpO ₂ Target and Clad Metallographic Sample D-3, Etched.	93
Figure 38. Irradiated NpO ₂ Target Metallographic Sample D-4, Etched. . .	94
Figure 39. Irradiated NpO ₂ Target Metallographic Sample C-6, Etched. . .	95
Figure 40. Irradiated NpO ₂ Target and Clad Metallographic Sample B-8, Etched.	96
Figure 41. Irradiated NpO ₂ Target Metallographic Sample A-11, Etched . .	97
Figure 42. Neptunium M α_1 X-Ray Intensity Versus Percent NpO ₂	104
Figure 43. Unirradiated Standard 2D-35 Microprobe Scan Showing ZrO ₂ -Rich Area.	105
Figure 44. Unirradiated Standard 2D-35 Microprobe Scan Showing NpO ₂ -Rich Area.	106
Figure 45. Sample 2A-11 Microprobe Scan.	107
Figure 46. Sample 2B-8 Microprobe Scan	108

LIST OF FIGURES (Continued)

	<u>Page</u>
Figure 47. Sample 2C-6 Microprobe Scan	109
Figure 48. Sample 2D-3 Microprobe Scan	110
Figure 49. Irradiated Sample 2D-3 Microprobe Scan.	111
Figure 50. Irradiated Sample 2C-6 Microprobe Scan.	112
Figure 51. Irradiated Sample B-8 Microprobe Scan	113
Figure 52. Irradiated Sample A-11 Microprobe Scan.	114
Figure 53. Sample 2A-11 Np and Pu X-Ray-Intensity Diametral Profile. . .	115
Figure 54. Sample 2B-8 Np and Pu X-Ray-Intensity Diametral Profile . . .	116
Figure 55. Sample 2C-6 Np and Pu X-Ray-Intensity Diametral Profile . . .	117
Figure 56. Sample 2D-3 Np and Pu X-Ray-Intensity Diametral Profile . . .	118
Figure 57. Pu/Np Diametral Profiles for 4 NpO ₂ Compositions.	121
Figure 58. Neptunium Rod No. 2 Thermal and Fast-Flux Profiles.	124
Figure 59. Neptunium Rod No. 2 Normalized Flux and Gamma Scan Profiles .	125
Figure 60. Flow Schematic for Recovery of Neptunium and Plutonium from Irradiated NpO ₂ -ZrO ₂ Target Rods	138

SUMMARY

Two neptunia-zirconia fueled target rods, containing four sections each of different neptunia concentrations, were fabricated and loaded into Connecticut Yankee Reactor for irradiation. Compositions of the target pellets in the sections were 14.65, 25.53, 44.47, and 71.69 w/o NpO_2 , with the balance of material being calcia-stabilized zirconia. Conventional ball milling, cold pressing, and sintering techniques were utilized for powder blending and pellet fabrication. Chemical analyses performed on selected pellets showed that total gas, moisture, and hydrogen contents, were considerably less than specified tolerances. Metallographic examination revealed a uniform porosity and grain structure which indicated that the distribution of constituents was homogeneous. This was confirmed by autoradiographic examination. Limited thermal expansion and thermal cycling tests were performed on several pellets to confirm their conformance to design specifications and probable stability to fracture during irradiation. All work was conducted according to rigid pellet fabrication and weld specifications, as well as stringent quality assurance procedures for each phase of the assembly operation.

After approximately 1 year's irradiation, the rods were removed from the reactor and transferred to the BCL Hot Lab Facility for postirradiation examination. A series of nondestructive examinations, including stereo visuals, diameter measurements, and gamma scans revealed that physical changes were minimal. Based on the gamma scans, Target Rod Number 2 was chosen for destructive testing and analysis. The target rod was punched and the cover gas collected and analyzed for molecular and atomic constituents. It was then slit open, examined visually, photographed, and specimens sectioned for metallographic examination, chemical analysis, and electron microprobe analysis. Cladding samples were also removed for neutron dosimetry.

Postirradiation chemical analyses included total plutonium and neptunium, ppm Pu-236/Pu-238, and plutonium isotopic abundance. In addition, electron microprobe analysis provided the relative Pu concentration across the pellet diameters, which is directly proportional to the flux depression. A summary of the results is as follows.

Section	Initial w/o NpO ₂	Np to Pu Conversion, percent	Percent Pu-238 in Pu	ppm Pu-236 in Pu-238	Percent Flux Depression (edge to center)
D	14.65	22.4	90.71	8.8	13.0
C	25.53	16.3	91.61	10.8	27.3
B	44.47	13.3	93.18	13.3	35.7
A	71.69	9.1	94.95	20.5	44.8

Dosimetry measurements were made at target locations by analysis of the 304 stainless steel cladding for Co-60 and Mn-54. Thermal and fast fluences were measured at 7.1×10^{20} and 2.9×10^{21} neutrons/cm², respectively.

Processing studies, performed on simulated irradiated pellets, indicated that the ground, irradiated material would be amenable to dissolution after treatment with either hot, concentrated HF or fuming H₂SO₄. In either case, the residue containing the neptunium and plutonium was soluble in hot 8N HNO₃. The resultant nitric acid solution served as a feed to the anion exchange recovery and separation of the neptunium and plutonium.

The feasibility of all the major operations involved in production of Pu²³⁸ by irradiation of Np²³⁷O₂ targets in commercial nuclear power reactors has been demonstrated. It is recommended that the demonstration be extended to a pilot-scale leading to installation of a full production capacity.

PRODUCTION OF Pu-238 IN COMMERCIAL POWER REACTORS:
TARGET FABRICATION, POSTIRRADIATION EXAMINATION,
AND PLUTONIUM AND NEPTUNIUM RECOVERY

by

M. Pobereskin, W. Langendorfer, L. Lowry,
D. Farmelo, V. Scotti, and O. Kruger

I. INTRODUCTION

The radioisotope thermoelectric generator (RTG) systems developed under sponsorship of the Space Nuclear Systems Division (SNSD) of the USAEC have compiled an enviable record for performance in a variety of space missions over the past decade. As a consequence, considerable interest has been generated in more extensive applications of such systems, not only in Government missions, but also in industrial and medical applications. This raises serious questions concerning availability of Pu²³⁸ to supply an expanding demand. Concomitantly, the development of much of this demand will depend upon a considerable reduction in cost of the currently very expensive Pu²³⁸.

Present capabilities for production of Pu²³⁸ within the USAEC Laboratories systems are limited. With the shutdown of plutonium production reactors, the Np²³⁷ target material has been derived primarily from the burning of costly U²³⁵. Thus, two target irradiations, with accompanying processing, are involved in the production operation. In the meantime, the installed capacity of light-water power reactors is rapidly increasing. Here is a ready source not only for Np²³⁷ target material, but also for neutron irradiation capacity to convert the Np²³⁷ to Pu²³⁸. It has been proposed, therefore, that one should look to commercial light-water power reactors as the basis for an industrial system capable of producing large quantities of Pu²³⁸ at relatively low cost.

A theoretical study of the feasibility of converting Np²³⁷ to Pu²³⁸ in commercial water reactors⁽¹⁾ was conducted in 1969 by Southern Nuclear Engineering (SNE), Division of Nuclear Utility Services, under sponsorship of the SNSD. The results of this work indicated that the approach was practical and the cost of Pu²³⁸ could be reduced appreciably with adequate profit margins for the utilities and other industrial components. Questions still remained regarding limitations of the one-dimensional model used for the calculations

and the unavailability of experimental data related to the behavior of the neptunium target form in a light-water-reactor environment. A project definition phase of a program aimed at generation of experimental and analytical data necessary to the critical analysis of the concept was initiated by SNE in 1970.⁽²⁾ This effort led to an agreement whereby Battelle's Columbus Laboratories (BCL) was responsible for the fabrication of two NpO_2 target assemblies for irradiation in the Connecticut Yankee Reactor owned by Connecticut Yankee Atomic Power Company (CYAPC). Details of this agreement, design drawings with full specifications, and the results of multidimensional calculations for the target rods in a pressurized water reactor have been reported.⁽³⁾

Specifications called for the fabrication of two target rod assemblies, each consisting of four separate sections with different neptunium compositions and mass-volume relationships, as listed in Table 1. The target material was to be composed of neptunium dioxide mixed with a suitable diluent in the form of pellets sintered to a fairly high density to promote heat transfer. Seamless Type 304 stainless steel tubing was specified as the cladding material. Fin-shaped spacers were located on the top ends of each segment of the targets to position the rod within the thimbles of the control rod assemblies which were chosen for the irradiation.

TABLE 1. SPECIFIED NEPTUNIUM CONTENT OF VARIOUS TARGET ROD SEGMENTS

Segment		Neptunium Density, g per cm^3	Total Volume of Fuel Segment, cm^3	Total Mass of Neptunium, g
1A	2A	5.44	18.88	102.69
1B	2B	2.72	18.88	51.35
1C	2C	1.36	18.88	25.67
1D	2D	0.68	81.17	55.20

II. TARGET ROD FABRICATION DEVELOPMENT

The time available for fabrication development was relatively short because of the necessity to meet an imminent deadline for insertion of the targets in the reactor. For this reason, and also to minimize the effort necessary to license the experiment for operation in the CYR, full advantage was taken of known reactor fuel technology. In this initial part of the program, effort was focused on experimental development and conduct of full quality assurance procedures for cladding examination, pellet fabrication, pellet characterization, some physical property measurements, rod segment welding, shipment, and, finally, assembly and welding at the reactor site.

Materials Selection

Target Pellet Constituents

Relatively few properties of NpO_2 have been reported in the literature, and furthermore there are few data relating to fabrication behavior. Ackermann, et al⁽⁴⁾, worked with small quantities of NpO_2 to study its vaporization characteristics. Their work showed that NpO_2 was the principal vapor species, although a tendency to become hypostoichiometric and form a lower oxide (probably Np_2O_3) through loss of NpO was found at high temperatures. In this respect, the phase relationships found in the neptunium-oxygen system seem to closely resemble those established for plutonium-oxygen.

The theoretical density of NpO_2 was calculated to be 11.13 g per cm^3 based on the lattice constant value of 5.434 Å reported by Ackermann. This datum was of immense value to this program, since it enabled calculation of reliable theoretical densities of neptunia solid solutions with the diluent material. These data in turn aided the interpretation of the sintering behavior as the approach to theoretical density was realized. Since little more was known of the intrinsic behavior of NpO_2 , an assumption was made that its melting point and phase interactions would closely parallel those of UO_2 and PuO_2 based on their actinide series relationships. Moreover, the sintering characteristics of NpO_2 were assumed to be about the same as those of UO_2 and PuO_2 , which effectively

bracketed the temperature range for attaining maximum densification between 1500 and 1700 C.

In order to conform to the reactor fuel geometry, a pellet-in-tube target geometry was designated. The optimum target appeared to be a column of pellets consisting of a dispersion of NpO_2 in some diluent added to reduce self-shielding of the neptunium. The term dispersion, as used here, is probably a misnomer, since some solubility, perhaps complete, would be predicted under the sintering conditions imposed to obtain pellets with a high degree of resistance to fracture and spalling coupled with the optimum attainable heat transfer. Materials and techniques normally used for target fabrication by the Savannah River Laboratories (SRL)⁽⁵⁾, e.g., powder metallurgical preparations of aluminum compacts with a uniform dispersion of NpO_2 , were unsuitable for this application because of the high temperatures involved in the irradiation and general incompatibility of aluminum with the reactor fuel and coolant system.

The desired characteristics of the diluent material are listed below.

- Low cross section
- Good irradiation stability in a water reactor environment
- Excellent high-temperature stability, i.e., to temperatures near the melting point of NpO_2 or ~ 2000 C (3632 F)
- High probability of predictable uniform sintering characteristics based on behavior with other actinide dioxides, e.g., UO_2 and PuO_2
- Compatible with Type 304 stainless steel cladding at 600 F, the normal reactor water temperature during operations.

Other factors taken into consideration were the low calculated heat evolution from the pins and almost negligible problems of swelling from fission products, etc., normally associated with reactor fuels.

Based on the above criteria, a decision was made to utilize CaO-stabilized ZrO_2 in solution with the NpO_2 . ZrO_2 was considered to be more favorable than Al_2O_3 because of possible deleterious side reactions associated with aluminum. Calcia stabilization of the zirconia appeared mandatory because of the complete lack of data on the $(\text{Np},\text{Pu})\text{O}_2$ - ZrO_2 system and the wide range of compositions called for in the target specifications.

Neptunium dioxide for this program was obtained from the Atomic Energy Commission via SRL. The powder was light green and was received with the specification sheet shown in Table 2. As a general observation, the impurity content of the NpO_2 powder, as determined by spectrographic analysis, was about the same as that expected in commercial-grade UO_2 and PuO_2 powders. The low plutonium content of this material was considered to be an asset for the planned irradiation.

The calcia-stabilized zirconia powder for use as the diluent with the neptunium dioxide was procured from the Zirconium Corporation of America (ZIRCOA). This material was ordered as nuclear-grade powder of minus 325 mesh ($<44\mu$ particle size) containing 10 to 12 w/o calcia. A typical chemical analysis for impurities in the powder furnished by ZIRCOA is given in Table 3, together with the results obtained at BCL. As can be seen, the BCL analysis is in fairly close agreement with that of the manufacturer. The relatively high silicon and sulfate contents of the powder were recognized as factors which could lead to fabrication difficulties, but no other substitute material could be obtained in time to meet the commitments of the program. Removal of chlorine during sintering was expected; therefore, the high chlorine content of the powder did not present any cause for concern.

The stabilized zirconia powder was examined by metallographic techniques in an effort to further characterize the material before blending with the neptunium. A photomicrograph from the mounted and polished powder specimen is shown in Figure 1. As expected, the particles were irregular in shape, and a cursory size analysis indicated that approximately 80 percent of the powder was $\leq 10\mu$ in maximum width. No similar evaluation of the NpO_2 was conducted; however, it was concluded that the particle size of the two constituents was sufficiently fine to give a highly sinterable powder blend with reasonable ball-milling periods.

Cladding Components

Type 304 stainless steel tubing for the target rods was supplied by Nuclear Materials and Equipment Corporation. This tubing, which conformed to the specification NPS-20A-Rev 1 (Reference NUMEC Drawing 10B323) was completely qualified for use in Connecticut Yankee core reload assemblies. The four tubes

TABLE 2. RESULTS OF CHEMICAL ANALYSES ^(a) ON NpO₂
POWDER RECEIVED FROM SAVANNAH RIVER

Run Identification	010HB-14
Oxide Weight, g	850.0
Neptunium Oxide Assay, %	99.54
Neptunium in Neptunium Oxide, %	88.1
Neptunium Weight, g	745.37
Thorium, w/o oxide	0.14
Uranium, w/o oxide	L 0.10
Weight loss at 800 C, w/o oxide	0.21
Total Plutonium w/o oxide	0.02

Plutonium Isotopic Distribution

²³⁸ Pu	78.32
²³⁹ Pu	18.98
²⁴⁰ Pu	2.19
²⁴¹ Pu	0.376
²⁴² Pu	0.140

Spectrographic Analysis, ppm

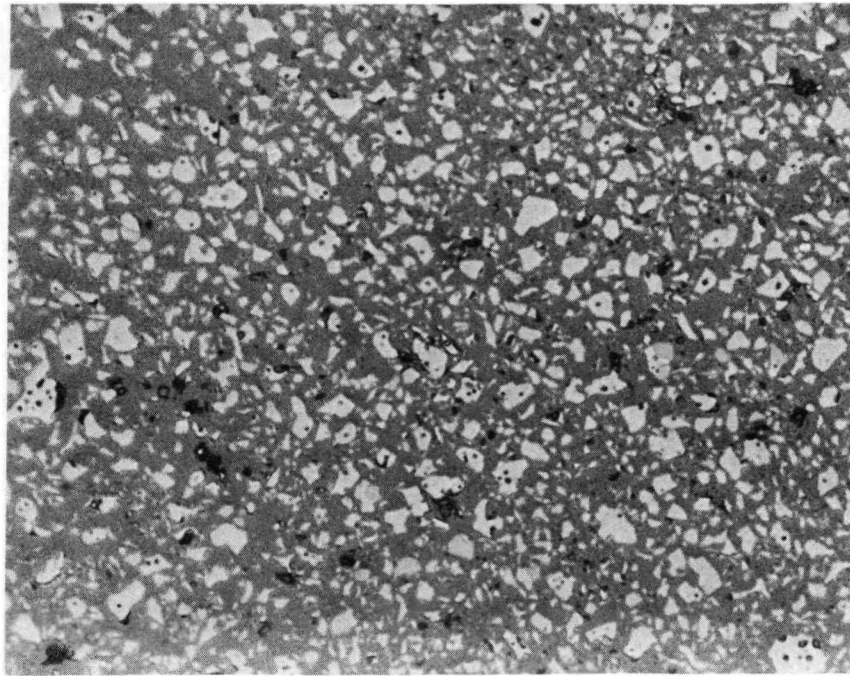
Al, 150	Fe, 200	Ni, L50
B, L20	K, L 200	P, L500
Be, L10	Mg, 10	Pb, L10
Ca, L50	Mn, L 50	Si, L100
Cd, L10	Mo, L 10	Sn, L50
Cr, 30	Na, L 20	Zn, L200
Cu, L50		

(a) L = less than.

TABLE 3. TYPICAL AND ANALYZED IMPURITIES IN THE
CALCIA-STABILIZED ZIRCONIA POWDER^(a)

Impurity	Impurity Content, ppm	
	Typical ZIRCOA Analysis	BCL Analysis
Aluminum	100-300	40
Boron	0.5-2	<5
Cadmium	<10	<10
Chlorine	10-20	40
Cobalt	<10	<10
Chromium	10-30	10
Copper	<25	<10
Iron	85-400	150
Hafnium	50-100	<100
Magnesium	100-150	50
Manganese	<10	5
Nickel	N.A.	20
Lead	<25	<10
Silicon	280-600	300
Tin	≈10	<10
Titanium	<10	20
Vanadium	≈10	<10
SO ₄	100-400	30
Loss on ignition	0.3% max	N.A.

(a) ZIRCOA reactor-grade zirconia containing 10 to 12 w/o CaO.
N.A. = not analyzed.



500X

As Polished

2F350

FIGURE 1. TYPICAL CaO -STABILIZED ZrO_2 PARTICLE CONFIGURATION AND SIZE DISTRIBUTION

received for this program were each approximately 10 feet long, and these were identified as S-557, -562, -566, and -569. Dimensions of this reactor-grade fuel rod tubing were 0.433 inch OD with a 0.0165-inch wall thickness. Results of chemical analyses for each of the tubes are presented in Table 4, along with the mill heat analysis and ASTM and SNE specifications. In general, all of the elements were within the standard specifications with the exception of the chromium content of Tube S-569, which was slightly on the low side. Battelle analyses for gaseous impurities fall within the ranges normally expected for these elements.

Further characterization included metallographic examination of transverse and longitudinal sections from each of the tubes. Typical microstructures of the various tube sections are shown in the photomicrographs of Figures 2 and 3 for Tube S-566. All of the sections were examined first in the as-polished condition to obtain a true picture of the inclusion distribution, and then in the etched condition for grain size evaluation. Small amounts of stringer-type inclusions seen in Figure 2b were present in all of the specimens examined in the longitudinal direction. These stringers were often found close to the surface, as is evident in Figures 2b and 3b. Generally, the microstructures were typical of those expected for this grade of stainless steel tubing. One of the tubes, S-566, appeared to have a somewhat higher concentration of inclusions; therefore, this length of tubing was held in reserve and utilized for preliminary testing of weld parameters and as cladding for compatibility capsules. Boroscope examination was conducted on all tubing after cutting to size. Some small pits and scratches were identified on the interior of all of the tubes, but in no case were these considered to be of sufficient magnitude to preclude the use of a tube for a target segment. As a result of this evaluation, however, all tubes were classified and subsequently utilized according to this listing.

Type 304 stainless steel rod for the various end fittings and other hardware components was procured in accordance with the SNE specification (Reference Drawing 69-646-11). The Battelle chemical analysis of this material is given in Table 5, together with the SNE specifications and the certified mill analysis. Concentrations of all elements were within the expected ranges. The high cobalt content specified for the stainless steel rod was appreciably above the generally accepted limit; however, it was necessary to relax the specification

TABLE 4. CHEMICAL ANALYSIS DATA FOR TYPE 304 STAINLESS STEEL TARGET TUBE MATERIALS ^(a)

Element	Specification Analysis		Mill Analysis ^(d)		Battelle Analysis of Indicated Tube ^(e)			
	NUMEC ^(b)	SNE ^(c)	Heat	Check	S-557	S-562	S-566	S-569
Oxygen	-	-	-	-	150 ppm	200 ppm	175 ppm	235 ppm
Hydrogen	-	-	-	-	4 ppm	7 ppm	4 ppm	3 ppm
Nitrogen	-	-	-	-	510 ppm	660 ppm	640 ppm	520 ppm
Carbon	0.08 max	0.04-0.08	0.04	0.04/0.04	0.038	0.041	0.037	0.035
Phosphorus	0.040 max	-	0.025	0.008/0.008	0.026	0.027	0.025	0.024
Sulfur	0.030 max	-	0.015	0.010/0.009	0.013	0.013	0.012	0.013
Chromium	18.0-20.0	-	18.89	18.30/18.30	19.6	18.7	18.5	17.8
Nickel	8.00-11.0	-	10.17	9.94/9.88	10.2	10.5	9.9	9.8
Manganese	2.00 max	-	1.17	1.13/1.15	1.23	1.01	1.13	0.94
Silicon	0.75 max	-	0.32	0.343/0.347	0.28	0.28	0.41	0.3
Cobalt	-	0.08 max	0.028	0.002/0.002	0.070	0.070	0.075	0.075
Boron	-	-	0.0005	<0.0005/<0.0005	N.A.	N.A.	N.A.	N.A.

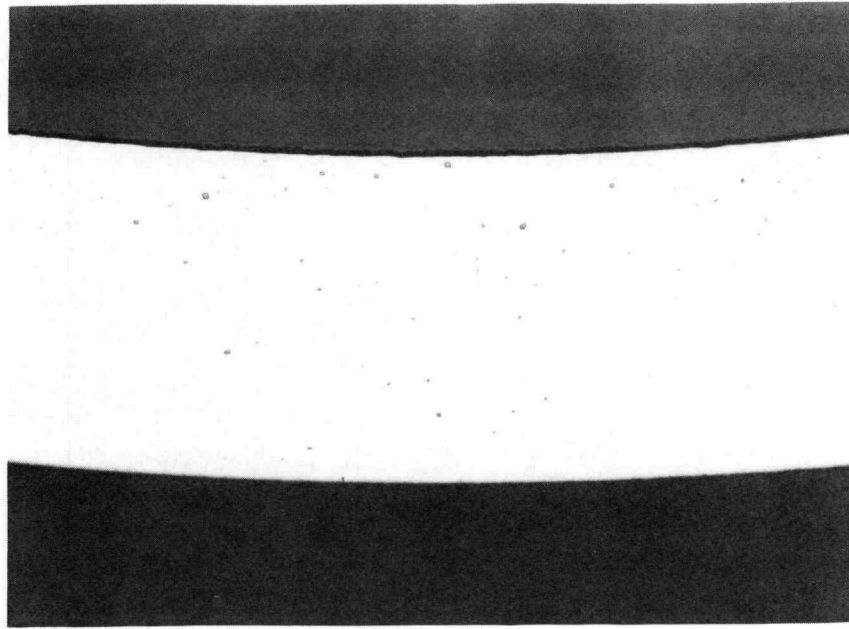
(a) Analysis data given as w/o unless otherwise indicated.

(b) NUMEC specification indicates material to conform to ASTM Standard A-213-66.

(c) SNE specification is same as NUMEC except for carbon and cobalt, as indicated.

(d) Mill analysis provided by Superior Tube Company for Heat No. M2918. Check analysis is at finish of processing.

(e) Samples taken from sections removed from one end of each tube. N.A. = not analyzed.

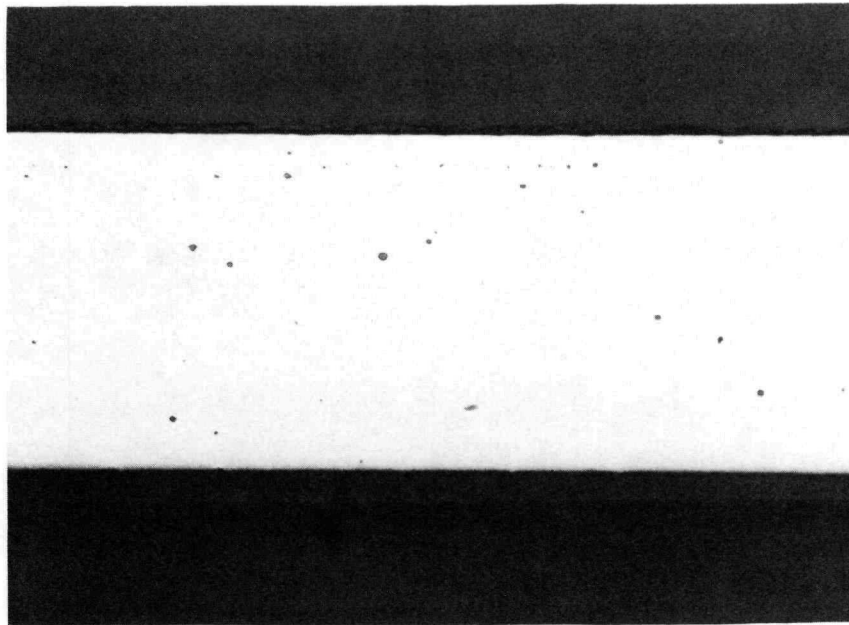


100X

As Polished

2F340

a. Transverse Section



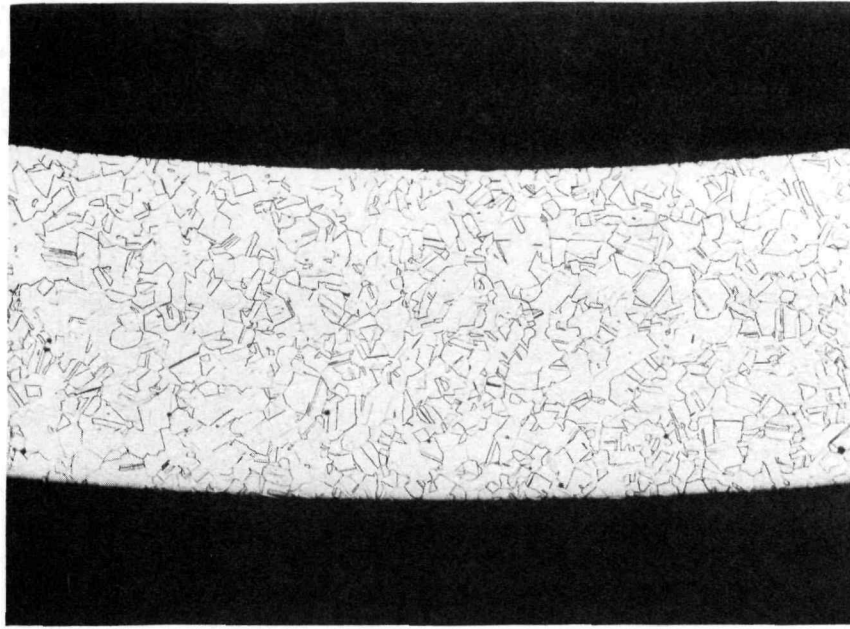
100X

As Polished

2F341

b. Longitudinal Section

FIGURE 2. UNIDENTIFIED INCLUSIONS (DARK) IN MATRIX OF SEAMLESS TYPE 304 STAINLESS STEEL TUBING

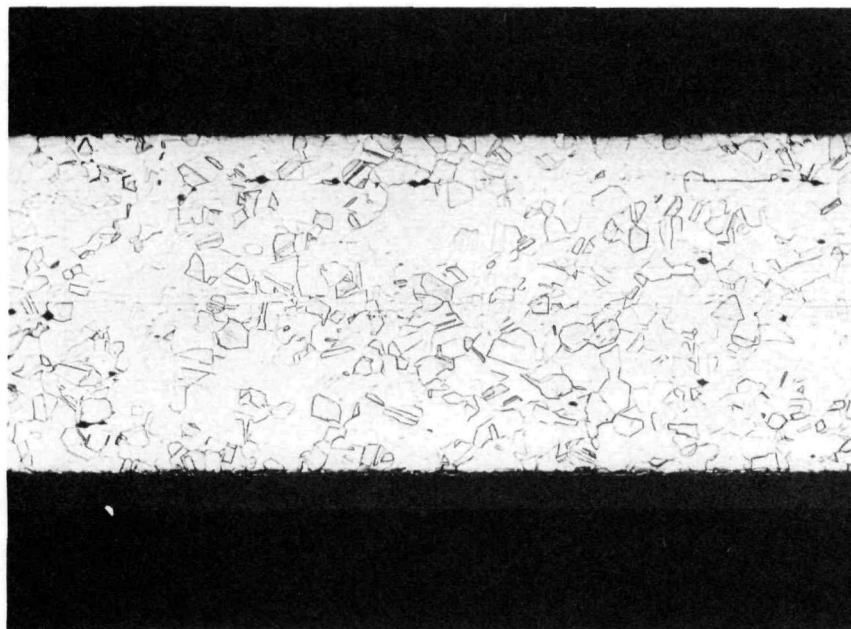


100X

Etched

2F342

a. Transverse Section



100X

Etched

2F343

b. Longitudinal Section

FIGURE 3. TYPICAL MICROSTRUCTURE OF TYPE 304 STAINLESS STEEL TUBING SHOWING GRAIN STRUCTURE AND STRINGER INCLUSIONS

TABLE 5. CHEMICAL ANALYSIS OF TYPE 304 STAINLESS STEEL ROD
USED FOR TARGET END COMPONENTS AND OTHER HARDWARE^(a)

Element	Specification Analysis ^(b)	Certification Analysis ^(c)	Battelle Analysis
Oxygen	-	-	600 ppm
Hydrogen	-	-	< 1 ppm
Nitrogen	-	-	300 ppm
Carbon	0.04-0.08	0.057/0.059	0.065
Phosphorus	0.045 max	0.022/0.023	0.027
Sulfur	0.030 max	0.021/0.019	0.025
Chromium	18.00-20.00	18.40/18.50	18.5
Nickel	8.00-12.00	8.36/8.36	8.25
Manganese	2.00 max	1.51/1.52	1.65
Silicon	1.00 max	0.52/0.52	0.46
Cobalt	0.15 max	0.13/0.13	0.12
Molybdenum	-	0.26/0.26	N.A.
Copper	-	0.20/0.20	N.A.

(a) Analysis data in w/o unless otherwise specified. N. A. = not analyzed.

(b) SNE Drawing 69-646-11 specifies ASTM Standard A-276, Type 304, centerless ground, Condition A, except for carbon, 0.04 to 0.08 w/o, and cobalt, 0.15 w/o max.

(c) Certified analysis from Williams and Company on Universal Cyclops Heat No. G5433.

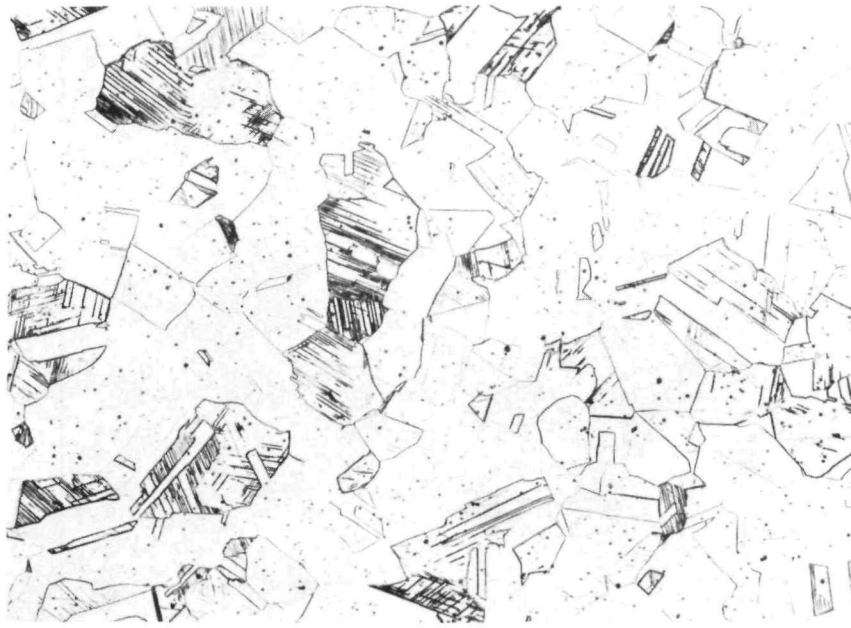
for cobalt somewhat in order to obtain material that would satisfy the immediate needs of the program. This bar stock was the only lot of stainless steel commercially available at the time the order was placed. Although stainless steel with a lower cobalt content can be obtained on special order, several months are required for delivery, and the quantity of steel ordered must be appreciably greater than warranted for this investigation.

Cursory evaluation of the effects associated with the high cobalt content of the cladding end fittings indicated that some degree of perturbation of the gamma scans of the target rods would be expected on postirradiation examination, but no serious or insurmountable problem was thought to exist. Metallographic examination of transverse and longitudinal center sections from the rod stock yielded the expected microstructures, as shown in Figure 4. Comparison of these microstructures with those of Figures 2 and 3 shows that the average grain size of this material was considerably greater than that of the cladding.

Pellet Preparation

Target Specifications

Initially, it was thought that extensive parametric processing studies could be avoided, since normal stringent performance characteristics associated with a reactor fuel were not specified for the targets, and there was no necessity for maintenance of excessively precise restrictions on density. As the work progressed and the goals of the program became more well-defined, however, it became obvious that there was a need for target pellet specifications equivalent in many ways to those for the fuel, so as not to jeopardize the operation of the reactor. This was further deemed necessary when the additional value of experimental data generated on pellets with a uniform density was considered in light of the ultimate goals for the program. In addition, a rigid diametral tolerance gave some assurance that appreciable void volume would form within the targets if the fuel-cladding gap closed during the course of the irradiation. The requirement for uniform clearance thus minimized the possibility of breaching the cladding. Control of pellet diameter was also found to be of significance, since this dimension affects the NpO_2 concentration per unit length,

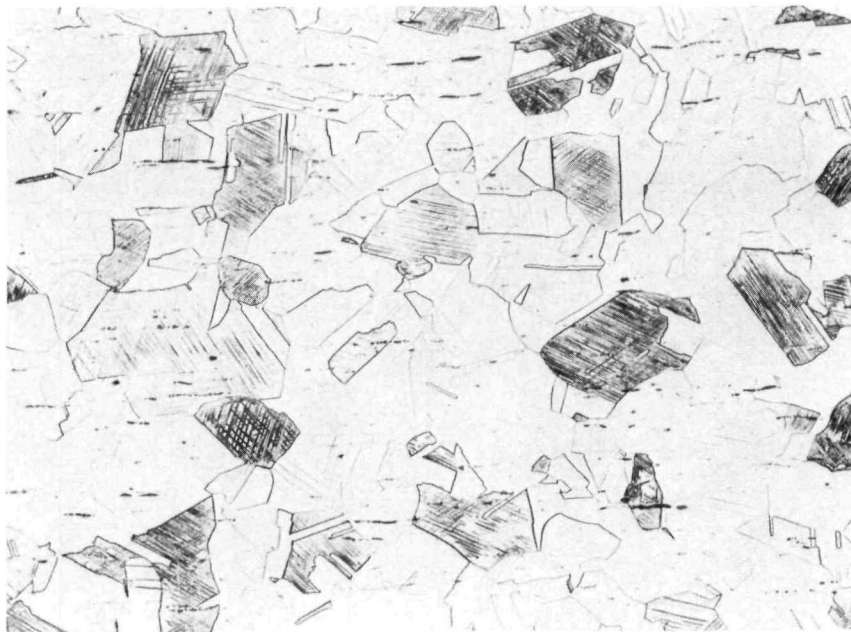


100X

Etched

2F381

a. Transverse Center Section



100X

Etched

2F383

b. Longitudinal Center Section

FIGURE 4. MICROSTRUCTURE OF TYPE 304 STAINLESS STEEL ROD STOCK

which, when held constant, provides a means of mapping the flux of the reactor through determination of the change in Pu^{238} concentration over the length of the target segment.

In view of the above, a pellet specification was written toward the completion of the target rod fabrication. This document is presented in Appendix A. The standards imposed on the target material closely parallel those normally required for UO_2 fuel. The only exceptions occur in the dimensional limits of surface flaws and in the allowable impurity elements, particularly in regard to the total equivalent boron content, since reactivity was of no consequence. Otherwise, the acceptable amount of chlorine, hydrogen, and total gas was the same as for the reactor fuel pellets. These limits and the consequences of preparing pellets that could not meet the specifications were factors that profoundly influenced the techniques chosen for pellet fabrication; these are discussed below.

Target Fabrication

Since data pertaining to the densification behavior of NpO_2 were virtually nonexistent, initial studies were directed toward obtaining some understanding of the powder blending characteristics and the change in density that could be expected on sintering the various compositions of interest. It was expected that this work would then provide the basic information needed to make adjustments in the processing scheme and thus zero in on the fabrication parameters that would meet the goals established for this phase of the program.

Neptunium concentrations specified for each of the target segments are given in the tabulation of Paragraph 5.1 of Appendix A. These values, which range from 77.22 to 15.18 w/o NpO_2 , essentially encompass the entire phase system in the pseudobinary NpO_2 -(10 w/o CaO-ZrO_2). Accordingly, an appreciable change in blending and densification characteristics could be expected for these compositions due to the tremendous difference in properties between the components.

As a first step in the investigation, various techniques for blending of the NpO_2 and 10 w/o CaO-ZrO_2 powders were evaluated according to the relative probability of obtaining a homogeneous dispersion of NpO_2 in the sintered pellets.

This was necessary because many standard methods are unsuitable for blending of powders with widely different densities, as is the case with NpO_2 and calcia-stabilized ZrO_2 , which have densities of 11.13 and about 5.0 g per cm^3 , respectively. A decision was eventually made to blend the powders by wet ball milling, on the basis of experience at Battelle with mechanically mixed UO_2 and PuO_2 together with an evaluation of previous work on UO_2 - PuO_2 - ZrO_2 fuels⁽⁶⁾.

Approximately 30 g powder batches* of various compositions were blended for the preliminary sintering trials. Each powder batch was blended for 8 hours in a rubber-lined mill containing zirconia balls and filled with distilled water. The powder slurry was removed, dried, and screened prior to pressing. Considerable foaming occurred during milling due to the sulfate content of the stabilized zirconia powder, but, aside from some inconvenience in cleaning, there was no deleterious effect on the dried powder. All work on this and other phases of the effort connected with pellet fabrication was conducted in glove boxes containing a dry nitrogen atmosphere. Pellets approximately 0.45 inch in diameter and 0.65 inch long were uniaxially cold pressed at 20,000 and 40,000 psi and sintered in a high-temperature resistance furnace employing a tungsten mesh heater at temperatures ranging from 1300 to 1800 C. An atmosphere of either flowing argon-8 v/o hydrogen or pure nitrogen was used throughout the sintering cycle. Pellets were placed on one of several tiers of a tungsten holder, which was positioned well within the hot zone of the furnace heater. Densities of the pellets were determined from their physical dimensions and weights. Theoretical densities of the various target segment compositions were calculated from a derived theoretical density for NpO_2 , based on the lattice constant data, together with an estimated density for 10 w/o CaO-ZrO_2 obtained from the manufacturer.

A compilation of the various process parameters investigated and the resulting densities of the pellets is given in Table 6. Duplicate pellets of the 48.76 and 77.22 w/o NpO_2 compositions were cycled to progressively increasing temperatures to determine the effect of temperature on shrinkage behavior.

* As defined in Appendix A, Paragraph 7.2.1, a batch of powder is defined as a blend of the initial constituents to obtain a specific composition.

TABLE 6. RESULTS OF INITIAL SINTERING STUDIES OF VARIOUS NpO_2 TARGET ROD PELLETS

Segment	Nominal Composition, w/o NpO_2	Ball-Milling Time, hr	Densification Pressure, psi	Sintering Temperature, C	Sintering Atmosphere	Density of Material		Diametral Shrinkage, percent
						G per cm^3	Percent of Theoretical (a)	
D	15.18	8	40,000	1700	Ar-8 v/o H_2	4.93	90.2	16
		8	40,000	1700	Ar-8 v/o H_2	4.98	91	-
		8	20,000	1700	Nitrogen	4.92	90.2	17
		8	20,000	1800	Nitrogen	5.07	92.7	17.6
		24	20,000	1800	Nitrogen	5.22	95.5	13.2
		24	20,000	1800	Nitrogen	5.25	96	13.3
		24	20,000	1700	Nitrogen	5.13	94.8	12.7
		24	20,000	1600	Nitrogen	4.97	91	11.4
		24	20,000	1675	Nitrogen	5.17	94.6	-
		24	20,000	1675	Nitrogen	5.16	94.4	12.4
		24	20,000	1675	Nitrogen	5.13	93.8	12.7
		C	28.06	8	40,000	1700	Ar-8 v/o H_2	5.37
8	40,000			1700	Ar-8 v/o H_2	5.28	89.1	-
8	20,000			1700	Nitrogen	5.38	91	18.2
8	20,000			1800	Nitrogen	5.38	91	18.1
24	20,000			1675	Nitrogen	5.47	92.4	-
24	20,000			1675	Nitrogen	5.39	91	12.9
B	48.76	8	20,000	1300	Nitrogen	4.53	66.3	9.1
		8	20,000	1500 (b)		5.13	75	13.3
		8	20,000	1700		6.04	88.3	17.2
		8	20,000	1800		6.03	88.3	17.6
		24	20,000	1675		6.37	93.2	13.7
A	77.22	8	20,000	1300	Nitrogen	5.67	65.2	11.1
		8	20,000	1500 (b)		7.16	82.5	17.6
		8	20,000	1700		7.15	82.5	18.0
		8	20,000	1800		7.74	89	19.9
		24	20,000	1675		8.70	100	16.8
		24	20,000	1675		8.54	98.2	16.5
A	77.22	Dry Blended	20,000	1400	Nitrogen	5.63	64.7	9.3
			1500	6.04		69.4	11.4	
			1600 (b)	6.58		75.6	14.2	
			1700	7.14		82	16.9	
			1800	7.14		82	-	
-	100	As Received	20,000	1400	Nitrogen	8.55	76.6	-
			1500	8.69		78	-	
			1600 (b)	-		-	-	
			1700	8.71		78	-	
			1800	8.71		78	-	

(a) Based on calculated theoretical densities of the 15.18, 28.06, 48.76, 77.22 and 100 w/o NpO_2 compositions of 5.46, 5.92, 6.84, 8.70, and 11.13 g per cm^3 , respectively. Calcia-stabilized ZrO_2 theoretical density is estimated to be 5.0 g per cm^3 .

(b) Same pellet(s) sintered at increasing temperatures.

In addition, small amounts of mechanically dry-blended powder containing 77.22 w/o NpO_2 , together with the as-received NpO_2 , were pelletized and sintered at increasing temperatures to obtain a measure of the benefits of reduction in particle size through ball milling. As soon as the data indicated that densities on the order of 90 percent of theoretical could be attained by high-temperature firing, batches of several hundred grams of powder were wet blended for a period of 24 hours and subsequently evaluated for densification characteristics.

Generally, sintering temperatures on the order of 1700 or 1800 C were needed to attain densities near 90 percent of theoretical with powder that was wet milled for 8 hours. Shrinkages were quite high and comparatively non-uniform, i.e., shrinkage was far greater in the radial direction than in the longitudinal direction and pellets were hourglass shaped or tended to be larger in diameter at one end. This behavior was attributed somewhat to the pressing techniques, but powder characteristics were thought to be primarily responsible. This was evident from the number of fissures, blow holes, and, in some cases, raised areas seen on the surface of the pellets which were apparently caused by impurities present in the as-received powders.

In comparison, pellets pressed from the as-received, dry-blended powders attained densities of only 82 and 78 percent of theoretical when sintered at temperatures up to 1800 C. This behavior demonstrated the greater activation of the wet-milled powder and enhanced densification through sintering that can be obtained by particle reduction. An additional and significant observation was the similarity among the surface characteristics of the pellets prepared from the as-received, dry-blended, and wet-milled powders. Further examination of the pellets by standard metallographic techniques showed that the porosity distribution was for the most part quite uniform except for occasional large void areas which appeared to be caused by gas formation from impurities. These voids were generally of less magnitude in the pellets prepared with wet-milled powders. This information, together with the somewhat greater dimensional uniformity of these pellets, suggested that a longer ball-milling time would be of value in enhancing ultimate densification and reducing surface defects. No evidence of metallic impurities was found in any of the microstructures and all specimens appeared to have a fairly equiaxed grain

configuration indicative of a single-phase $\text{NpO}_2\text{-CaO-ZrO}_2$ solid solution. Similarly, there was no indication of the presence of the ZrO_2 monoclinic phase when the specimens were examined with polarized light.

Further reference to Table 6 shows that there was no increase in sintered density from either the use of high densification pressure, i.e., 40,000 psi as compared with 20,000 psi, or the change of sintering atmosphere from pure nitrogen to argon-8 v/o hydrogen. Data pertaining to the densification characteristics of pellets prepared from the large batches of powder milled for 24 hours are also shown. A general increase in density was noted with the longer ball-milling time for all compositions, but the change was more significant in the pellets with the higher NpO_2 content. This trend is more readily seen by comparison of the data pertaining to the 77.22 w/o NpO_2 powder batches where material ball milled for 8 hours achieved a density of only 82.5 percent of theoretical on sintering to 1700 C, while the 24-hour-milled powder treated in the same manner sintered to densities close to the calculated theoretical value. Another quite noticeable change occurred in the shrinkage characteristics of the powder milled for the longer period. The diametral shrinkage of pellets with sintered densities in the range of 90 to 95 percent of theoretical was considerably less than found in earlier work. For example, initial shrinkage values generally fell within the range of 17 to 18 percent when the various powder blends were sintered at about 1700 C for 2 hours. Calculations also indicated that the shrinkage was nonuniform, with the ratio of the diametral to longitudinal change being about 1.1. The trend was similar to that observed for overall densification, i.e., the greatest amount of diametral shrinkage occurred in the 77.22 w/o NpO_2 composition, and the dimensional non-uniformity or degree of hourglass configuration was also greatest in this material.

Evaluation of the sintering characteristics of the 24-hour-milled 15.18 w/o NpO_2 powder showed that hourglassing could be minimized by sintering at 1800 C; however, the densities of these pellets were near 96 percent of theoretical, which was greater than desired in this work. When the sintering temperature was lowered to 1600 C, dimensions of the pellets were generally somewhat irregular, indicative of nonuniform shrinkage within the fired specimens. Although the calculated densities of pellets sintered at 1600 C were very

close to the desired value of 90 percent of theoretical, the best compromise in regard to dimensional stability and appearance was obtained by treatment at 1675 C. Time did not permit the same type of study with other compositions. In any event, the 1675 C sintering temperature was found to be satisfactory for the 28.06 and 48.76 w/o NpO_2 compositions as well. A decision was made to lower the sintering temperature of the 77.22 w/o NpO_2 pellets to 1600 C on consideration of the near theoretical densities attained by firing at the slightly higher temperature of 1675 C.

Throughout the above study, shrinkages were obtained on one or two pellets of a given composition, and these data were then used to calculate the die sizes needed to prepare densified pellets within several thousandths of an inch of the specified mean diameter of 0.3825 inch. Early results established the difficulties associated with an original intent to sinter the pellets to size. Therefore, dry centerless grinding was incorporated into the fabrication process as an additional, but necessary, step to insure uniform clearance between the pellets and cladding wall.

A flow diagram outlining the various process steps utilized in the fabrication of the target pellets is shown in Figure 5. This general scheme was used to prepare six batches* of pellets, as described in Table 7. All pellets were centerless ground to a diameter of 0.383 ± 0.001 inch. The densities shown in Table 7 were obtained on randomly selected pellets. All values were quite close to the mean for the various batches of material. This excellent reproducibility was achieved only through exceedingly close control of all process variables including pressing techniques, heating and cooling rates during sintering, and gas flow through the furnace.

Zirconia Pellet Fabrication

According to specifications, each end of the four target segments composing the two rods required nonfissile zirconia pellets to act as barriers between the hot center of the target columns and the stainless steel components.

* Paragraph 7.2.1 of the Appendix defines a pellet batch as those compacts pressed and sintered under identical conditions in the same furnace cycle.

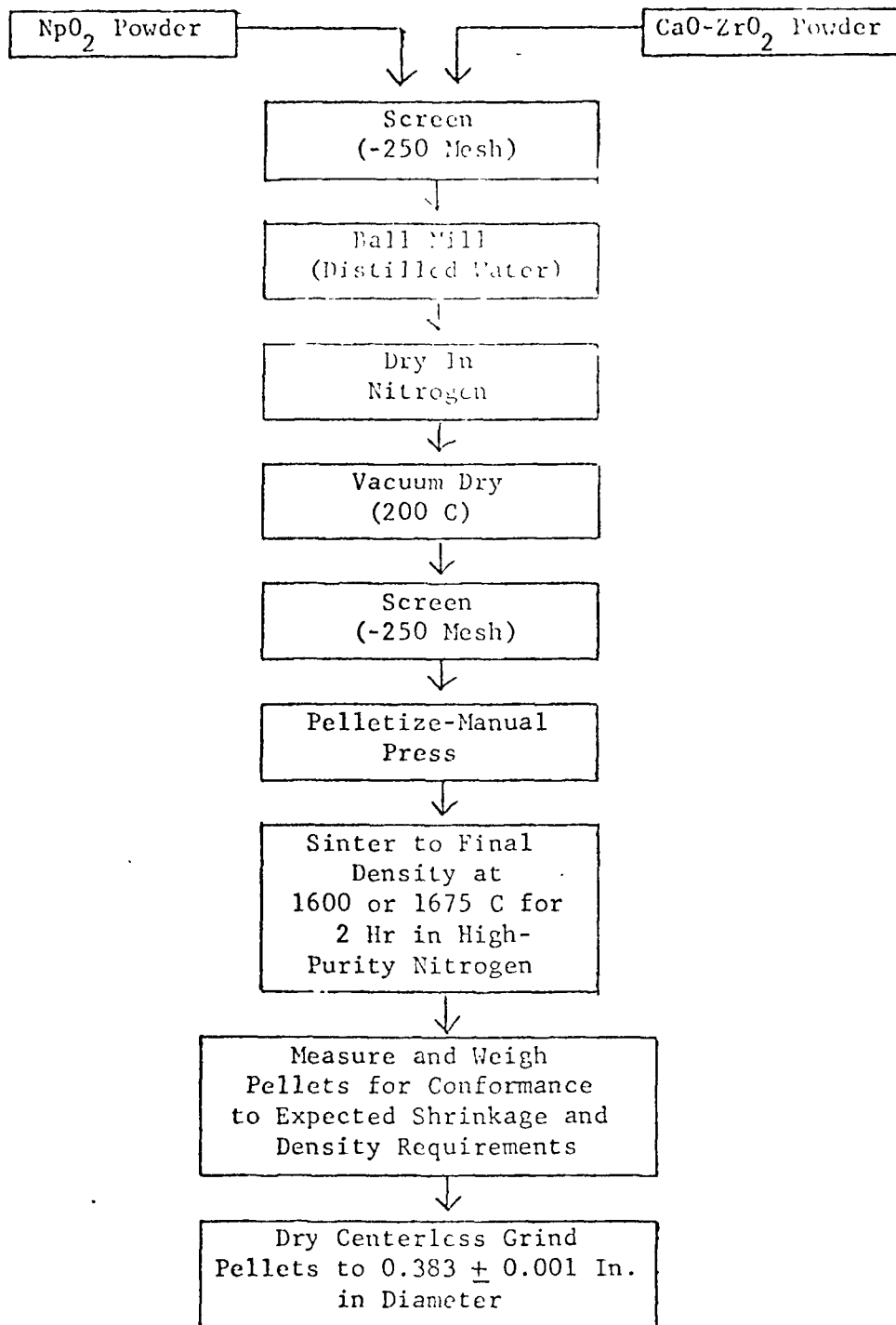


FIGURE 5. PROCESS FLOW DIAGRAM FOR PELLET FABRICATION

TABLE 7. PROCESS PARAMETERS AND DENSITIES OF NpO₂ TARGET PELLETS

Target Segment	Batch Identification	Nominal Composition, w/o NpO ₂	Densification Pressure, psi	Temperature of Nitrogen Sinter, C	Density, ³ g per cm	Density Percent of Theoretical
1A	4	77.22	20,000	1600	8.61	99.0
					8.65	99.4
					8.65	99.4
2A	4	77.22	20,000	1600	8.61	99.0
					8.61	99.0
					8.61	99.0
1B	5	48.76	20,000	1675	6.15	90.0
					6.13	89.7
					6.16	90.0
2B	5	48.76	20,000	1675	6.18	90.4
					6.14	90.0
					6.20	90.6
1C	6	28.06	20,000	1675	5.42	91.6
					5.42	91.6
					5.51	93.0
2C	6	28.06	20,000	1675	5.31	89.7
					5.45	92.1
					5.40	91.3
1D	2	15.18	20,000	1675	5.10	94.0
					5.11	94.0
					5.13	94.6
	1	15.18	20,000	1675	5.12	94.5
					5.13	94.6
					5.08	93.6
2D	3	15.18	20,000	1675	5.03	92.8
					5.04	92.9
					5.12	94.5

Characterized calcia-zirconia powder, obtained for preparation of the target pellets, was also used for this purpose.

Pellets were pressed from the stabilized zirconia powder at a pressure of 60,000 psi and subsequently sintered at 1800 C for 2 hours. Heating and cooling rates ranged between 200 and 300 C per hour. A flow of pure nitrogen was maintained through the furnace during the entire sintering cycle.

Dimensions of the densified pellets were 0.433 to 0.438 inch in diameter by about 0.5 inch long. All pellets were dry centerless ground to a diameter of 0.384 ± 0.001 inch and ends were faced to leave the pellets at their maximum length. Determinations of the density of several pellets gave values ranging between 90 and 93 percent of theoretical.

Pellet Characterization

Chemistry

Two pellets were selected from each batch of material for chemistry studies. One of these was used for immediate analysis of total gas, moisture, spectrographic impurities, and major constituents NpO_2 , CaO , and ZrO_2 . The other pellet was stored as an archive sample to be available if needed during examination of the targets after irradiation. Specifications also called for the determination of the typical hydrogen content of the gas released from the pellets and measurement of the chlorine content of a typical 15.18 w/o NpO_2 pellet. The latter analyses were to serve as backup data if total gas and moisture approached or exceeded specifications.

Gas collection and moisture analysis were conducted in low-volume glass apparatus that had been thoroughly outgassed by heating and evacuation. The apparatus was divided into two sections by appropriate valves, with the lower section containing the pellet and moisture probe, and the upper section a pressure gage and collection bulb. The analytical procedure consisted of heating a pellet to 1000 C in a system previously evacuated to 10^{-6} torr with a mercury diffusion pump, followed by immediate collection and analysis of all evolved gas. Each pellet was held at temperature for 30 minutes. The moisture

content of the gas was monitored continually by an EMF probe*, and the amount of total gas was obtained by measurement of the pressure change in the calibrated volume portion of the apparatus.

The results of these analyses are given in Table 8. In all cases, the total gas was far less than the 0.05 cm^3 per g specified for the target pellets, and the moisture content was exceedingly low at less than 1 ppm. Although samples of evolved gas were taken from all pellets, only one was analyzed, as per previous agreement with CYAPC and SNE. This approach seemed quite reasonable in view of the fact that all pellets received the same prior treatment and the total gas and moisture contents were generally very low. The values obtained from the mass spectrometric analysis of the gas from a 77.22 w/o NpO_2 pellet are given in Table 9. As can be seen, the offgas was composed primarily of nitrogen and carbon monoxide. Hydrogen, which was to be held to <10 ppm, was present in an insignificant amount.

By analogy in processing, it can be assumed that the distribution of the various species present in the evolved gas did not change appreciably with composition. It is interesting to note that conversion of the percentage moisture in the gases to ppm by weight yielded values ranging between 0.9 and 0.07, which is in relatively close agreement with the results obtained by use of the electrolytic probe. This correlation essentially substantiated earlier predictions that very little hydrogen and moisture would be found in the pellets. In addition, since the total amounts of evolved gas were all quite low, one can be quite confident that there was no introduction of impurities into a particular pellet batch that would have gone undetected by the procedures used in these analyses.

A separate determination of the chlorine content of the 15.18 w/o NpO_2 composition was conducted to obtain some indication of the amount of this impurity present after processing. A pellet of the high ZrO_2 composition was chosen for analysis because of the high chlorine content of the as-received calcia-stabilized zirconia powder. The analytical technique employed for the measurement involved pyrohydrolysis by passage of a moisture-saturated argon

* Panametrics hydrometer, Model 1000, Waltham, Massachusetts.

TABLE 8. TOTAL GAS RELEASE AND MOISTURE CONTENTS
OF SELECTED NpO_2 PELLETS

Sample Designation	Nominal Composition w/o NpO_2	Gas Volume, cm^3 per g (STP)	H_2O , ppm
22	15 (Batch 1)	0.0022	<0.38
36	15 (Batch 1)	0.0079	0.08
34	15 (Batch 2)	0.0050	<0.10
38	15 (Batch 3)	0.0280	<0.10
28	28	0.0270	0.05
30	48	0.0240	<0.10
21	77	0.0150	0.10

TABLE 9. RESULTS OF MASS SPECTROMETRIC ANALYSIS
OF GAS FROM 77 w/o NpO_2 PELLETT

Species	Amount, v/o
CO_2	0.98
H_2O	0.60
O_2	0.32
CO	57.6
N_2	25.6
H_2	14.0
C_2H_6	0.59
CH_4	0.16
SO_2	<0.02
Unknown component	0.27

gas stream over a crushed pellet while it was being heated at 950 C. The gas was passed through a solution of potassium acetate and acetic acid which was treated with mercuric thiocyanate in ethanol containing ferric alum, and this solution was then read spectrophotometrically. A value of about 8 ppm chlorine was obtained by use of this analytical method. This result showed that chlorine was removed in processing and was within the limit of 10 ppm established in the target specification. Although other batches of pellets were not analyzed for chlorine, from all indications, these compositions would contain far less of this impurity than the 15.18 w/o NpO_2 material.

After completion of the total gas analysis, the pellets were broken and divided to obtain sections for general spectrographic analysis and metallography. Sections for spectrographic analysis were specifically taken from the surface of the pellets in an effort to obtain analyses that would be representative of the highest levels of impurities that could be expected in these materials. As seen from the results of this work, shown in Table 10, the impurities present in various material batches were of little consequence, aside from those of iron, magnesium, manganese, chromium, and silicon. Generally acceptable impurity levels for UO_2 pellets are given in this table for comparison.

Analysis of the constituent elements of the pellets was performed according to the following procedures. Duplicate 0.3 g samples of ground pellets were dissolved in HNO_3 -HF solutions. For neptunium analysis, these solutions were evaporated and fumed twice with sulfuric acid. The resulting sulfuric acid solution was passed through a Jones reductor and titrated with ceric ammonium sulfate. For zirconium and calcium analysis, the neptunium was removed from the nitric acid solution by absorption on a Dowex 1 resin column. Zirconium was precipitated as $\text{Zr}_2\text{P}_2\text{O}_7$ by addition of diammonium phosphate to the eluate, and converted to ZrO_2 by ignition at 1000 C. Calcium was precipitated as oxalate from the supernatant solution, filtered and redissolved in dilute sulfuric acid, and then titrated with a standard KMnO_4 solution. The results of these analyses are presented in Table 11.

Except for the 70 percent NpO_2 composition, the mass balance values for these samples are satisfactory, although somewhat narrower precision limits might have been expected. There is an obvious discrepancy between nominal and measured compositions of the order of 10 percent at the higher levels of

TABLE 10. IMPURITIES PRESENT IN SELECTED PELLETS FROM VARIOUS BATCHES OF MATERIAL AFTER SINTERING

Element	Impurity Content, ppm							UO ₂
	Sample 22, 15 w/o NpO ₂ (Batch 1) ²	Sample 36, 15 w/o NpO ₂ (Batch 1) ²	Sample 34, 15 w/o NpO ₂ (Batch 2) ²	Sample 38, 15 w/o NpO ₂ (Batch 3) ²	Sample 28, 28 w/o NpO ₂	Sample 31, 48 w/o NpO ₂	Sample 21 77 w/o NpO ₂	
Bi	<2	<2	<2	<2	<2	<2	<2	2
B	<0.3	<0.3	<0.3	<0.3	<0.3	<0.3	<0.3	1
Cd	<5	<5	<5	<5	<5	<5	<5	1.0
Cr	80	95	95	95	85	80	80	500.0
Cu	11	3	5	11	3	2	2	25.0
Fe	375	280	520 ^(a)	700 ^(a)	375	125	220	500.0
Li	<0.5	<0.5	<0.5	<0.5	<0.5	<0.5	<0.5	0.1
Mg	200	200	225	200	200	200	150	50.0
Mn	75	95	50	55	75	12	75	10.0
Mo	<6	<6	<11	<11	<6	<11	<6	150.0
Ni	8	<8	25	35	8	<12	<8	300.0
P	<210	<210	<210	<210	<210	<210	<210	-
Pb	40	40	<4	<4	40	<4	<40	20.0
K	<125	<125	<250	<250	<125	<250	<125	-
Si	110	70	300	300	60	80	<34	500.0
Ag	<0.1	<0.1	<0.1	<0.1	<0.1	<0.1	<0.1	0.3
Na	80	50	<40	<40	80	<40	160	-
Sn	20	20	10	20	20	10	20	5.0
V	<11	<11	<11	<11	<11	<11	<11	1.0
Zn	<50	<50	<50	<50	<50	<50	<50	20.0

(a) Contaminated with iron during sampling

TABLE 11. SUMMARY OF MAJOR OXIDE CONSTITUENT ANALYSES
FOR THE TARGET PELLETS

Nominal Composition, w/o NpO_2	Batch	Sample	NpO_2 Content, w/o	ZrO_2 Content, w/o	CaO Content, w/o	Mass Balance, w/o
15.18	1	22 ₁	15.20	71.65	13.34	
		22 ₂	14.35	70.64	12.93	
15.18	1	36 ₁	14.94	71.28	11.88	
		36 ₂	14.94	68.46	12.30	
Batch 1	Average		14.86±0.25	70.51±1.0	12.61±0.52	97.98±1.17
15.18	2	34 ₁	14.98	72.49	12.75	
		34 ₂	14.98	74.02	12.65	
Batch 2	Average		14.98±	73.25±0.77	12.70±0.05	100.93±0.77
15.18	3	38 ₁	14.91	71.55	11.79	
		38 ₂	14.90	73.51	11.71	
Batch 3	Average		14.91±0.05	72.53±0.98	11.75±0.04	99.19±0.98
28.06	6	28 ₁	25.34	62.06	9.61	
		28 ₂	25.65	65.04	10.01	
Batch 6	Average		25.30±0.05	63.55±1.49	9.81±0.2	98.66±1.50
48.76	5	30 ₁	43.05	48.07	8.44	
		30 ₂	42.96	47.75	8.43	
Batch 5	Average		43.01±0.04	47.91±0.16	8.44±0.05	99.36±0.17
77.22	4	21 ₁	74.69	20.48	4.69	
		21 ₂	68.21	20.67	4.69	
		21 ₃	69.26	-	-	
		21 ₄	67.92	-	-	
Batch 4	Average		70.02±2.34	20.56±0.08	4.69±	95.27±2.34

neptunium content. Some slight zirconium gain in the powder mix might have occurred during ball milling. Considering the difficulty in dissolving the samples, however, it seemed more realistic to ascribe the discrepancy in neptunium content to incomplete dissolution or incomplete valence state adjustment. Accordingly, a second series of samples was analyzed for neptunium, taking drastic measures to dissolve the samples (6NHC1-1NHF), and carrying out the ultimate analysis by controlled potential coulometry. The results of these analyses are reported in Table 11A, and these data are used in the remainder of the program to designate the neptunium content of the specimens.

TABLE 11A. NEPTUNIUM CONTENT OF TARGET PELLETS

Nominal Composition, w/o NpO ₂	Batch	Sample	Actual Composition, w/o NpO ₂	<u>Average</u>
15.18	1	22 ₁	14.61	14.65 ± 0.04
		22 ₂	14.68	
28.06	6	17 ₁	25.55	25.53 ± 0.02
		17 ₂	25.50	
48.76	5	31 ₁	44.46	44.47 ± 0.01
		31 ₂	44.47	
77.22	4	32 ₁	71.8	71.69 ± 0.10
		32 ₂	71.5	
		32 ₃	71.6	
		32 ₄	71.8	
		32 ₅	71.5	
		32 ₆	71.8	

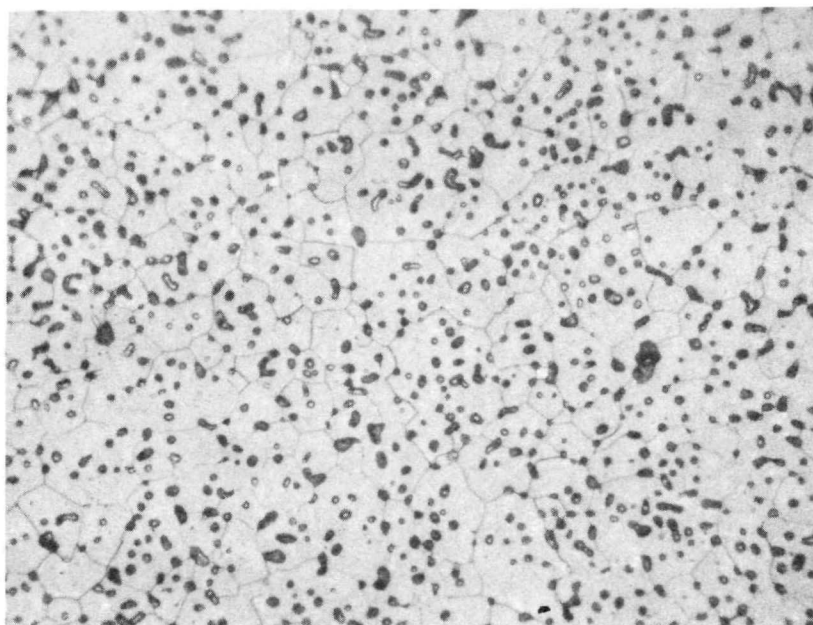
Metallographic Examination

Standard metallographic procedures were used to mount, grind, and polish samples from pellets designated for chemistry studies. An attempt was made to obtain longitudinal sections for examination, but, in most cases, the pellets fractured into several pieces which were not truly representative of this configuration. Microstructures of the various pellet sections are shown in Figures 6 through 11. A slight chemical attack of the pore areas was noted when the samples were etched to obtain grain structure. This behavior should be taken into account when the pore areas are compared with apparent void volumes for each composition, easily derived from the density values given in Table 7. Offhand, there appears to be a close correlation between the observed porosity and the amounts thought to exist from the density calculations, i.e., the densities of 90 to 94 percent of theoretical are consistent with the microstructures. The very high densities of 99 percent of theoretical (see Table 7) determined for the 71.69 w/o NpO_2 pellets were verified by the microstructure of this material seen in Figure 11. Only a few pores present at the triple points of the grain boundaries are in evidence.

The grain size for various batches of pellets was quite uniform, considering the wide range of compositions prepared. Average values determined from the photomicrographs varied from 8 to 10μ . This factor, in conjunction with the uniformity of observed porosity in all specimens, pointed to the conclusion that the distribution of the neptunia and stabilized zirconia was homogeneous.

Autoradiography

The procedure utilized for autoradiography was one developed for routine examination of plutonium-containing material. These checks were conducted on each of the metallographic specimens to obtain a positive record of the uniform distribution of the component materials and as a necessary criterion to comply with the pellet specifications. As can be seen in Appendix A, areas with neptunia concentrations of greater than 200μ were unacceptable.

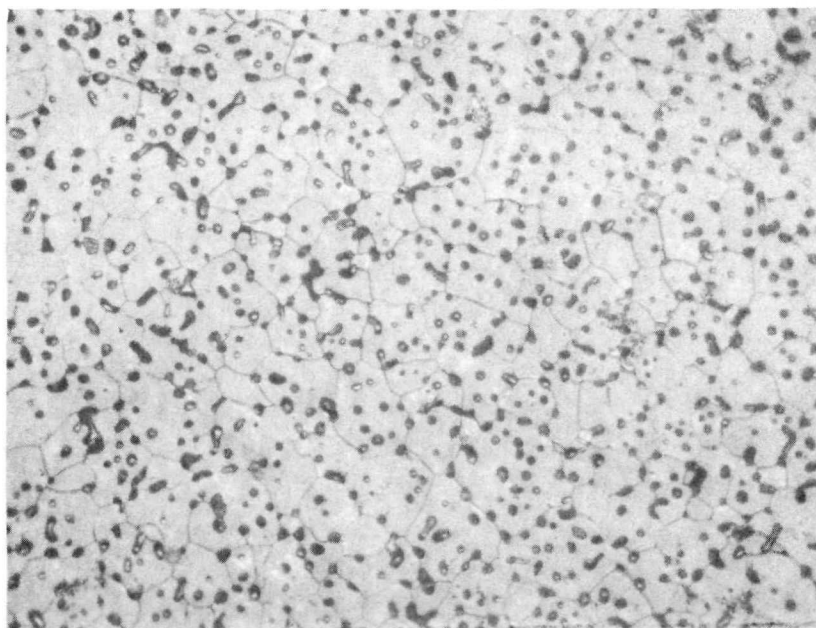


500X

Etched

PL8736

FIGURE 6. TYPICAL MICROSTRUCTURE OF 14.65 w/o NpO_2 COMPOSITION AFTER SINTERING AT 1675 C FOR 2 HR (PELLET BATCH 1)

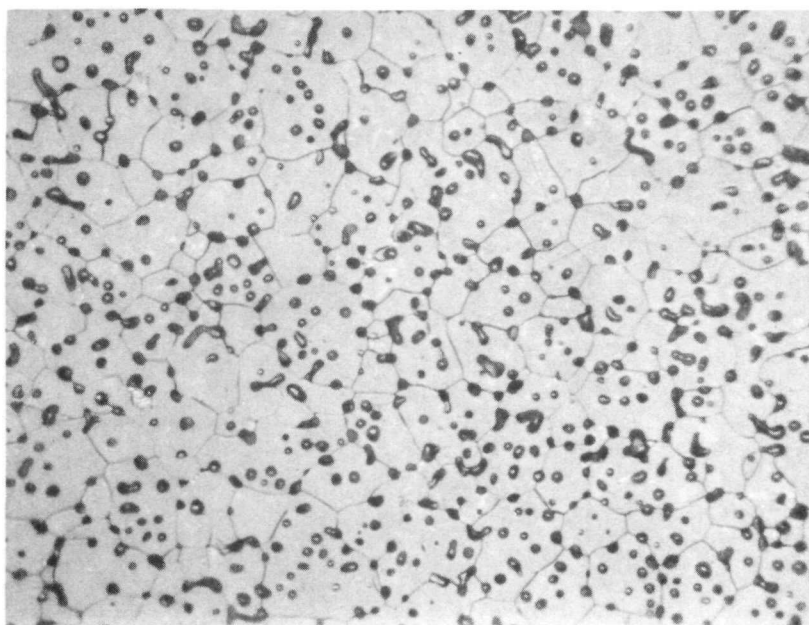


500X

Etched

PL8749

FIGURE 7. MICROSTRUCTURE OF TYPICAL PELLET FROM BATCH 2 CONTAINING NOMINAL 15.18 w/o NpO_2

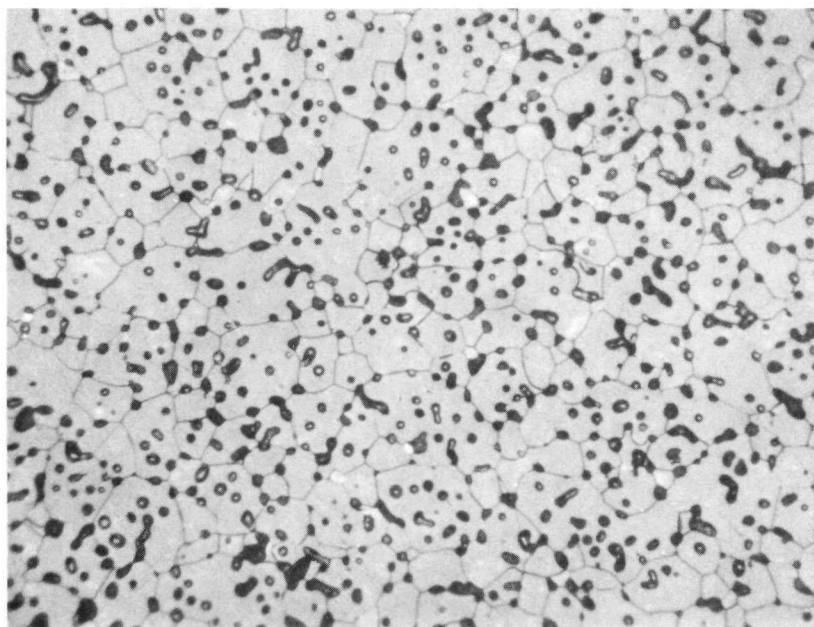


500X

Etched

PL8753

FIGURE 8. MICROSTRUCTURE OF TYPICAL PELLET FROM BATCH 3 CONTAINING NOMINAL 15.18 w/o NpO_2

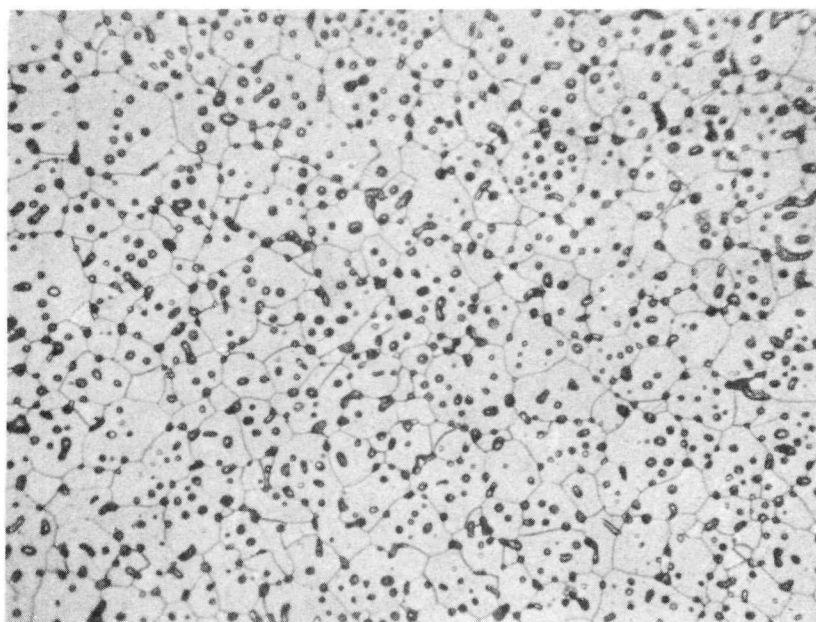


500X

Etched

PL8741

FIGURE 9. MICROSTRUCTURE OF 25.53 w/o NpO_2 COMPOSITION BATCH (PELLET BATCH 6) AFTER SINTERING AT 1675 C FOR 2 HR

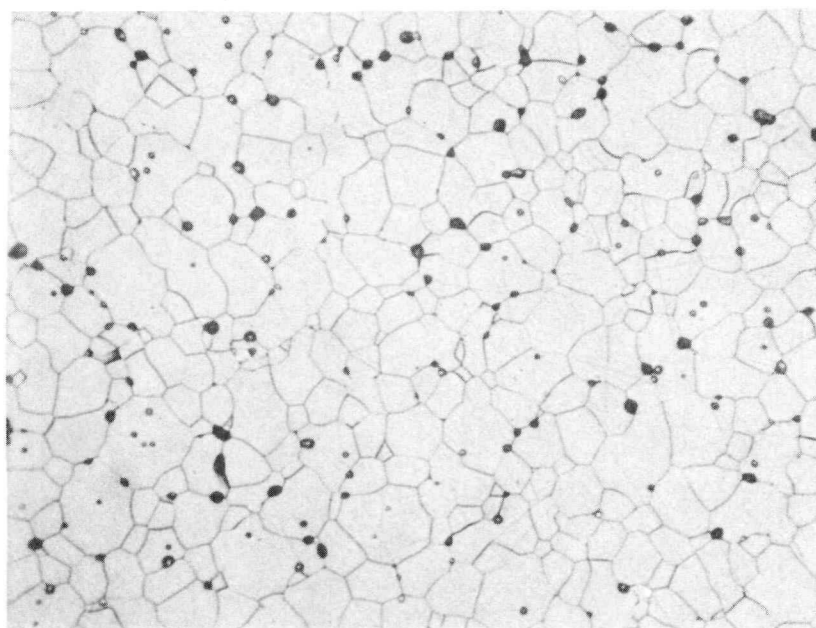


500X

Etched

PL8745

FIGURE 10. MICROSTRUCTURE OF 44.47 w/o NpO_2 COMPOSITION (PELLET BATCH 5) AFTER SINTERING AT 1675 C FOR 2 HR



500X

Etched

PL8731

FIGURE 11. TYPICAL MICROSTRUCTURE OF 71.69 w/o NpO_2 COMPOSITION (PELLET BATCH 4) AFTER SINTERING AT 1600 C FOR 2 HR

Note high density typified by absence of large pore volume (black areas).

The examination technique consisted of placing the polished and cleaned surface of the metallographic samples in contact with a very fine grain photographic film* in total darkness. To prevent alpha contamination of the film, a thin sheet, <0.001 inch of polyester** was placed over the specimen surface. Previous work showed that this thin layer of polyester has very little effect on alpha particle resolution. All samples were weighted throughout the time of exposure to maintain intimate contact of the polished surface with the polyester and film. Exposure periods ranged from 20 to 30 minutes for all compositions, with the shorter time giving the best results for the specimens containing the highest concentration of neptunia.

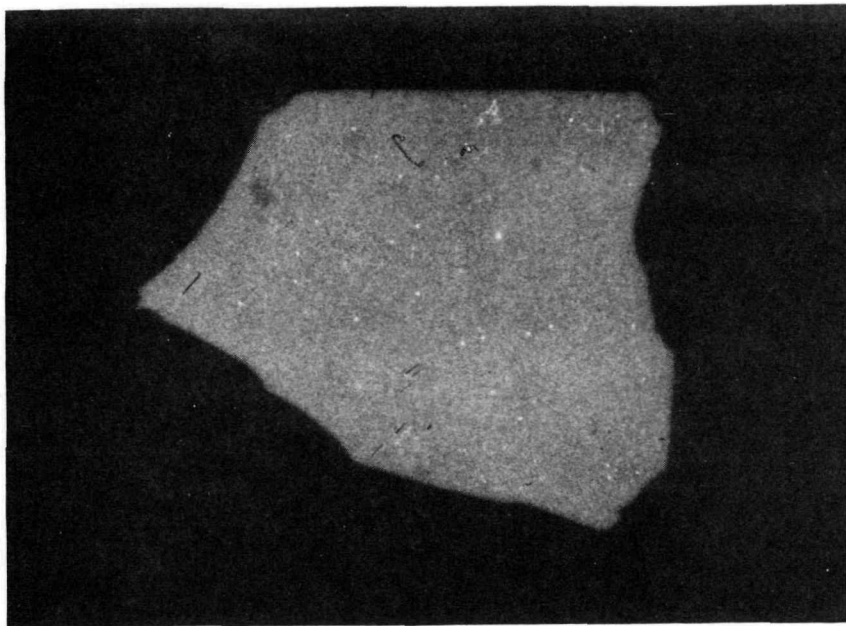
Negatives produced from the developed film were enlarged eight times to obtain the autoradiographic prints shown in Figures 12a through 12f. No significant dark areas or variations in contrast which would indicate a non-uniform distribution of neptunia were found on any of these prints. In several instances, very small light areas can be seen, which are attributed to incomplete removal of plutonium particles from the specimen surface during cleaning. Striations on the autoradiograph of the 44.47 w/o neptunia sample (Figure 12e) are scratches made during placement or removal of the sample from the film, since an almost identical exposure showed the same type of marks on the opposite end. Furthermore, the autoradiograph of the 71.69 w/o neptunia sample (Figure 12f) shows a dark curlicue emanating from an apparent imperfection on the surface, which is probably a remnant from the cloth used for cleaning. The obvious sharp delineation of surface imperfections is a good indication of the resolution of the technique. Therefore, these autoradiographs generally verify the metallographic observations, and are further evidence of the homogeneous nature of all the pellets.

Property Measurements

As part of the overall evaluation of the pellets, an effort was made to determine the thermal expansion characteristics of the 14.65 w/o NpO_2

* Kodak contrast process Ortho film.

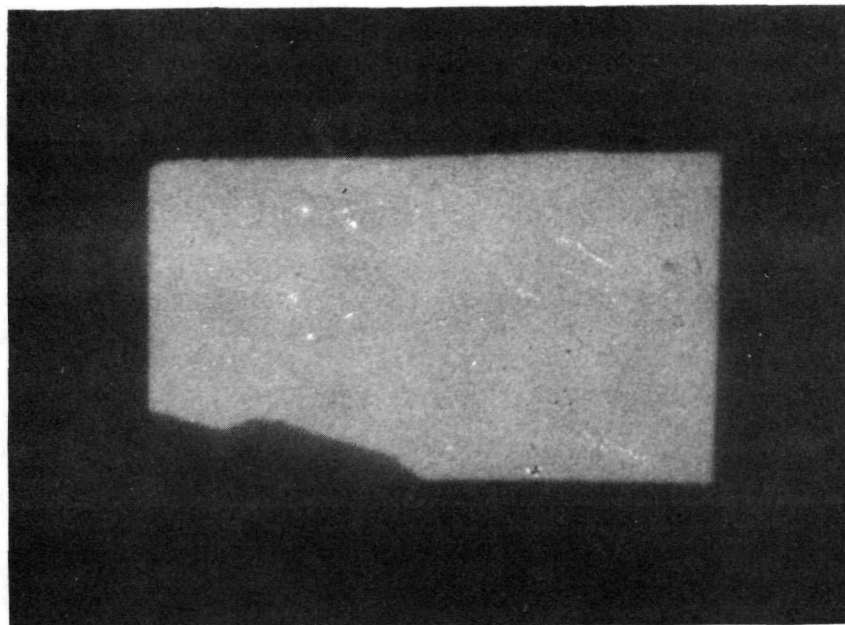
** Melinex polyester film, Type S.



8X

PL8869

a. 14.65 w/o NpO₂ (Batch 1)

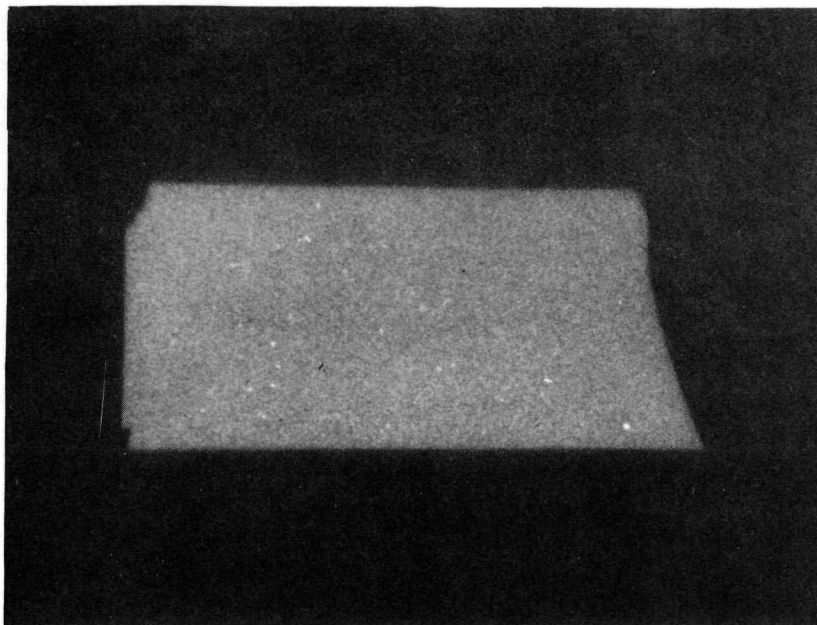


8X

PL8866

b. Nominal 15.18 w/o NpO₂ (Batch 2)

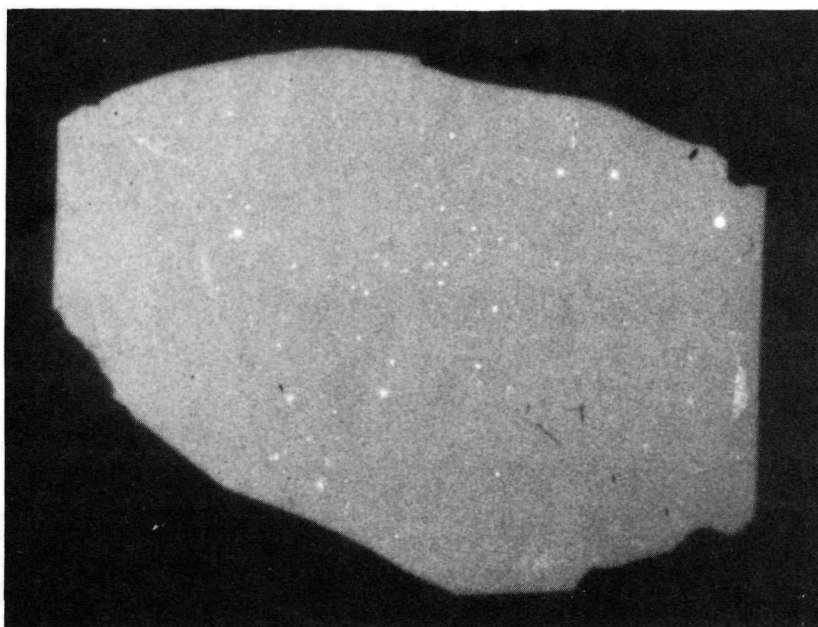
FIGURE 12. AUTORADIOGRAPHS OF VARIOUS METALLOGRAPHIC SPECIMENS



8X

PL8871

c. Nominal 15.18 w/o NpO_2 (Batch 3)

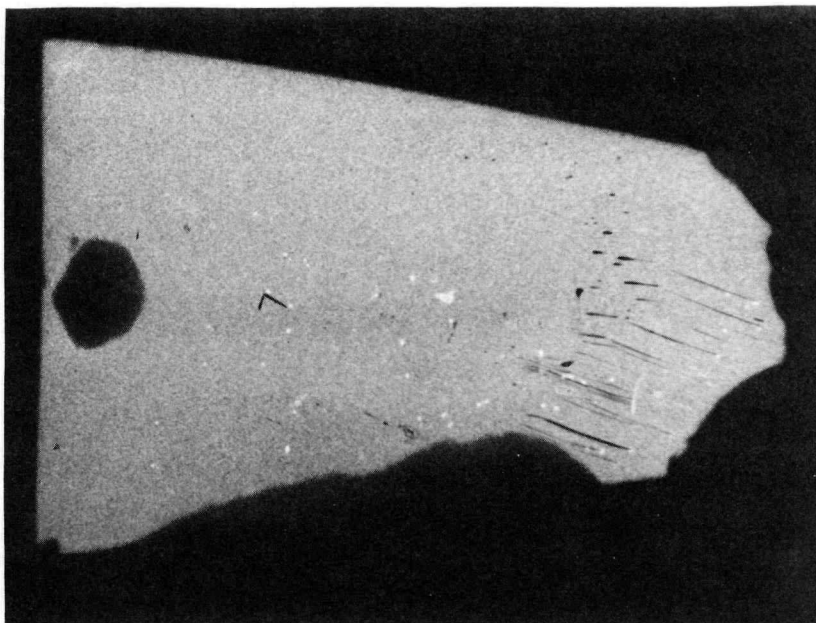


8X

PL8863

d. 25.53 w/o NpO_2

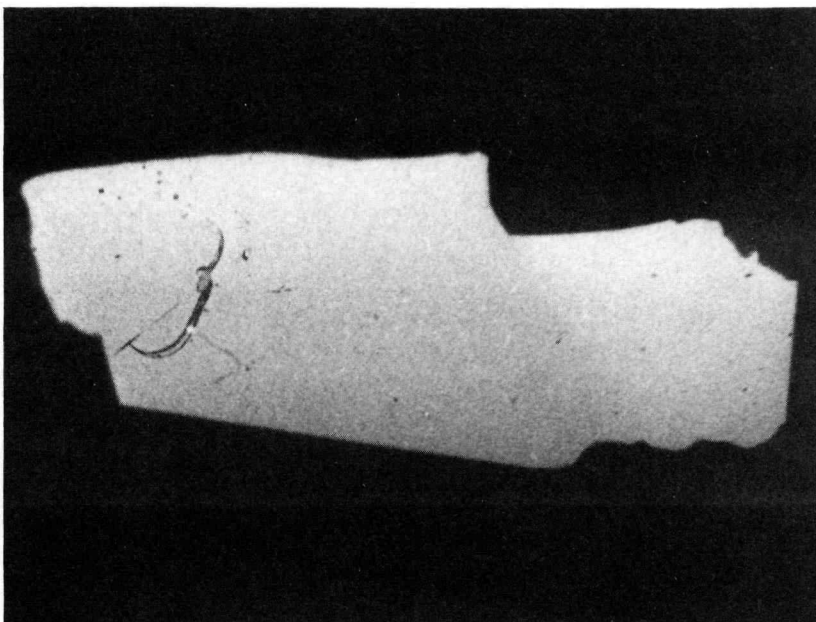
FIGURE 12. (Continued)



8X

PL8864

e. 44.47 w/o NpO_2



8X

PL8858

f. 71.69 w/o NpO_2

FIGURE 12. (Continued)

material and the thermal cycling behavior of all compositions. These measurements, although not intended to be thorough investigations, were considered to be the minimum backup data needed to provide some assurance that design parameters were correct and the targets would perform as expected after placement in the reactor.

Thermal Expansion

The 14.65 w/o NpO_2 composition was selected for measurement because the possibility of a phase transformation was highest in this material and deviations from design values would have the greatest effect, since these pellets make up the longest length target specimen of approximately 43 inches. An existing recording dilatometer was used for the measurement. This apparatus was calibrated with a high-purity alumina specimen prior to the run with the unknown. The specimen consisted of two pellets stacked to give an overall length of about 1 inch. These pellets were slowly heated to 1000 C in a period of about 12 hours. Flowing, high-purity nitrogen was used as a protective atmosphere throughout the time of measurement.

The thermal expansion curve depicting dilation as a function of temperature is shown in Figure 13. No discontinuities were observed in the temperature range studied. The linear thermal expansion coefficient of 8.2×10^{-6} per C (4.56×10^{-6} per F) calculated from these data was somewhat less than expected based on an assumed behavior for NpO_2 similar to that of PuO_2 and existing data for ZrO_2 . In any case, this measurement was satisfactory to show that design values were conservative for this and, by inference, the other target segments.

Thermal Cycling

Fairly early in the program, it was apparent that some degree of testing would be required to verify the thermal shock resistance of the pellets under simulated reactor conditions. Compositions thought to have the least resistance were those containing the greatest amount of zirconium dioxide, a material known to have excellent insulating properties and generally poor

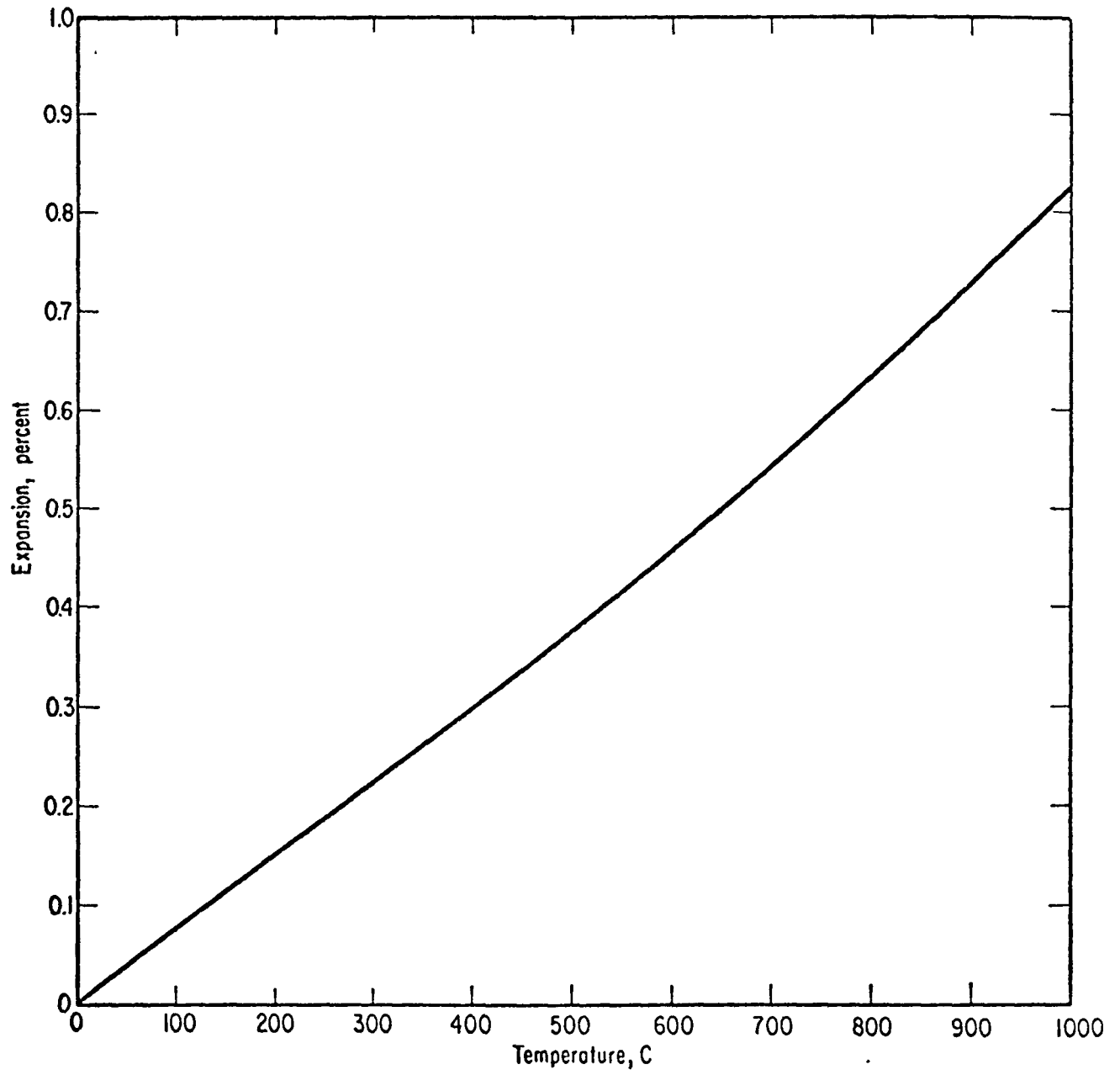


FIGURE 13. THERMAL EXPANSION CURVE OF THE 14.65 w/o NpO_2 MATERIAL

thermal shock behavior. Neptunia was assumed to behave similarly to urania, but the lack of properties data on this material made its behavior in the reactor an unknown. The possibility of pellet fracture and ratcheting of the cladding prompted considerable thought directed to cycling tests. Further incentive to conduct these tests was provided by the inadvertent rapid cooling of a furnace from high temperatures during one of the initial sintering runs which resulted in fracture of an entire batch of 14.65 w/o NpO_2 pellets.

A decision was made at this time to conduct a limited series of thermal cycling experiments that would simulate cooling of the pellets during a reactor scram, the most rapid transient expected throughout the irradiation period. To obtain a series of curves approximating this condition, SNE conducted a computer analysis which determined the rates of cooling of various radial nodes for each different target composition. The results of this work are given in the SNE report describing their experimental and analytical program⁽³⁾. An attempt was then made at BCL to approximate the curves for the centerline transients.

Three thermal cycles consisting of a slow heatup, a short hold, and rapid cooling were performed on the various different target pellets. Tests were performed in a low-heat-capacity furnace to facilitate cooling. In addition, the furnace was purged with helium at a high flow rate the instant that power to the furnace was turned off. This procedure gave quite rapid cooling, but, even under these conditions, the actual curves obtained on the pellets deviated appreciably from the calculated ones, as may be seen in Figure 14. It should be noted that the maximum temperature reached in the various tests increased with the neptunia content of the pellets. Also, all three thermal cycles were identical; therefore, the curves given in Figure 14 are a composite of the typical behavior observed for specific compositions. Pellets containing 14.65 w/o NpO_2 (Segment D) were not cyclic tested, since calculations indicated that the maximum center temperature of the target segment loaded with this material would be only several hundred degrees Fahrenheit above the ambient water temperature of the reactor.

Although the cooling curves obtained on the pellets are significantly different from the calculated centerline curves, it can be rationalized that these tests were as severe as the cyclic changes actually expected for the

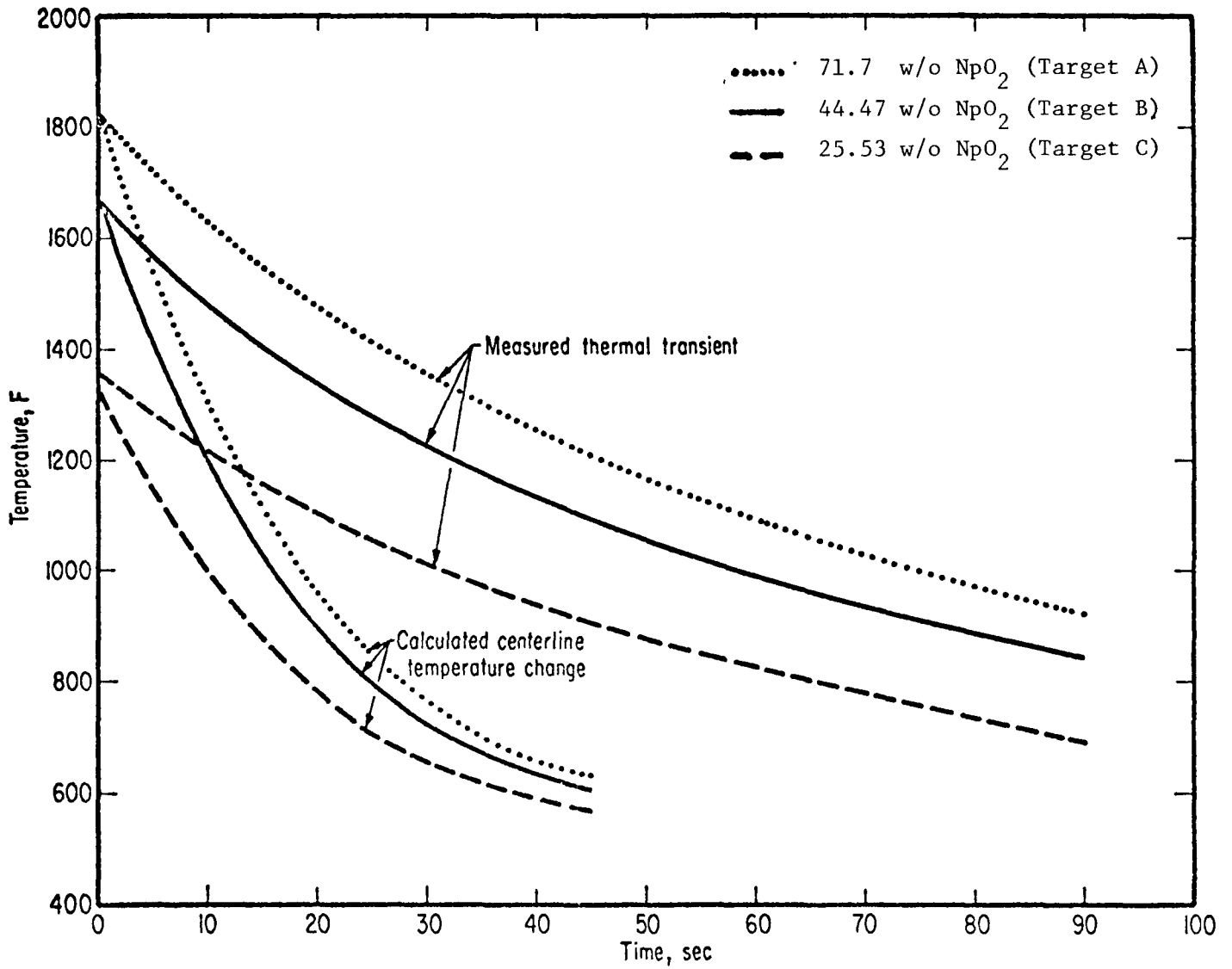


FIGURE 14. COMPARISON OF CALCULATED AND MEASURED TEMPERATURE CYCLES OF VARIOUS NpO_2 TARGET COMPOSITIONS

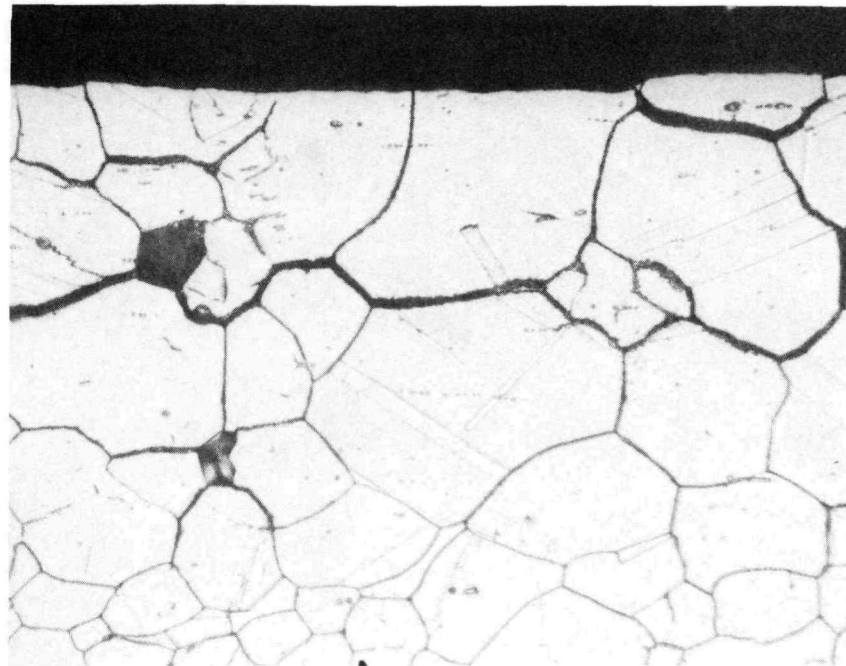
average radial node of the targets and, hence, are satisfactory for the purpose intended. In fact, the test performed may be overly severe because cooling was initiated from temperatures considerably higher than those calculated for the midradial nodes.

All pellets were examined closely for cracks after testing, and in no case was a pellet changed from its original appearance. These studies showed that the pellets could withstand the severest transient expected during irradiation, a reactor scram.

Compatibility Testing

Demonstration of the long-term compatibility of the pellets with the Type 304 stainless steel cladding under conditions far exceeding those expected within the reactor was required as part of the testing phase of the program. However, no definite criteria existed as to the best conditions for these tests, so a temperature of 500 C (932 F) for a period of 1 month was chosen as a satisfactory goal. This decision was based primarily on the choice of a reasonably high testing temperature, which would be, in effect, an accelerated test equivalent to a 1-year treatment of the cladding at the normal reactor operating temperature of 315 C (600 F). In addition, UO_2 and PuO_2 are known to have no solid-state interaction with stainless steel at 500 C; therefore, identical behavior for the NpO_2 target pellets would demonstrate the similarity of this material with common fuels.

One pellet of each target composition was encapsulated under conditions identical to those described later for the target rods, i.e., in helium, by TIG techniques. After heat treatment, the capsules were examined in the longitudinal direction for diffusion interaction between the pellets and the cladding wall. No evidence of a solid-state reaction was found on any of the capsules; however, close examination of the cladding revealed areas of grain pullout, which, in some instances, affected 20 percent of the cladding wall. A typical microstructure of an affected area is shown in Figure 15. Disturbed areas were found in all of the capsules, but there was no indication of a systematic change in the depth of penetration with pellet composition.



250X

Etched

PL8685

FIGURE 15. TYPICAL APPEARANCE OF LONGITUDINAL SECTION FROM TYPE 304 STAINLESS STEEL CAPSULE WHICH CONTAINED PELLET AFTER HEAT TREATMENT AT 500 C (932 F) FOR 1 MONTH

Note grain pullout (black areas) and grain separation (black outline) near the surface of the cladding.

At this point in the program, the seriousness of the situation was assessed and steps were taken to obtain as much information as possible in the short period of several weeks available before a final decision was mandatory in regard to loading of the target rods into the reactor during the spring refueling operation. Specifically, it was decided to section all of the metallographically mounted cladding specimens in the transverse direction to obtain a separate view of the phenomenon, which might aid interpretation. One cladding specimen with the most severe grain pullout was repolished and examined on the electron microprobe. Finally, additional capsules were made up and heat treated according to the conditions listed in Table 12. In addition, several BCL experts on stainless corrosion were consulted as to the possible significance of the problem and rate of attack expected at the somewhat lower temperatures (600 F) of actual reactor operation. The general consensus of opinion was that the phenomenon would not occur at 600 F even under prolonged periods of more than a year.

TABLE 12. SUMMARY OF HEAT-TREATMENT CONDITIONS FOR THE SECOND GROUP OF TEST CAPSULES

Capsule Identification	Description	Heat Treatment	
		Temperature	Time, days
1	Blank (helium filled)	500 C (932 F)	12
2	14.65 w/o NpO ₂ pellet	315 C (600 F)	10
3	Al ₂ O ₃ grinding medium (pieces)	500 C (932 F)	12
4	NpO ₂ pellet (pieces)	500 C (932 F)	12
5	CaO-stabilized ZrO ₂ pellet	500 C (932 F)	9
6	UO ₂ pellet	500 C (932 F)	9

Examination of the cladding sections mounted in the transverse direction confirmed the fact that the pullout was localized to a number of areas on the inner surface of the cladding. Electron microprobe examination showed that there was no penetration of neptunium, calcium, or zirconium into the cladding. The specimen was also checked for other impurities that could have inadvertently been present on the surface of the pellets, e.g., aluminum, silicon, manganese, sulfur, and chlorine. None were found. Although this examination was inconclusive as to the cause of grain pullout, it unquestionably verified the absence of diffusional attack of the cladding, which was the initial goal of these studies.

Further efforts were directed toward the metallographic examination of the capsules assembled and heat treated as indicated in Table 12. Since the heat treatment was substantially shorter, significant changes in the cladding were not expected. However, by this time, there was a strong indication that the grain pullout was related to sensitization of the stainless steel (precipitation of chromium carbides at the grain boundaries) and somehow tied to the numerous inclusions (see Figures 3 and 4) present in certain sections of the cladding material. Based on this assumption, the type of grain structure and grain size present after heat treatment were noted and compared with those found initially as a means of obtaining some indication of a change in the stainless steel that could be related to carbide precipitation.

Pullout to the extent seen previously was not detected in any of the capsules from this group, but a blank capsule containing only pure helium and another containing the UO_2 pellet exhibited very slight grain separation in some areas, forming what appeared to be the initial stages of the process. Grains in these and some of the other stainless steel capsules heat treated at 500 C (932 F) were more equiaxed and the etchant attack produced a fairly clear delineation of the grain boundaries. In comparison, the grains of the capsule containing the 14.65 w/o NpO_2 pellet remained unchanged after the heat treatment at 600 F. No attack of the cladding was seen in any of the capsules, including those containing pure NpO_2 , pure ZrO_2 (calcia stabilized), and the alumina bonding medium. Based on these results, the pellet gas analyses, and discussions with representatives from SNS, AEC, SNE, and CYAPC, a decision was made to proceed with the irradiation of the NpO_2 target rods.

Encapsulation and Quality Assurance

As a necessary part of the project, all work from this point forward was conducted according to written quality assurance procedures to insure proper assembly and checking of the target rod segments. This phase of the effort included construction of a welding alignment bench, determination of welding parameters through prequalification testing, weld qualification, and writeup of procedures for assembly, welding, decontamination, visual inspection, helium leak testing, and radiography. These procedures were then submitted to SNE for approval prior to actual conduct of the various operations.

Weld Qualification

Requirements for the alignment of the assembled segmented target rods were such that only a few thousandths of an inch deviation from the center axis could be tolerated for the attachment of the end plugs to the cladding tubing. In order to meet this specification, a TIG welding unit was attached to an optical bench, which was bolted to a surface-ground steel channel, as shown in Figure 16. With this welder design, the electrode revolves around the rod, which is held stationary in the alignment fixtures. The entire assembly, including the fixtures for holding the cladding tube and end fitting, was aligned within 0.0015 inch over the span of the optical bench.

Additional specifications pertaining to welding techniques were (1) less than a 0.0015-inch rise on the weld zone and (2) positively no abrasion of the weld. These conditions, which are quite strict for normal water reactor fuel pins, were imposed to guarantee the proper water flow through the thimbles containing the target assemblies and to prevent generation of cracks or stress concentration after welding.

Parameters for welding, i.e., the best distance of the electrode to the piece, power setting, and rotational velocity of the electrode, were established through trials with appropriately machined end fittings and shortened tube sections. Each weld was sectioned and examined by standard metallographic techniques to determine the amount of penetration obtained with the power and rotational variations. Although the optimum weld parameters were quickly

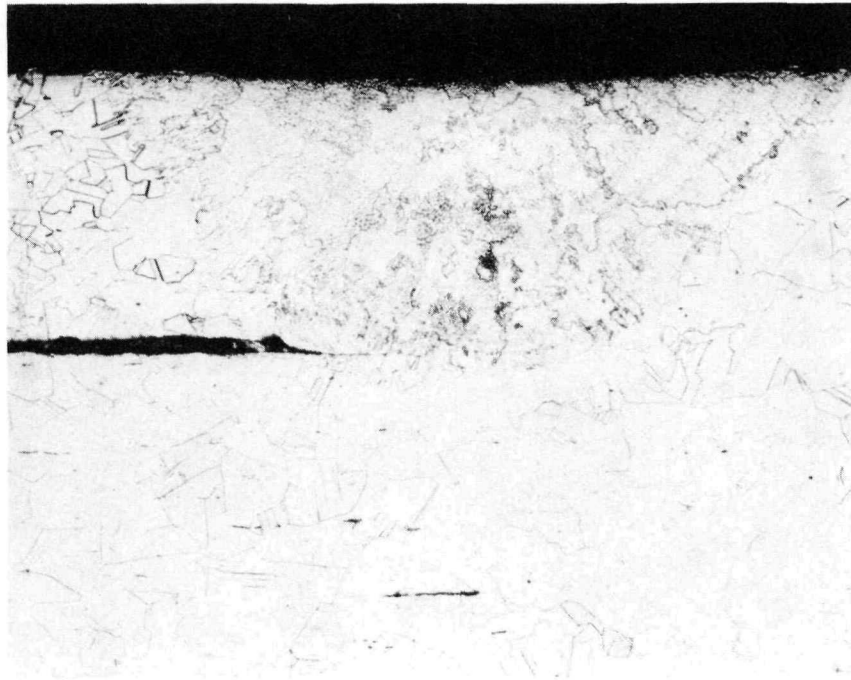


FIGURE 16. VIEW OF WELDING FIXTURE
AS SET UP IN GLOVE BOX

established, a slight misalignment from the center axis, sometimes as much as 0.009 inch, was noted on the joined pieces. As the problem became better defined, a decision was made to shim the end fittings and connectors slightly to compensate for shrinkage on cooling. This technique was quite successful in bringing the overall alignment of the welded section to within a few thousandths of an inch of the center axis, which was within the straightness of the stainless steel tubing.

Three test welds were then made under identical conditions to demonstrate repeatability of the operation. In all cases, metallographic examination showed the required 100 percent penetration. A typical microstructure of a weld area is shown in Figure 17. These results completed qualification of the welding process; therefore, all appropriate fittings and connectors were joined to the cladding sections while the unit was outside the glove box. The eight circumferential welds were then examined by use of the postemulsifiable-penetrant inspection technique. This method is extremely sensitive to surface-connected discontinuities, since the weld area is inspected with ultraviolet light. All welds appeared to be perfect, except for two which were subsequently checked with a binocular microscope and found to have very slight surface imperfections. Although these welds were readily acceptable, the sensitivity of the technique was also demonstrated to the extent that there was no question of the integrity of the welds as regards microcracking and surface defects.

At the end of this phase of the work, the welding apparatus, as assembled on the alignment bench, was transferred into a glove box. Modifications were then made to the box to obtain a helium atmosphere and accommodate the electrical and gas feeds for the welding equipment. A test weld was then attempted under conditions identical to those used for qualification, but in the presence of a high-purity helium atmosphere. Metallographic examination of weld area showed that the amount of penetration was identical to that obtained by welding outside the glove box.



75X

Etched

FIGURE 17. TYPICAL MICROSTRUCTURE OF WELD ENCOMPASSING THE TYPE 304 STAINLESS STEEL CLADDING-END FITTING INTERFACE

Encapsulation Procedures

Centerless-ground pellets were wiped clean and visually examined for defects in accordance with limits described in the pellet specifications. Following a thorough examination, the pellets were placed on a "V" bar to obtain a stacking length measurement prior to loading. The bar used for this purpose was scribed with marks to accurately indicate the tolerances for the pellet stack lengths in each of the two target rod segment categories, i.e., 10.000 ± 0.125 and 43.000 ± 0.125 inch. At this point, pellets for chemistry determinations and archive storage were selected and placed in appropriately marked containers for identification. Dimensions and weights of several pellets typical of those to be loaded were measured and geometric or bulk densities were obtained from these figures. No effort was made to keep track of individual pellets throughout processing and loading; however, different batches of pellets were carefully identified as to position within the target rod segment.

Pellet stack lengths were adjusted within tolerances either by selection or grinding of the pellets. A properly dimensioned calcia-stabilized zirconia pellet was then inserted into the appropriate target rod tube and the neptunia pellets followed. Dimensions taken from the open end of the tube verified a flush fit between pellets. A second zirconia pellet was then ground to the length necessary to obtain the specified spring pressure of 1.0 and 2.5 pounds for the short (10 inches) and long (43 inches) target rod segments, respectively. Spring deflections were checked under loads of 1.1 and 2.2 pounds to insure conformance to specifications.

All welds were performed with a qualified operator according to procedures and parameters established earlier in the program. The glove box, which normally contained high-purity nitrogen, was switched over to helium flow and flushed thoroughly for several hours before initiation of the pellet loading and end fitting weld operations.

Extreme care was taken to keep the open end of the tube and the end fitting in the vicinity of the weld free of contamination. The end fittings were held securely, but slightly shimmed to compensate for shrinkage during cooling. Visual and dimensional examination of the welds indicated that no

defects were present and the total diametral rise did not exceed 0.002 inch. Deviation of the end fittings from the center axis of the target segment was less than 0.008 inch per foot. Qualification welds made before and after a series of welds were examined metallographically, and, in all cases, full penetration, i.e., 100 percent of the wall thickness, was observed.

Fabrication data for each target segment are summarized in Table 13. Original design specifications are also included in this table for comparison. Generally, the as-fabricated neptunium concentrations were exceedingly close to those initially specified, except in case of the Segment A values. The reason for this discrepancy was pointed out earlier during the discussion of the sintering data, since it relates to the very high density obtained on the 71.7 w/o NpO_2 pellets. A decision was made to shorten the stack lengths of the "A" segments by one pellet to provide sufficient archive samples, since material of this composition was limited. Average pellet diameters were generally within a few ten-thousandths of an inch of the values shown. This pellet diameter of 0.383+ inch fixed the pellet-cladding gap in the range between 0.003 and 0.004 inch.

Cleaning and Inspection

All rods were decontaminated by standard techniques, i.e., cleaning with various detergent solutions followed by several rinses with ethyl alcohol. Smear counts taken after cleaning showed that no loose contamination remained on the surface. Direct counting of the surface, as well as the weld areas, verified the absence of contamination on the entire surface of every target segment.

A visual check was subsequently performed on all rods in accordance with quality assurance procedures. All rods were found to be free of surface defects and were approved accordingly.

Following decontamination, each rod segment was immediately subjected to a helium leak check in the following manner. Several rods, or a single one if this was all that was available at the time, were loaded into a chamber which was pressurized overnight to 150 psi with helium. A thorough calibration of the leak detector with a standard leak of $7.3 \times 10^{-7} \text{ cm}^3$ per second was initiated concurrently with this operation to assure smooth sequential movement

TABLE 13. NpO_2 TARGET SEGMENT EXPERIMENTAL AND DESIGN DATA

Segment	NpO_2 Concentration, w/o	Stack Length, inches	Average Pellet Diameter, inch	Total Target Volume, cm^3	Total Target Weight, g	Average Segment Density g/cm^3	NpO_2 Mass, g	Neptunium Mass, g		Neptunium Content per Total Target Volume, g/cm^3	
								Actual	Specified	Actual	Specified
1A	71.69	9.468	0.3835	17.92	152.62	8.52	109.43	96.30	102.69	5.38	5.44
2A	71.69	9.406	0.3835	17.80	152.33	8.56	109.22	96.11	102.69	5.40	5.44
1B	44.47	9.937	0.3835	18.81	116.14	6.18	51.64	45.44	51.35	2.42	2.72
2B	44.47	9.937	0.3837	18.83	116.84	6.20	51.96	45.72	51.35	2.43	2.72
1C	25.53	9.906	0.3834	18.74	100.53	5.36	25.67	22.59	25.67	1.21	1.36
2C	25.53	9.906	0.3838	18.78	101.00	5.38	25.79	22.70	25.67	1.21	1.36
1D	14.65	43.030	0.3834	81.41	412.85	5.07	60.48	53.22	55.20	0.65	0.68
2D	14.65	43.046	0.3835	81.48	410.90	5.04	60.20	52.98	55.20	0.65	0.68

of the segments from one step to the next. Individual rods were then rapidly moved to a chamber attached to the leak detector and evacuated. Meter readings significant of the helium present in the chamber were taken at 5-minute intervals for a period of approximately 20 minutes. The rate of change of the detector with the target rod present was then compared with the rate observed under identical conditions with the chamber empty and the blank rate after pumping for a period of several hours, which was usually about $1.7 \times 10^{-8} \text{ cm}^3$ per second. Analysis of the data indicated that the rate of helium dissipation found for the various rod segments was almost identical to that for the empty chamber and that readings less than the standard leak rate were attained within several minutes after the start of pumpdown.

Radiography of the target segments had two objectives: (1) to obtain a full view or composite shot to verify close spacing of the pellets within the cladding and (2) to verify full penetration of the circumferential welds in the vicinity of the end fittings. The latter was accomplished by taking radiographs of both sides of the weld at 0-, 60-, and 120-degree rotations. This approach provided a total of six views of the weld, which was considered ample to detect gross defects. This reasoning was also predicated on the performance of a continuous and uniform weld, which was a necessary criterion invoked in the quality assurance procedure.

To satisfy the first objective, radiographs were taken at a fairly low power setting with brass bars located adjacent to the cladding to reduce scatter. Some of these shots were also acceptable for weld examination; however, in most instances a different technique was needed to obtain a clear delineation of the weld zone and void at the fitting-cladding interface. This technique consisted of placing stainless steel shape corrections, machined to closely fit the contour of the rod, in the weld zone to equalize the beam penetration and reduce scatter. With this arrangement, power settings were increased to produce a dark film which was examined with a high-intensity arc light source. Resolution of the weld zone was substantially increased with this procedure; therefore, all subsequent radiographs were taken in an identical manner.

The detection limit, or penetration resolution, was judged to be less than 0.002 inch with the latter technique, and this value was somewhat higher initially. These figures are based for the most part on examinations of

penetrometer holes and visibility of the void between the end fitting and cladding wall which extended into the cladding about 0.7 inch. All welds were judged to be free of defects and of 100 percent penetration within the limits of detection.

Shipment and Assembly

Early in the program, a decision was made to ship the target rods to the reactor site in a total of four segments (two for each rod) and to carry out final assembly at the pool side. A bench consisting of closely aligned plywood standoffs on a 10-foot-long steel channel was constructed to facilitate final joining of the rod sections and loading into a reactor fuel assembly. The entire unit comprising the eight segments and flow mixer was then assembled at BCL prior to shipment.

The three lower segments of each rod, i.e., Segments A, B, and C, were joined according to plan at the laboratory. This operation involved the following steps: (1) use of a torque wrench to tighten adjoining segments, (2) drilling and reaming of a hole through the assembled fittings, (3) pin insertion, and (4) welding of the peripheral surface of the pin to the fitting. A photograph of the assembled target rods fastened to the bench is shown in Figure 18. Note the modified flow mixer assembly at the far end of the target rods.

The two rods were then disassembled into the four remaining segments and transported to Connecticut Yankee Reactor together with the flow mixer, alignment bench, and other tools needed to complete the assembly operation. The rod segments were joined at the reactor pool area without difficulty and loaded into an appropriate fuel assembly for storage until reactor reloading.

The fuel assembly containing the neptunium target rods was loaded into Connecticut Yankee Reactor on May 8, 1971.

Fabrication Optimization Studies

After results of irradiation of the target rods were available, attention was directed toward optimization and generalization of the

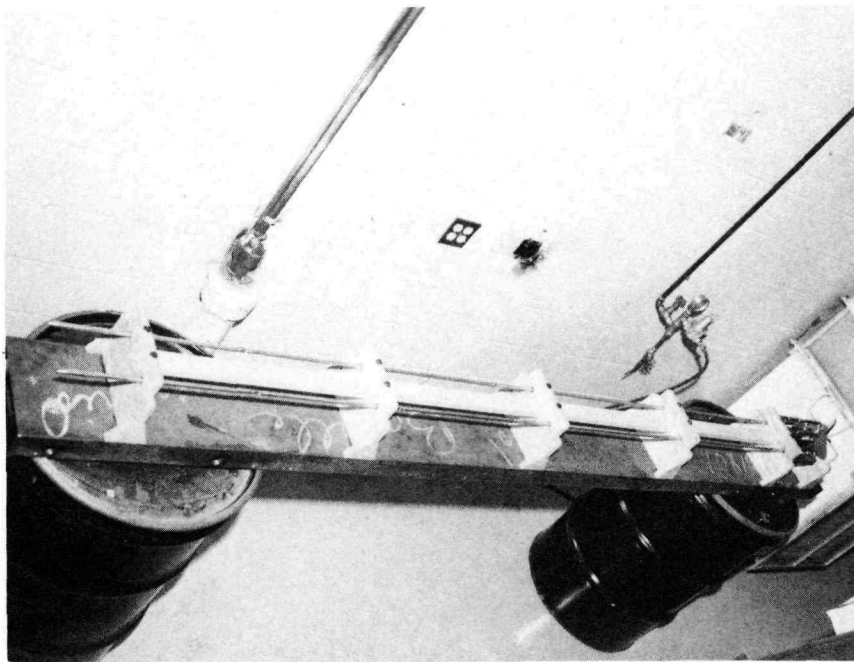


FIGURE 18. NEPTUNIUM TARGET RODS ASSEMBLED
AND FASTENED TO BENCH

Note modified flow mixer (far right)
attached to the top end of the rods.

fabrication process in order to lay the groundwork for large-scale operations leading to production of Pu²³⁸ on the scale of 10 to 100 kg per year. As an initial step in the program, numerous processing variables were assessed from all possible angles including their effect on production rate, impurity pickup, control of composition, and desired characteristics of the powder feed for the pressing operation, etc. Consideration of various trade-offs associated with each of the operations provided considerable insight for selection of the optimum processing route for pellet production. A simplified flow diagram of the various basic steps in the process is shown below.

Powder Blend → Slug → Granulate → Press → Sinter

Some of the options for the blending operation are shown in variations (a) through (g). Additional variables include the type of rubber lining in the mill, which can be either low-ash rubber or neoprene.

- (a) Dry ball mill NpO₂ and ZrO₂ (combined)
- (b) Dry ball mill NpO₂ initially--add ZrO₂, continue milling
- (c) Ball mill NpO₂ and "V" blend NpO₂ plus ZrO₂
- (d) Ball mill wet with conditions shown in (a) through (c) and
(e) through (g)
- (e) Use rubber-lined mill with ZrO₂ balls
- (f) Use rubber-lined mill with SS balls
- (g) Use SS mill with SS balls.

Previous studies had shown that mechanical blending of the as-received powders resulted in density of fired compacts no greater than 80 percent of theoretical. Based on the behavior noted from the postirradiation examination of the targets, the low pellet density appears to be quite acceptable. However, other considerations, particularly those related to licensing of the targets, suggested that a somewhat higher density of 90 percent of theoretical would be a better choice for a specification. This viewpoint stems primarily from recent problems with reactor fuel densification. In order to achieve the higher density, some comminution of the NpO₂ powder is required. Of the various alternatives described above, wet ball milling still seems to be the most desirable method. The main concern with this technique is introduction of impurities that

might alter the irradiation performance. To circumvent potential problems, the milling time should be kept as short as possible, probably less than four hours^(7,8). Use of a liquid medium is essential to prevent powder agglomeration and improve milling efficiency due to the vastly different densities of the components.

Based on the above considerations, initial fabrication studies were to be carried out according to the following processing scheme. The neptunia and calcia-stabilized zirconia powders were to be wet blended for four hours in a neoprene-lined mill using ZrO_2 slugs. This powder was to be subsequently dried, screened, and tested as feed for the automatic press. Preliminary efforts were to be made to press as-received calcia-stabilized zirconia powders in the automatic mode. If some difficulty was experienced with this powder, a lubricant was to be added to the blended mixture prior to pressing. Compaction pressure was to be investigated by use of four variations, which, hopefully, would bracket a range in behavior. Initially, pressures of 10,000, 20,000, 30,000, and 40,000 psi were to be studied. Several pellets were to be pressed at each pressure and sintered at 1600 C. Data obtained on these pellets was to be evaluated prior to the incorporation of changes in the processing scheme.

Because of time and funding limitations, it was not possible to execute the program defined above. Instead, the abbreviated study whose results are described below was carried out. The neptunia target composition of 20 w/o was selected on the basis of the postirradiation results relating to maximum Pu^{238} production with minimum Pu^{236} contamination as a function of NpO_2 target composition. It is estimated that a compositional variation of plus or minus 8 w/o would not significantly change the conclusions.

Cladding Specification

Various fabrication and testing requirements for the stainless steel tubing to be used as cladding for the targets have been assembled into a specification. This effort was conducted by reviewing similar specifications for LWR and FBR tubing. Generally, the specification is more stringent than the one supplied by NUMEC for the tubing used in the irradiation target rods. However, the additional criteria are easily justified on the basis of the

potential problems that could occur if the tubing were to fail during irradiation, the move toward better QA throughout the nuclear industry, and the numerous defects that were found in one of the qualified tubes received from NUMEC. A copy of the suggested specification is attached as Appendix B.

Pellet Specification

A preliminary general specification for the neptunia target pellets is proposed in Appendix C. Generally, the requirements are about the same as those written for the $\text{NpO}_2\text{-ZrO}_2$ irradiation targets. Spectrographic impurity limits have been increased somewhat because of the relatively low temperature of the targets during irradiation. Limits for moisture, fluorine, and chlorine contents were also placed at about the maximum acceptable level based on the same reasoning.

An acceptable value for pellet density is still in question. One would prefer to keep the density in excess of 90 percent of theoretical; however, this may be difficult to achieve in production without accepting a high level of Fe, Ni, and Cr contamination. Furthermore, the excellent results achieved in the irradiation suggest that a pellet density as low as 85 percent of theoretical may pose no problem if the pellets are fired at a temperature of 1600 C. In this case, stability under irradiation would occur through stabilization of the structure at a relatively high temperature as compared with the irradiation temperature, in combination with a large particle size of the constituents. On the other hand, low-density pellets usually absorb moisture rapidly and would probably give problems with dimensional stability when mass produced.

Specifications for the dispersion of neptunia have been set at a level wherein the maximum increase in Pu-236 content would be ~ 0.33 ppm. This may at first seem to be too stringent, but the presence of an appreciable quantity of neptunia agglomerates of a size of 1000 microns or greater generally signifies sloppy production techniques. In our original targets, at least 95 percent of the neptunia particles were less than 10 microns in diameter. Based on these results, we feel that there is no need to accept a lesser quality and any effort to do so might jeopardize the performance characteristics of the targets.

Although a specific sampling program has not been determined, a typical program has been provided for guidance purposes. This program, based on a furnace run of about 300 pellets in a batch, will require substantial modification, which will depend on the number of pellets fabricated and sintered at a time and the potential for contamination of the powder during processing.

Pellet Fabrication

Pellet fabrication studies were initiated by ball milling of NpO_2 - CaO-ZrO_2 powder using available ZrO_2 balls. Powder batches weighing approximately 75 g were wet ball milled for periods of 4, 8, and 12 hours. The powder was then dried, screened, and pressed into pellets.

Pellets pressed at pressures greater than 10 tsi were generally laminated and fell apart on subsequent handling. Trials were then conducted to find a more satisfactory range of pressing parameters which could be used for the densification studies. The range finally selected was 2.5, 5, and 10 tsi.

A total of 54 pellets were prepared for sintering, two for each of the parameters given below.

<u>Milling Time,</u> <u>hour</u>	<u>Densification</u> <u>Pressure, tsi</u>	<u>Sintering Temperature,</u> <u>C</u>
4	2.5	1350, 1500, 1650
4	5	1350, 1500, 1650
4	10	1350, 1500, 1650
8	2.5	1350, 1500, 1650
8	5	1350, 1500, 1650
8	10	1350, 1500, 1650
12	2.5	1350, 1500, 1650
12	5	1350, 1500, 1650
12	10	1350, 1500, 1650

Cold-Pressing Characteristics. Data for cold-pressed pellets including ball milling and pressing parameters are shown in Table 14. Pellets for this evaluation were selected from one of the duplicate pellets pressed for the sintering studies. The theoretical density used for the calculations was 6.22 g/cm^3 . As can be seen, the cold-pressed density does not appear to be significantly influenced by ball milling time; therefore, densities attained by pressing at the various parameters of 2.5, 5, and 10 tsi were averaged and plotted in Figure 19. Each point on this plot represents the average of 9 values. A curve drawn through the points indicates that there is a smooth, almost linear relationship between cold-pressing parameters and green density. This type of behavior was expected. It should also be noted that the range of densification is quite small, i.e., from 52.2 to 56.4 percent of theoretical; consequently, the pressed density seems to be somewhat insensitive to pressing pressure.

Sintering Behavior. Pellets pressed at various parameters were sintered in flowing high-purity nitrogen for a period of 3 hours at maximum temperatures of 1350, 1500, and 1650 C. Data for each of these pellets are given in Table 15. Generally, the density values for pellets that were green pressed at various pressures but were otherwise treated identically, i.e., ball milled for a specific time and sintered at one of the three specified temperatures, fall within a close band. Exceptions to this statement seem to occur primarily when the pellets are incompletely densified from sintering at the lowest temperatures of 1350 C.

In order to get a better perspective on the sintering behavior, all data for a given ball milling time and sintering temperature were averaged. These results are shown in Table 16 and plotted in Figures 20 and 21. Therefore, the points in these figures and Table 16 are the average of six values from Table 15. Correlation of the data appears to be excellent, since trends in most instances vary smoothly with changes in processing parameters. Increasing the ball milling time from 4 to 12 hours has a significant effect on the density of pellets sintered at 1350 C (see Figure 20). However, the overall effect of variations in the ball milling time of 4 to 12 hours diminishes as the sintering temperature is increased to 1650 C. The data point for the ball milling time of 8 hours appears to be slightly to the left of the curve for the

TABLE 14. COMPILATION OF GREEN DENSITY DATA FOR PELLETS
 PRESSED AT DIFFERENT PARAMETERS FROM BALL
 MILLED POWDER

Specimen Designation	Ball Milling Time, hr	Cold Pressing Pressure, tsi	Cold-Pressed Density, percent of theoretical
1-C	4	2.5	59.4
2-C	4	10	55.7
3-C	4	5	54.5
4-C	8	5	53.3
5-C	8	10	55.5
6-C	8	2.5	50.8
7-C	12	2.5	50.8
8-C	12	5	52.8
9-C	12	10	55.3
10-C	4	2.5	51.8
11-C	8	2.5	51.3
12-C	12	2.5	50.7
13-C	4	5	53.5
14-C	8	5	53.5
15-C	12	5	55.1
16-C	4	10	57.4
17-C	8	10	57.2
18-C	12	10	56.0
19-C	4	2.5	53.5
20-C	4	5	54.7
21-C	4	10	57.2
22-C	8	2.5	50.8
23-C	8	5	53.6
24-C	8	10	56.7
25-C	12	2.5	51.0
26-C	12	5	53.6
27-C	12	10	56.4

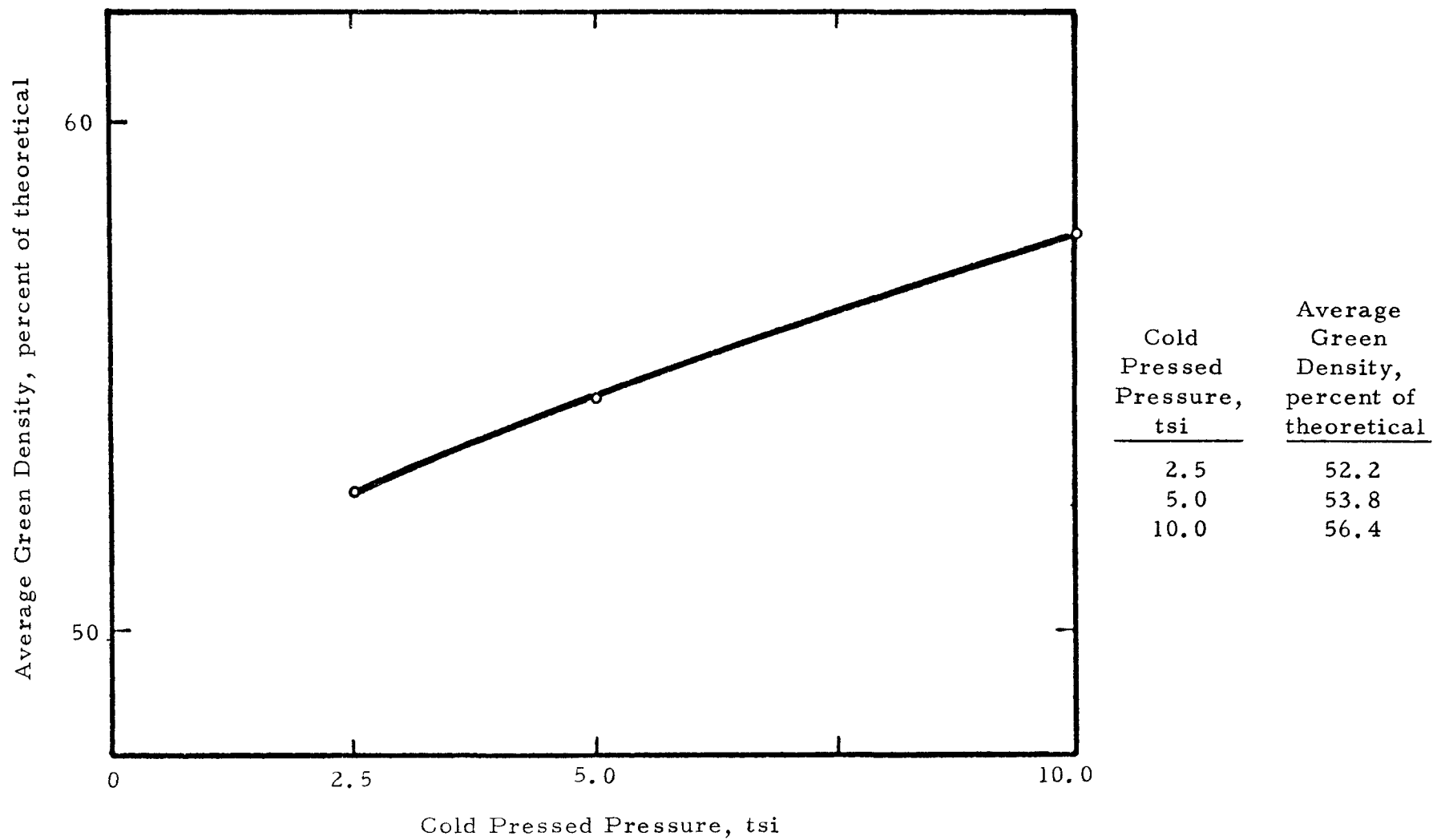


FIGURE 19. CHANGE IN AVERAGE GREEN DENSITY OF PELLETS WITH PRESSING PRESSURE

TABLE 15. SUMMARY OF DATA FOR VARIOUS PROCESSING PARAMETERS

Specimen Designation	Sintering Temperature, C	Ball Milling Time, hr	Cold Pressing Pressure, tsi	Sintered Density, percent of theoretical
1	1350	4	2.5	62.2
2	1350	4	2.5	66.4
3	1350	4	5	58.7
4	1350	4	5	59.7
5	1350	4	10	68.6
6	1350	4	10	65.4
7	1500	4	2.5	77.3
8	1500	4	2.5	76.6
9	1500	4	5	75.0
10	1500	4	5	75.4
11	1500	4	10	78.1
12	1500	4	10	78.1
13	1650	4	2.5	81.3
14	1650	4	2.5	81.8
15	1650	4	5	84.0
16	1650	4	5	83.6
17	1650	4	10	85.9
18	1650	4	10	86.8
19	1350	8	2.5	73.7
20	1350	3	2.5	75.1
21	1350	3	5	71.5
22	1350	3	5	72.2
23	1350	8	10	79.4
24	1350	8	10	76.4
25	1500	8	2.5	81.0
26	1500	8	2.5	81.2
27	1500	8	5	80.5
28	1500	8	5	82.0
29	1500	3	10	83.0
30	1500	3	10	83.2
31	1650	8	2.5	86.0
32	1650	8	2.5	86.9
33	1650	8	5	79.3
34	1650	8	5	79.1
35	1650	8	10	86.3
36	1650	8	10	87.7
37	1350	12	2.5	81.1
38	1350	12	2.5	79.7
39	1350	12	5	76.5
40	1350	12	5	74.1

TABLE 15. (Continued)

Specimen Designation	Sintering Temperature, C	Ball Milling Time, hr	Cold Pressing Pressure, tsi	Sintered Density, percent of theoretical
41	1350	12	10	79.5
42	1350	12	10	80.8
43	1500	12	2.5	85.1
44	1500	12	2.5	84.8
45	1500	12	5	85.2
46	1500	12	5	84.4
47	1500	12	10	84.5
48	1500	12	10	85.8
49	1650	12	2.5	86.9
50	1650	12	2.5	88.3
51	1650	12	5	87.0
52	1650	12	5	86.6
53	1650	12	10	87.7
54	1650	12	10	88.1

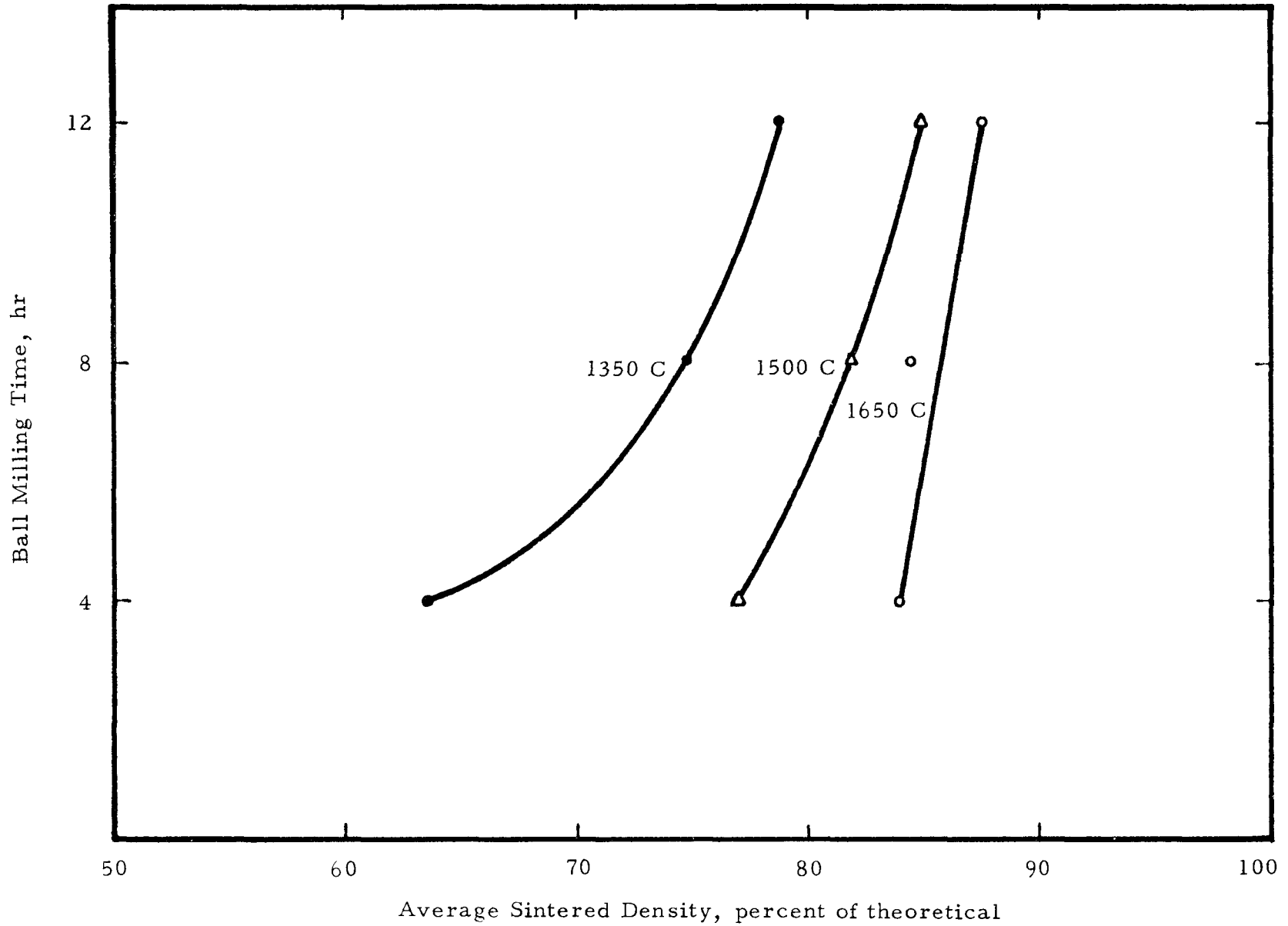


FIGURE 20. VARIATION OF PELLET SINTERED DENSITY AS A FUNCTION OF BALL MILLING TIME AND SINTERING TEMPERATURE

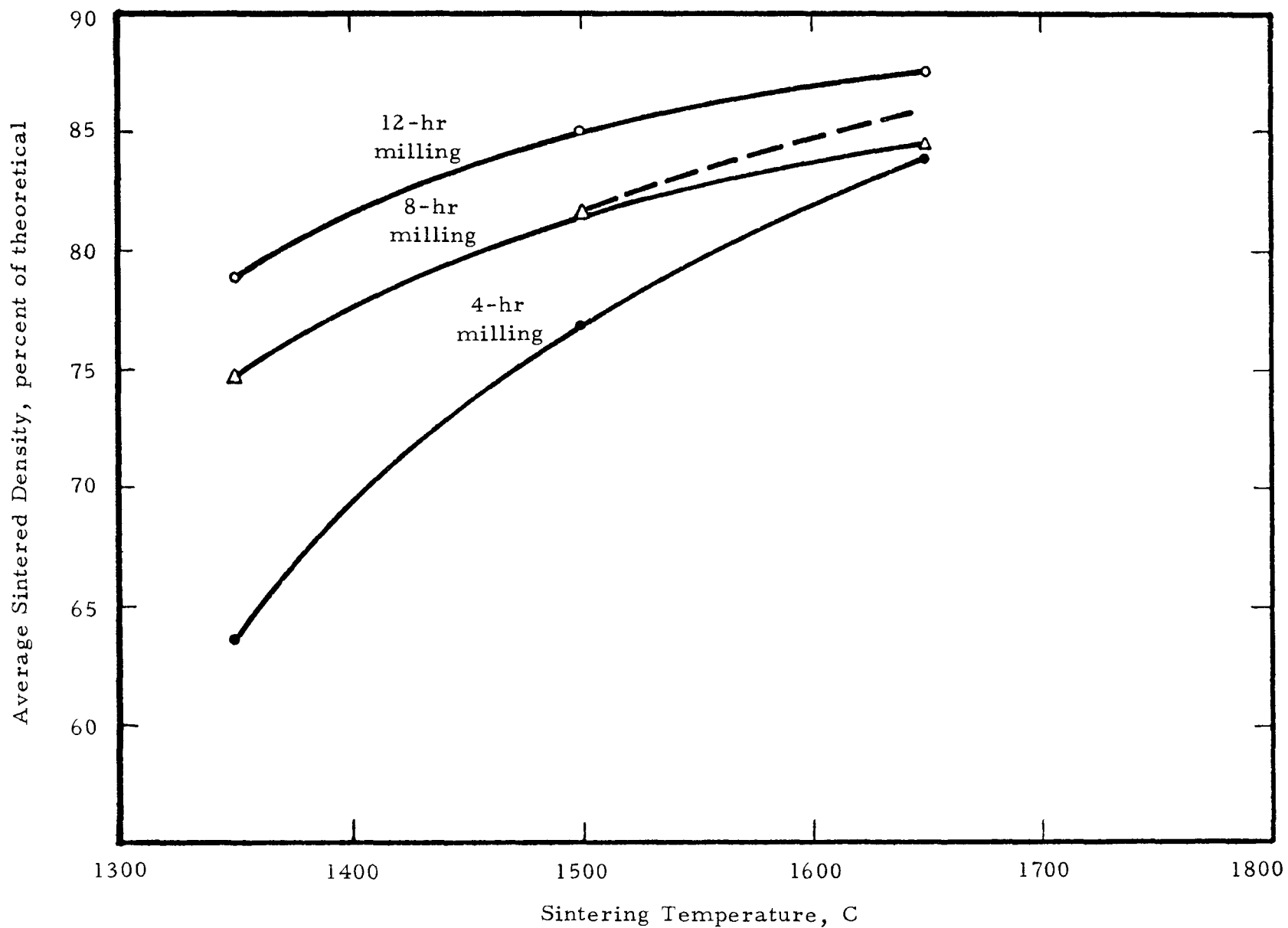


FIGURE 21. VARIATION OF PELLET SINTERED DENSITY AS A FUNCTION OF SINTERING TEMPERATURE FOR CONSTANT BALL MILLING TIME

TABLE 16. AVERAGE SINTERED DENSITY OF PELLETS PREPARED FROM
POWDER PROCESSED UNDER DIFFERENT CONDITIONS

Sintering Temperature, C	Ball Milling Time, hr	Average Sintered Density, percent of theoretical
1350	4	63.5
	8	74.7
	12	78.6
1500	4	76.8
	8	81.8
	12	85.0
1650	4	83.9
	8	84.2
	12	87.4

1650 C sintering temperature. This is due to the two low densities obtained on pellets pressed at 5 tsi (see Table 15). It seems reasonable to assume that this low-density value is erroneous. Projection of the 1650 C curve to a 24-hour ball milling time used for fabrication of the target pellets gives a density of approximately 94 percent of theoretical. This value is in excellent agreement with our earlier work.

Density data from Table 16 are plotted as a function of sintering temperature for constant ball milling periods in Figure 21. The dashed line for the 8-hour ball milling curve is probably closer to the true behavior based on the above discussion. The trend of these curves shows that increasing the sintering temperature above 1650 C would have little effect on the sintered density of pellets. From all indications, 1650 C is about optimum for production of high-density material.

Where chemical dissolution is desired, pellets sintered at a lower temperature would probably be preferred. The curves in Figure 21 indicate that densities above 80 percent of theoretical can be attained by ball milling the powder mixtures for more than 12 hours and sintering above 1375 C. The lower sintering temperatures would undoubtedly lead to larger dimensional variations in the pellets and irregularities in the density, but considering the purposes intended, this should cause no problem during irradiation.

III. POSTIRRADIATION EXAMINATION

The two target rods were irradiated in the Connecticut Yankee Reactor for 361.64 equivalent full power days to a total fluence of approximately 3.6×10^{21} n/cm². They were removed from the reactor on June 9, 1972, and each rod was cut between Sections C and D (see Figure 22). The gas tightness of each section (A, B, C, and D) was preserved. On June 18, 1972, the four segments, resulting from the cutting of the two target rods, were removed from the spent fuel pit and shipped to the BCL Hot Laboratory at West Jefferson, Ohio, for postirradiation examination. A flow diagram for the destructive testing of the target rod is given in Figure 23.

The primary objective of the postirradiation examination was to check experimentally the validity of the initial theoretical predictions by determining the Pu-238 yield in the four compositions of NpO₂ and to evaluate the effect of flux depression and flux spectral changes as a function of the NpO₂ concentration. The secondary objective was to determine the irradiation stability of the four target compositions and the compatibility of the various fabrication materials.

Stereo Visual Examination

Upon receipt at BCL, the four sections of the target rods were transferred into the high level cell and each of the four sections was visually examined and photographed at 0, 90, 180, and 270 degrees. Photographs of the as-received rods are given in Figure 24. The rods external condition was excellent with no detectable irregularities such as bow, corrosion, or crud deposits. Diameter measurements using a micrometer were made at five evenly spaced intervals along each of the four sections and at the same circumferential orientation at each point. These readings were repeated at 90-degree rotations of each section. The results of these measurements, tabulated in Table 17, indicate no significant diametral changes. The postirradiation diameter measurements in the area of the fuel

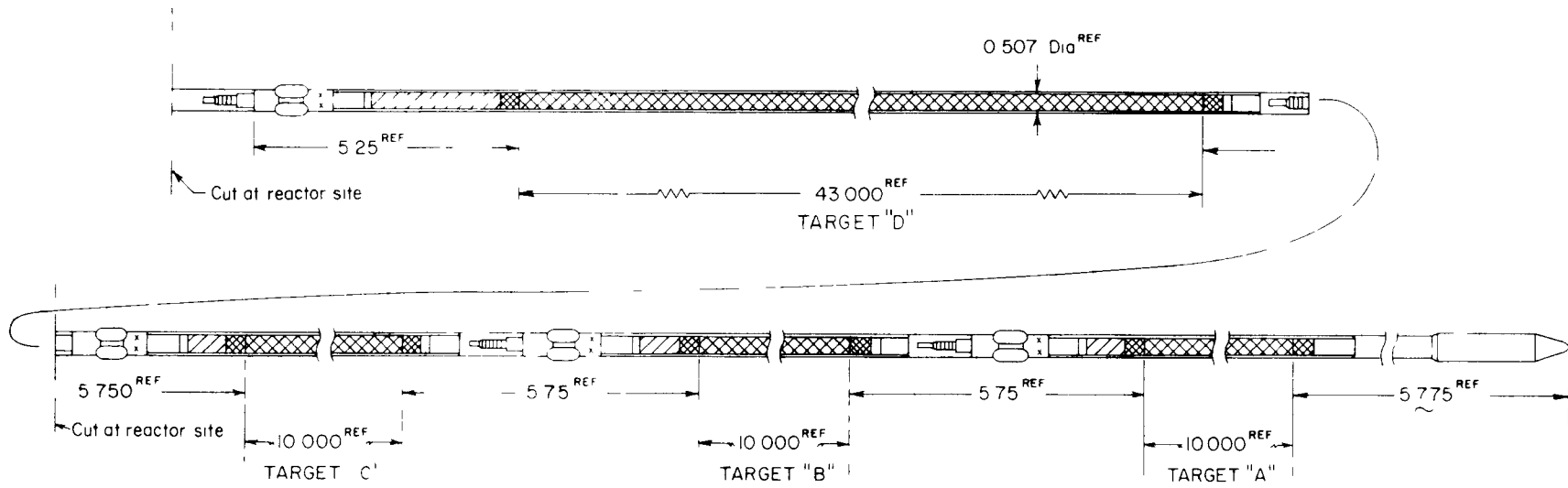
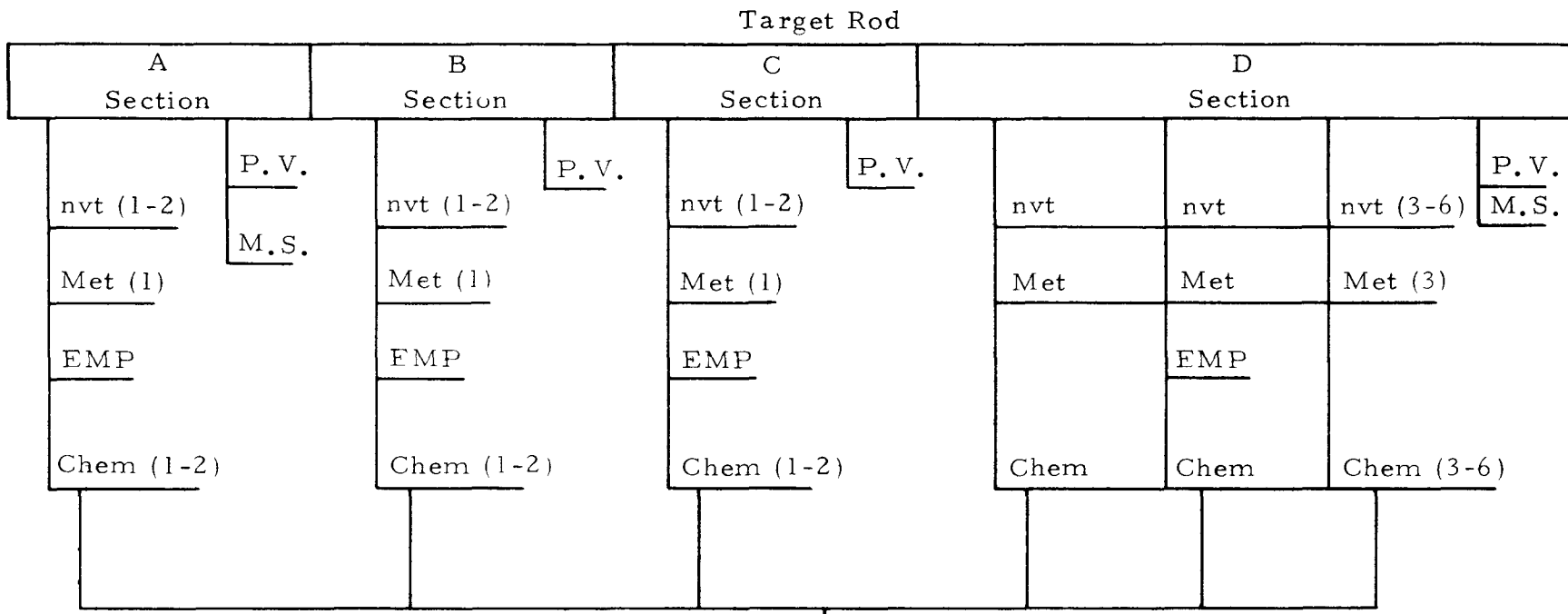
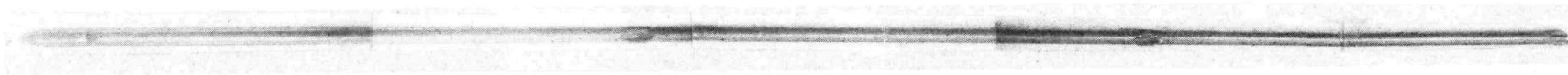


FIGURE 22. NEPTUNIUM FUEL ASSEMBLY J-14 WITH TARGET ROD ASSEMBLY



<p>nvt = Neutron dosimetry</p> <p>P. V. = Measure of quantity of gas in the target rod section</p> <p>M.S. = Mass Spectrometer gas analysis</p> <p>Met = Metallographic examination</p> <p>E.M.P. = Electron Microprobe analysis</p> <p>Chem = Chemical analysis</p>	<p><u>Pu Total</u></p> <p><u>Pu isotopic</u></p>
--	--

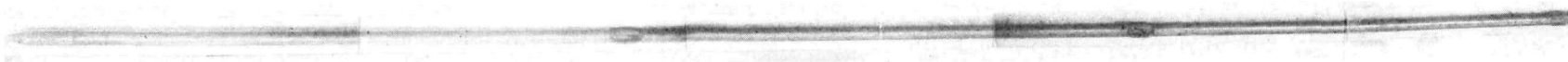
FIGURE 23. FLOW DIAGRAM FOR DESTRUCTIVE EXAMINATION



a. Rod 1 - Sections A, B, and C



b. Rod 1 - Section D



c. Rod 2 - Sections A, B, and C



d. Rod 2 - Section D

FIGURE 24. AS-RECEIVED NEPTUNIUM TARGET RODS 1 AND 2

TABLE 17. NEPTUNIUM ROD DIAMETERS

Rod No.	Section	Measurement No. (1)	Diameter Measurements	
			0°	90°
1	A	1	0.4219	0.4217
1	A	2	0.4219	0.4215
1	A	3	0.4214	0.4217
1	A	4	0.4215	0.4213
1	A	5	0.4218	0.4218
1	B	1	0.4215	0.4214
1	B	2	0.4210	0.4215
1	B	3	0.4208	0.4208
1	B	4	0.4209	0.4212
1	B	5	0.4227	0.4227
1	C	1	0.4218	0.4210
1	C	2	0.4218	0.4213
1	C	3	0.4214	0.4205
1	C	4	0.4216	0.4219
1	C	5	0.4228	0.4230
1	D	1	0.4210	0.4225
1	D	2	0.4216	0.4215
1	D	3	0.4214	0.4215
1	D	4	0.4211	0.4213
1	D	5	0.4212	0.4218
2	A	1	0.4224	0.4216
2	A	2	0.4218	0.4210
2	A	3	0.4214	0.4212
2	A	4	0.4212	0.4216
2	A	5	0.4227	0.4227
2	B	1	0.4214	0.4220
2	B	2	0.4216	0.4219
2	B	3	0.4210	0.4215
2	B	4	0.4216	0.4219
2	B	5	0.4230	0.4230
2	C	1	0.4211	0.4212
2	C	2	0.4209	0.4213
2	C	3	0.4208	0.4216
2	C	4	0.4211	0.4210
2	C	5	0.4220	0.4221
2	D	1	0.4217	0.4230
2	D	2	0.4221	0.4220
2	D	3	0.4214	0.4219
2	D	4	0.4213	0.4205
2	D	5	0.4210	0.4203

(1) Measurements were evenly spaced along each section and were made at the same circumferential orientation at each point.

pellets averaged 0.421 in. as compared to the preirradiation average diameter of 0.422 in. The maximum postirradiation diameter measurements near the stabilizing fins were 0.430 in. as compared to the maximum preirradiation diameter of 0.427 in.

Gamma Scan

The four sections of the $\text{NpO}_2\text{-ZrO}_2$ target rods were gamma scanned using a 50-mil slit collimator. The signal from a single channel analyzer, with a gamma ray energy window from 0.770 to 0.776 Mev in conjunction with a 2-in. NaI (Tl) crystal, was used to drive a strip chart recorder. The gamma ray peak at about 0.775 Mev is the $\text{Zr}^{95}\text{-Nb}^{95}$ decay energy peak. The strip chart time markers represent 1/16-in. rod intervals. Gamma-scan strip charts are graphically represented in Figure 25. The fuel column stack heights before and after irradiation are given below. The gamma-scan showed gaps within some columns and the gap widths are tabulated below.

<u>Rod</u>	<u>Section</u>	<u>Height Before Irradiation, in.</u>	<u>Height After Irradiation, in.</u>	<u>Total (Summed) Pellet Gaps After Irradiation, in.</u>
1	A	9.468	9.563	0.188
1	B	9.937	10.188	0.313
1	C	9.906	10.125	0.250
1	D	43.030	42.875	0
2	A	9.406	9.626	0.313
2	B	9.937	10.188	0.313
2	C	9.906	9.875	0
2	D	43.046	43.313	0.375

Using the gamma scan chart as a guide, six rod positions were chosen from which specimens would be sectioned for metallographic examination, for chemical analysis, and for electron microprobe analysis. The rod positions from which eight cladding neutron dosimetry samples were to be removed were also chosen.

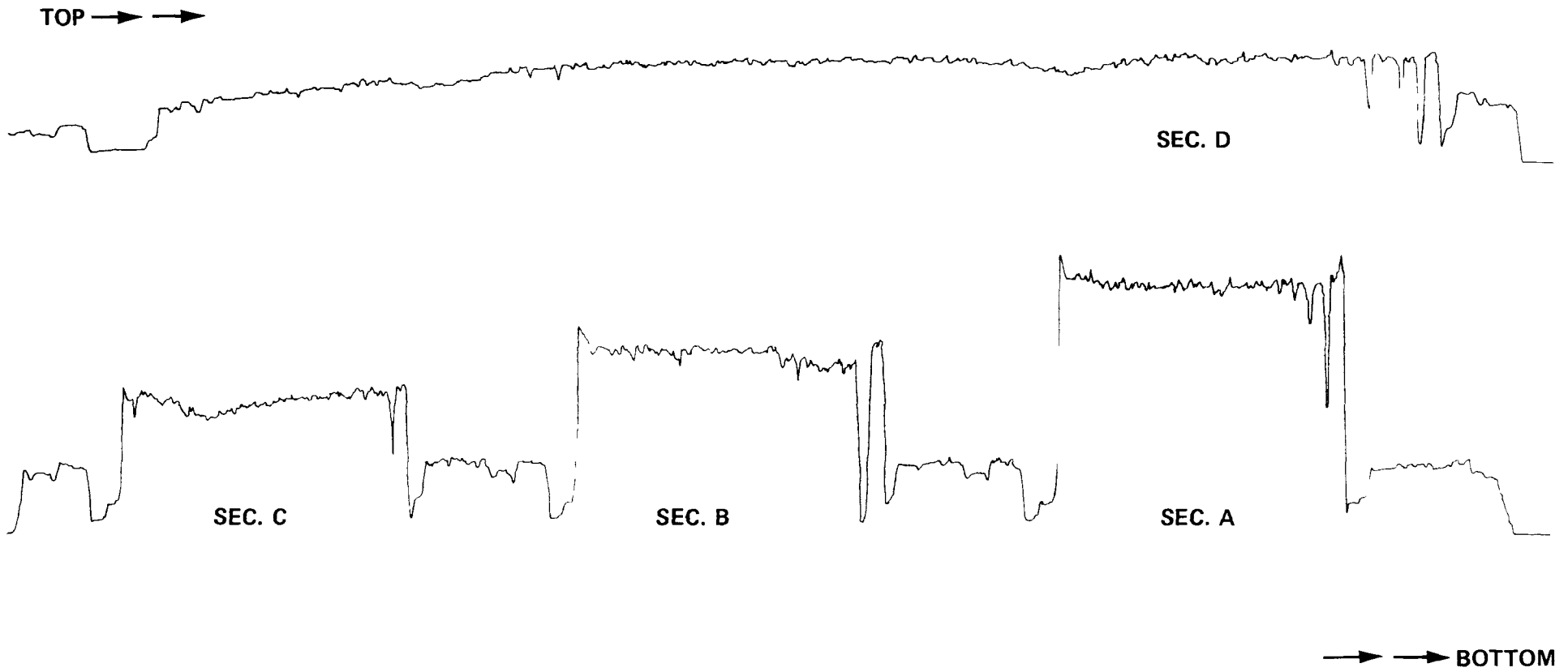


FIGURE 25. NEPTUNIUM TARGET ROD GAMMA SCAN

A tabulation of the initial neptunia concentration is compared with gamma scan intensity for Rod Number 2 below.

<u>Rod</u>	<u>Section</u>	<u>Concentration NpO₂, w/o</u>	<u>Average Gamma Scan Intensity (C/min)</u>
2	D	14.65	30 K
2	C	25.53	40 K
2	B	44.47	55 K
2	A	71.69	75 K

The target rod gamma intensity and the amount of Pu-238 produced from the Np-237 fuel should be related since both are a function of the neutron flux. The gamma scan intensities indicate that the Pu-238 yield should increase with increased Np concentration but the increase will not be linear (see Figure 26). The equation for the curve of NpO₂ concentration versus gamma scan intensity is $Y = (1.4X^{0.88} + 15)(10^3)$, where Y is the relative gamma intensity and X is the initial weight percent NpO₂ concentration. The non-linearity of this relationship stems in part from increased flux depression at higher NpO₂ concentrations, partly from activation of the zirconium in the ZrO₂ diluent, and probably partly from species activated in the clad.

Cover Gas Analysis

Sections A, B, C, and D of neptunium Rod Number 2 were punctured and the cover gas collected using mercury diffusion pumps and a Toepler pump. A minimum of 95 percent of the gas was collected from each section and the gases from Sections A and D were mass analyzed. The volume percents of the molecular and atomic constituents are tabulated in Table 18. The xenon and krypton isotopic analysis results are given in Table 19. The gases from Sections B and C were stored. The quantity of gas in Section A was 1.82 cc at STP and in Section D was 3.36 cc at STP. In both Sections A and D the mass spectrometric analysis indicated 0.03 volume percent of an undetermined hydrocarbon, probably a C₃ compound, and in Section D about 0.08 volume

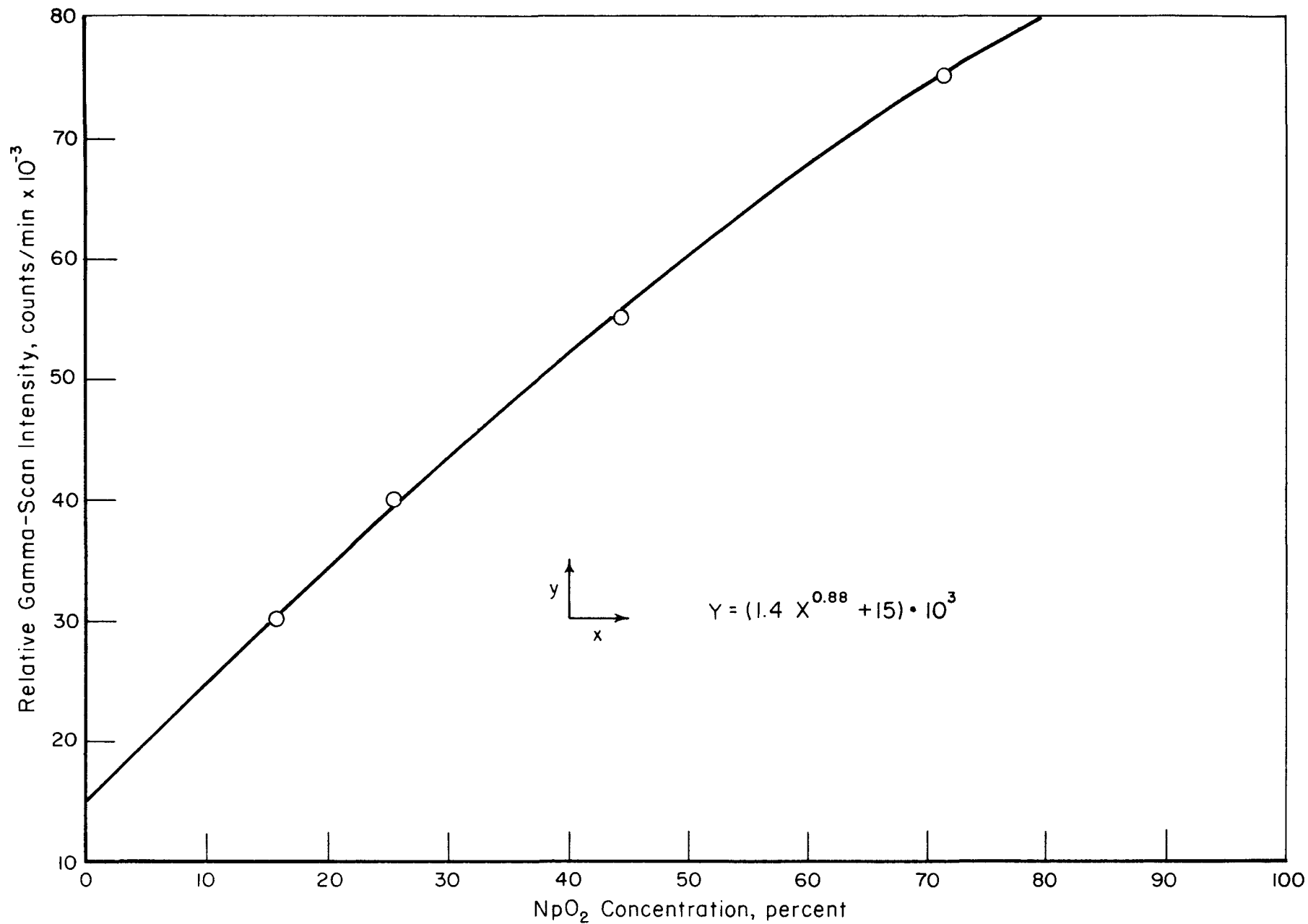


FIGURE 26. PLOT OF INITIAL NpO₂ PERCENT CONCENTRATION VERSUS RELATIVE GAMMA-SCAN INTENSITY

TABLE 18. GAS ANALYSIS

Rod	Section	Total Collection System Volume, cc	Gas ⁽¹⁾ Volume, cc	Volume Percent										
				H ₂	He	CH ₄	H ₂ O	O ₂	N ₂	A	CO ₂	Kr	Xe	Xe/Kr
2	A	148.7	1.82	17.0	31.4	<0.01	2.6	1.60	4.42	42.3	0.12	0.06	0.48	8.00
2	D	502.8	3.36	43.1	40.7	0.04	1.9	1.59	4.43	5.68	0.93	0.12	1.35	11.25

(1) The quantity of gas is at STP.

TABLE 19. XENON AND KRYPTON ISOTOPIIC ANALYSIS

Rod	Section	Isotopic Percent Krypton				Isotopic Percent Xenon			
		83	84	85	86	131	132	134	136
2	A	20.2	30.0	9.3	40.5	12.6	21.5	27.6	38.3
2	D	19.2	29.4	7.7	43.7	11.9	20.3	26.7	41.1

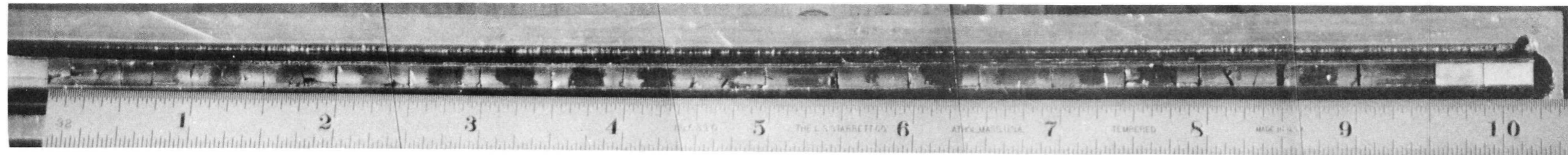
percent benzene (C_6H_6). These carbon compounds do not appear significant and may have been introduced during collection and analysis. The total hydrogen content of the cover gas including the amount contributed by water is less than 2.5 ppm of fuel and the water content in the gas is less than 1 ppm of fuel.

There appears to have been some air contamination or gases released from the pellets since the mass spectrometer analysis indicates some concentration of water, oxygen, and nitrogen. The volume and isotopic percents of xenon and krypton are about the values expected. However, the argon is assumed to have been introduced during fabrication of the targets.

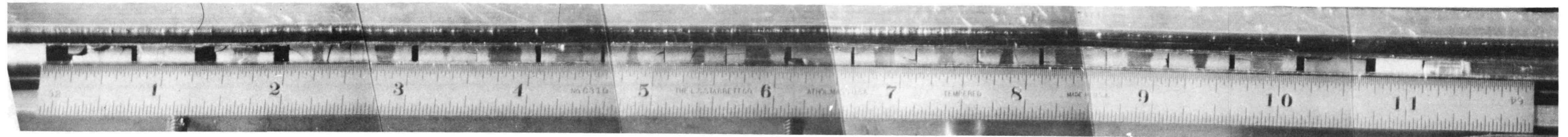
Target Rod Disassembly

Target Rod Number 2 was chosen by SNE and BCL personnel for further destructive testing. A slitting device was used to open Sections A, B, C, D top, and D bottom and expose the fuel pellets for visual examination. Composite pictures of these sections are included (see Figures 27 and 28). The cladding inner surface was bright and shiny and there was no evidence of fuel-cladding incompatibility. The cladding was relatively ductile.

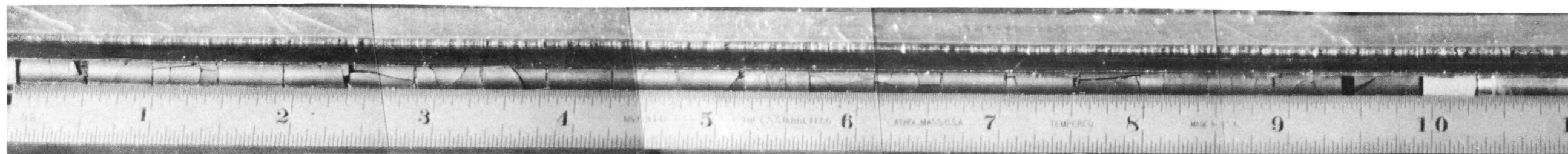
The fuel pellets were cracked to varying degrees, from virtually no cracks (whole pellets) to numerous cracks; however, there was no evidence of pulverization. The cracking was probably due to thermal stresses. The pellets were light to dark gray. The A and B sections showed color variations within a pellet with the ends being very light gray and the centers (longitudinally) being darker gray as shown in the composite pictures. The reason for this discoloration is not known at this time. However, the pellet cracking and discoloration did not appear to have been deleterious to the irradiation performance. The irradiated target rods were in excellent mechanical and chemical condition.



A



B



C

FIGURE 27. NEPTUNIUM TARGET ROD 2 — SECTIONS A, B, AND C
(SLIT OPEN FOR VISUAL EXAMINATION)

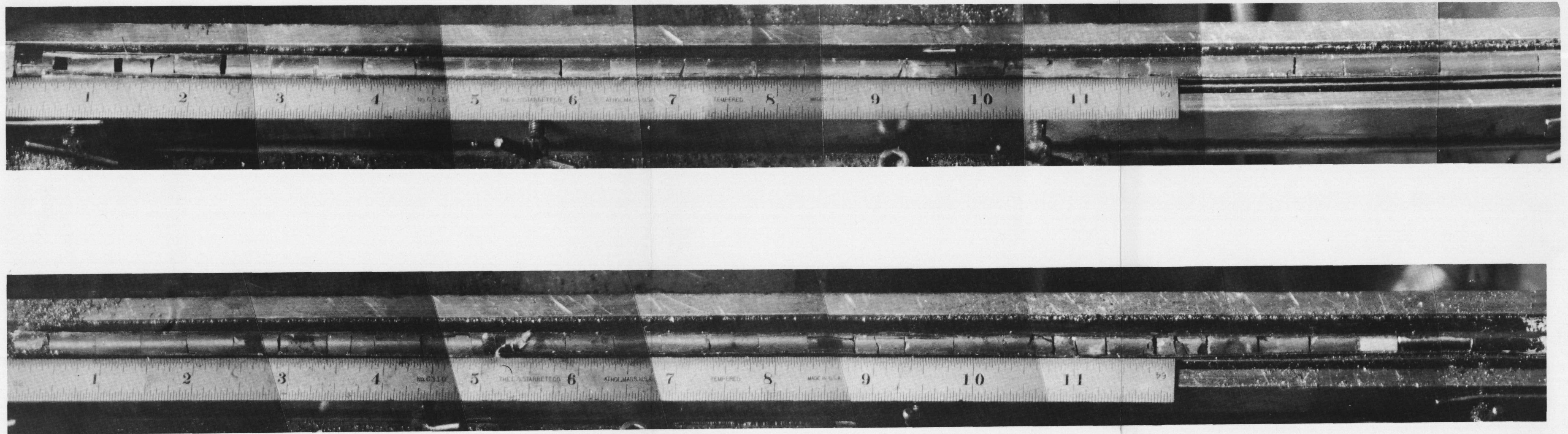


FIGURE 28. NEPTUNIUM TARGET ROD 2 - SECTIONS D TOP AND D BOTTOM
(SLIT OPEN FOR VISUAL EXAMINATION)

Metallographic Examination

Using the preliminary area choices indicated on the gamma scan chart and viewing the photographs taken after the slitting operation, six pellet specimens from Rod Number 2 were removed. The specimen numbers, the types of mounts, the specimen positions with respect to the top of each section, and the preirradiation weight percents of neptunium dioxide are given below.

<u>Rod</u>	<u>Rod Specimen and Specimen No.</u>	<u>Specimen Mounted</u>	<u>Inches From Top of Section</u>	<u>Preirradiation w/o NpO₂</u>
2	D, Met 1	Longitudinally	4.0 - 4.5	14.65
2	D, Met 3	Transversely	19.25 - 19.75	14.65
2	D, Met 4	Longitudinally	39.0 - 39.5	14.65
2	C, Met 6	Longitudinally	3.75 - 4.25	25.53
2	B, Met 8	Transversely	4.5 - 5.0	44.47
2	A, Met 11	Transversely	5.5 - 6.0	71.69

A schematic drawing of target Rod Number 2 and the sampling positions are shown in Figure 29.

The six metallographic specimens mounted in epoxy were wet ground with 120, 240, 400, and 600-grit SiC papers and polished with Linde A plus 2 percent CrO₃ on Texmet cloth. In the as-polished condition, a macroscopic photograph (3.5X), traverse photographs from center to edge at 100X, and 500X photographs of center and edge were taken for each specimen. The macrograph and the 500X center and edge photographs and a 100X typical photograph are included in this report (see Figures 30 through 35).

The specimen photographs for Sections C and D show very little variation in density; however, the specimen from Section B has fewer voids than either Section C or D. The A section specimen has almost no voids. A comparison of preirradiation and postirradiation metallographic photographs indicated that no detectable density changes occurred during irradiation.

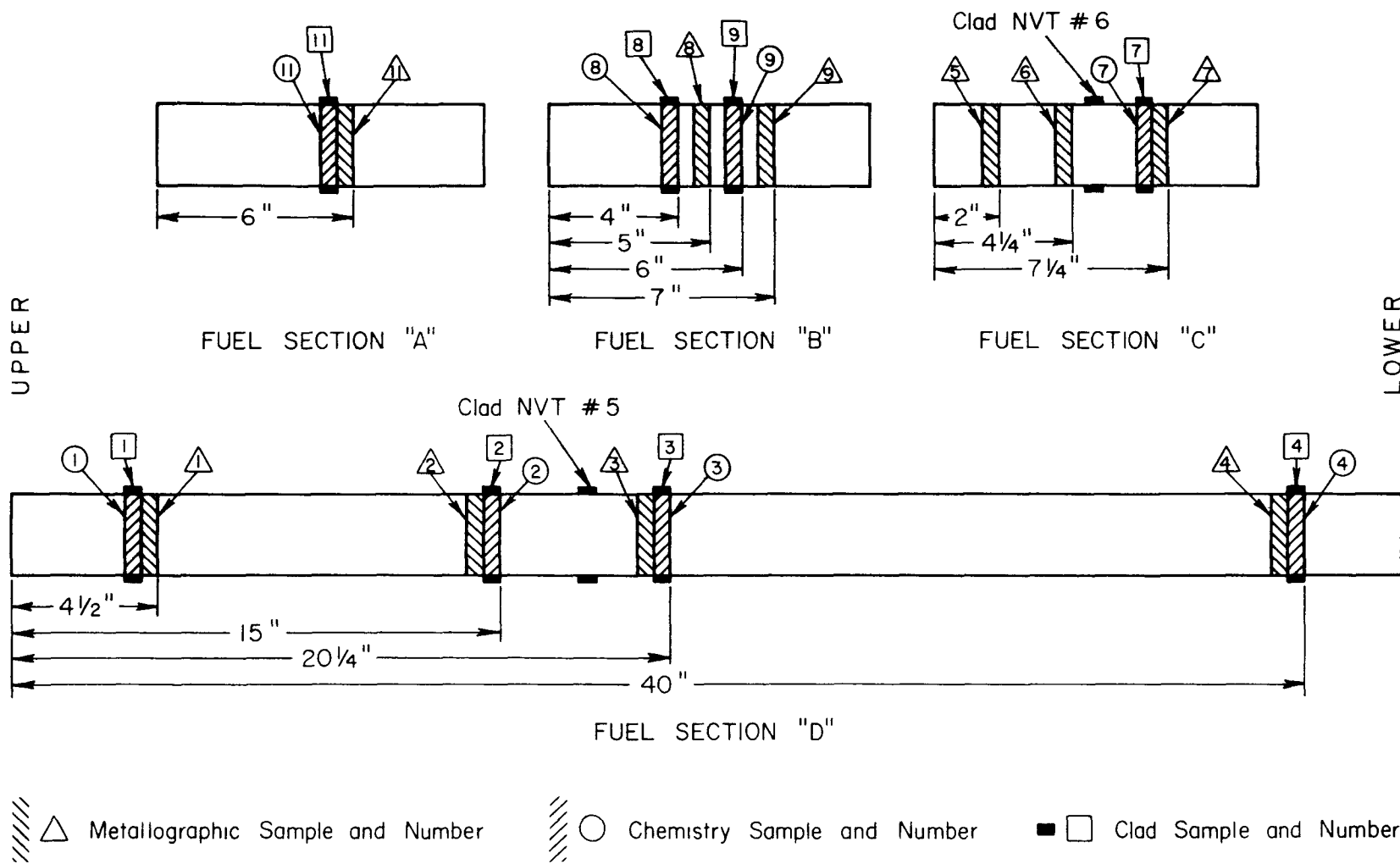
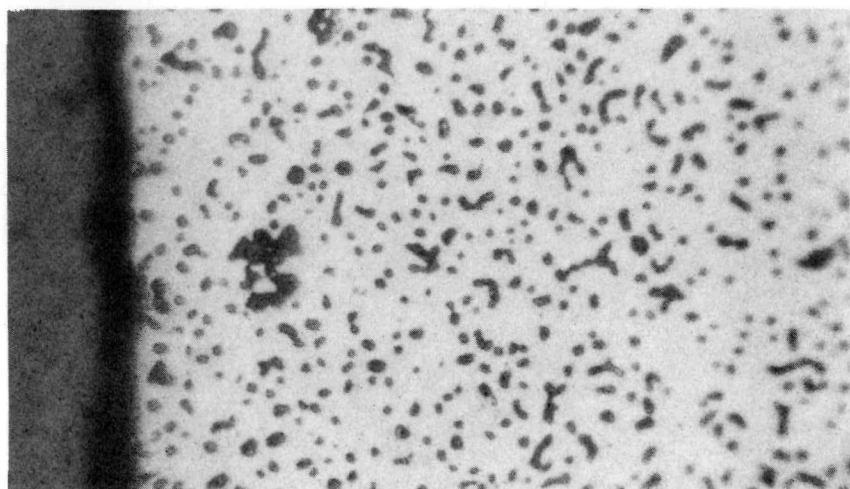


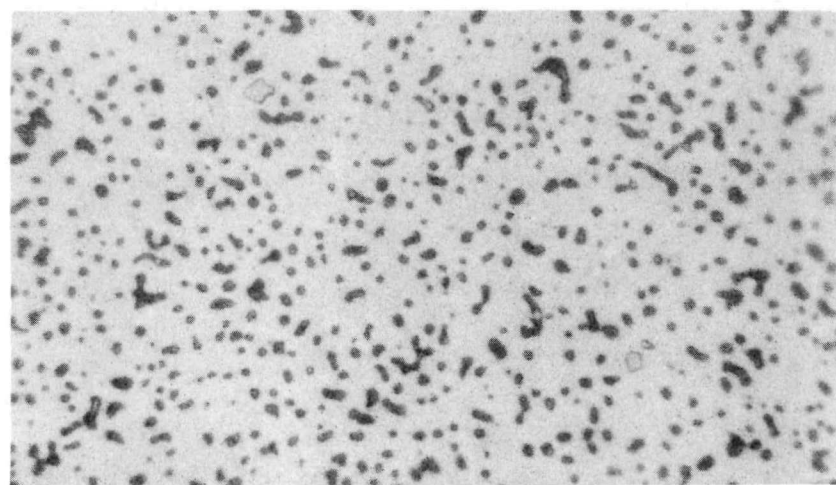
FIGURE 29. NEPTUNIUM ROD NUMBER TWO SECTIONING SCHEMATIC



500X

HC32414

a. Edge



500X

HC32413

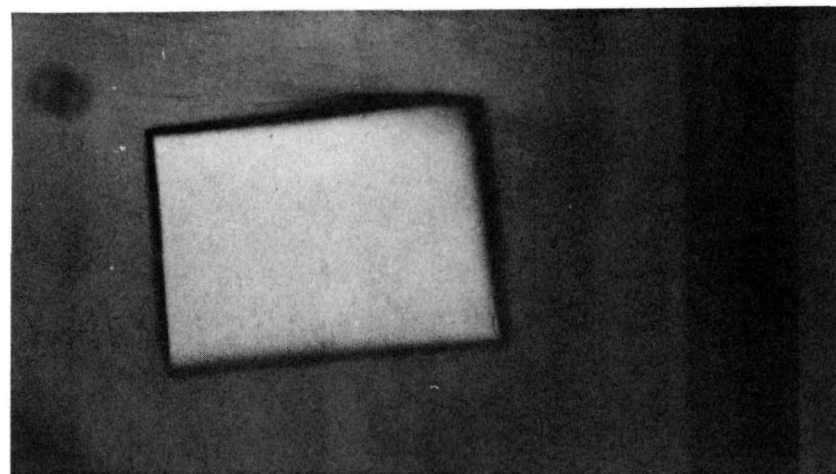
b. Center



100X

HC32409

c. Typical

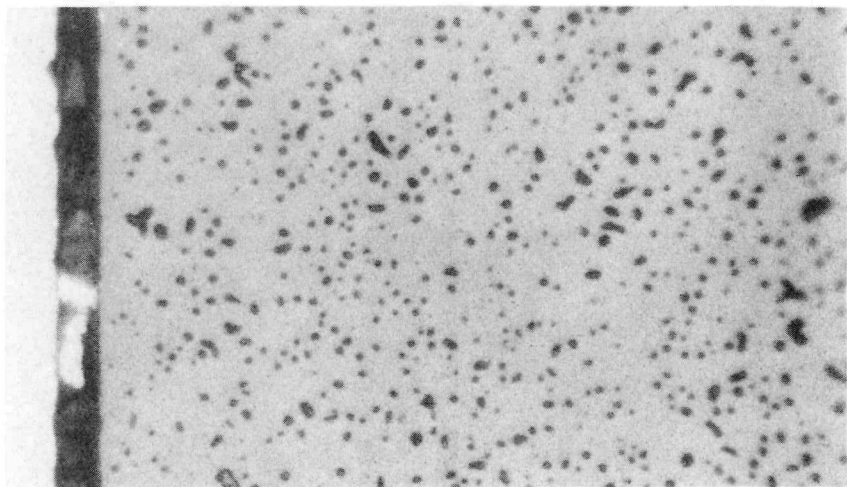


3.5X

HC32364

d. Macro

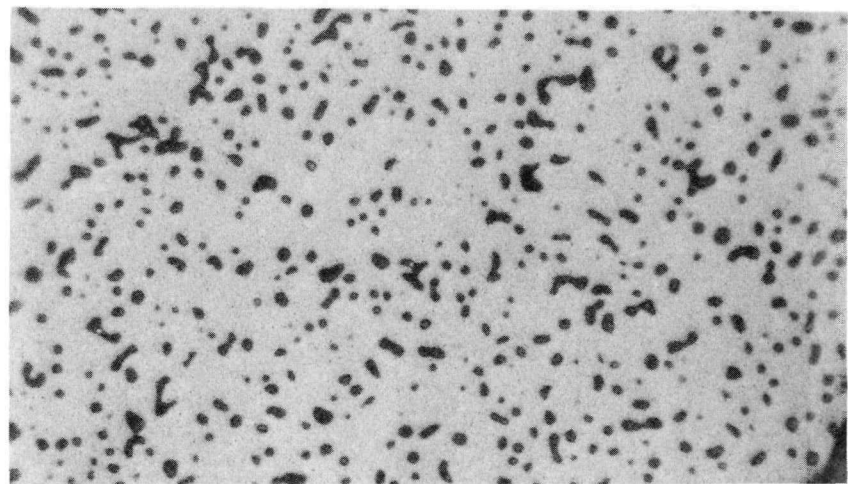
FIGURE 30. NEPTUNIUM TARGET ROD 2 AS-POLISHED METALLOGRAPHIC SAMPLE 1 FROM SECTION D



500X

a. Edge

HC32405



500X

b. Center

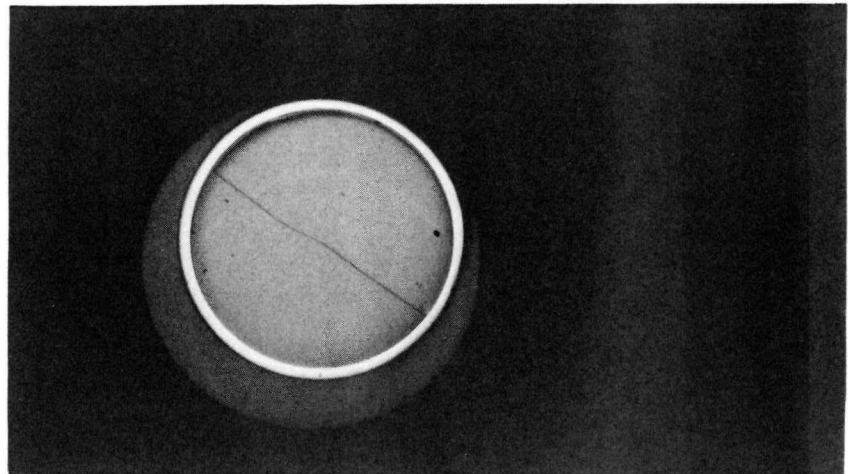
HC32404



100X

c. Typical

HC32401

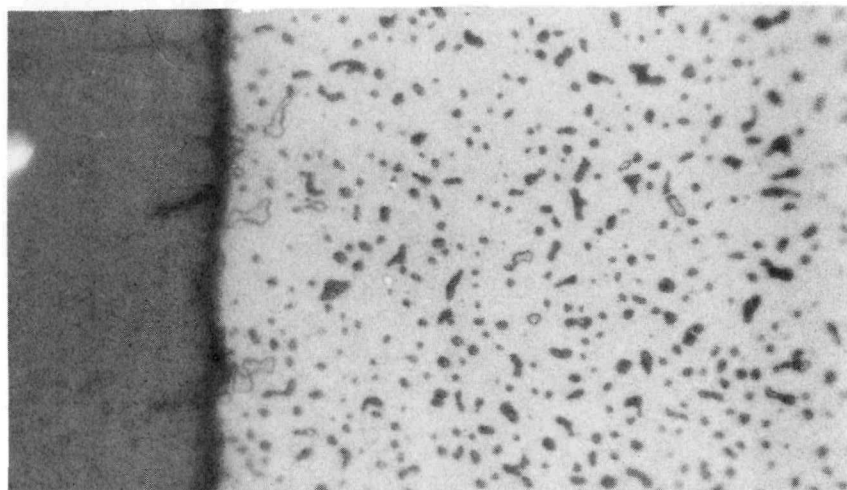


3.5X

d. Macro

HC32363

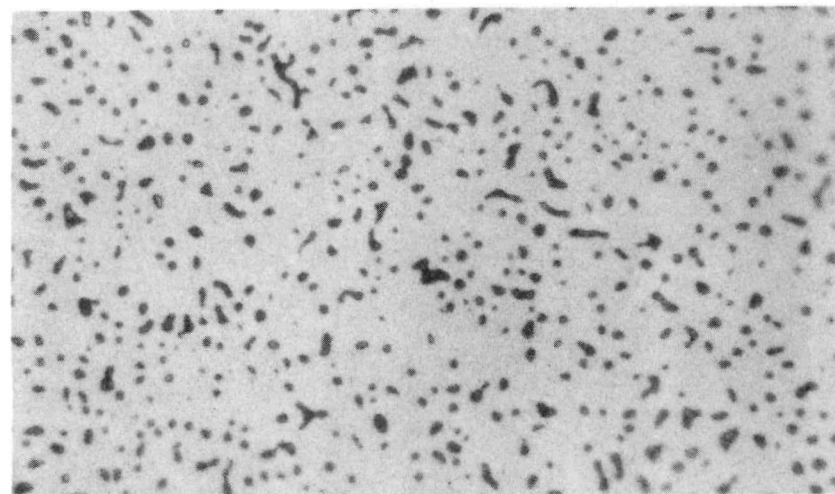
FIGURE 31. NEPTUNIUM TARGET ROD 2 AS-POLISHED METALLOGRAPHIC SAMPLE 3 FROM SECTION D



500X

HC32397

a. Edge



500X

HC32396

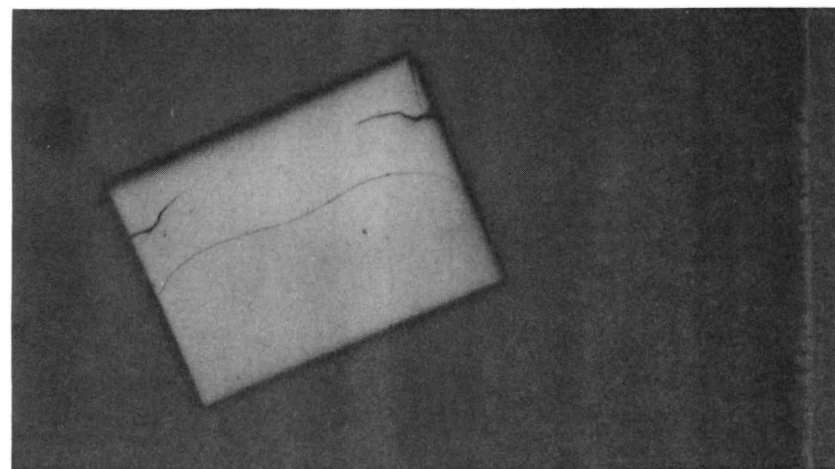
b. Center



100X

HC32392

c. Typical

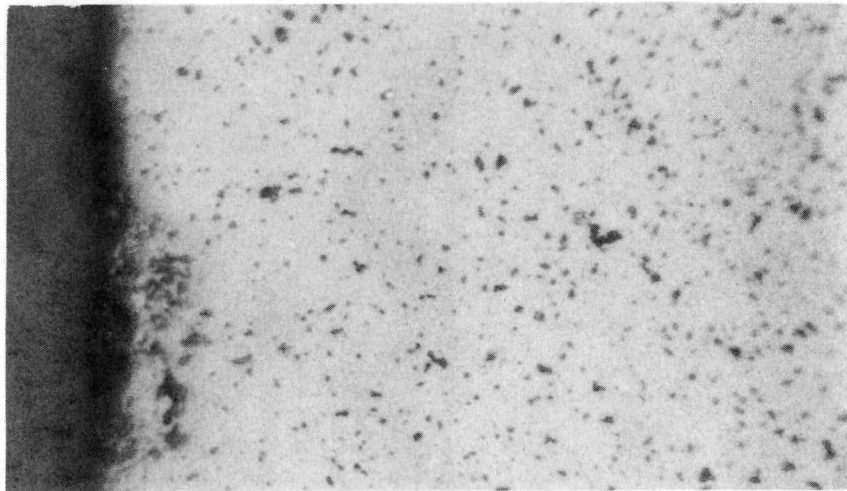


3.5X

HC32362

d. Macro

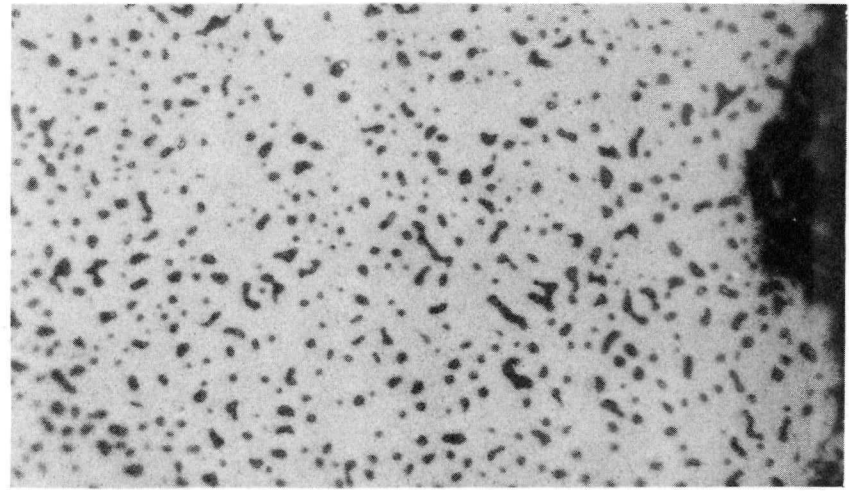
FIGURE 32. NEPTUNIUM TARGET ROD 2 AS-POLISHED METALLOGRAPHIC SAMPLE 4 FROM SECTION D



500X

a. Edge

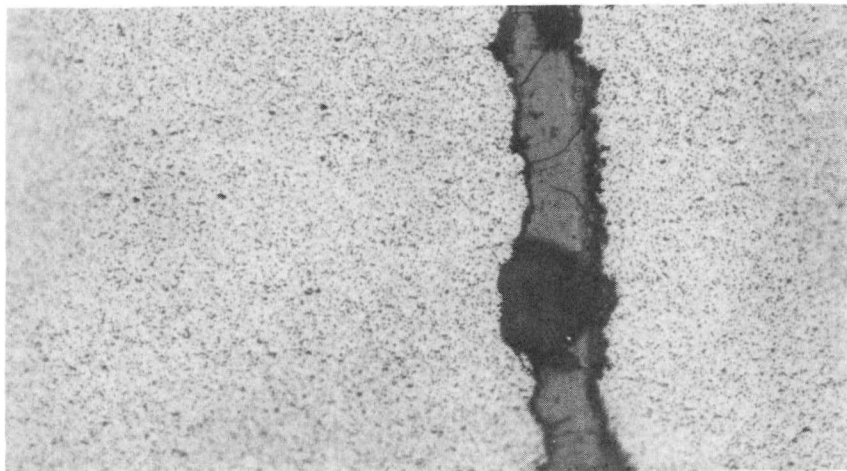
HC32389



500X

b. Center

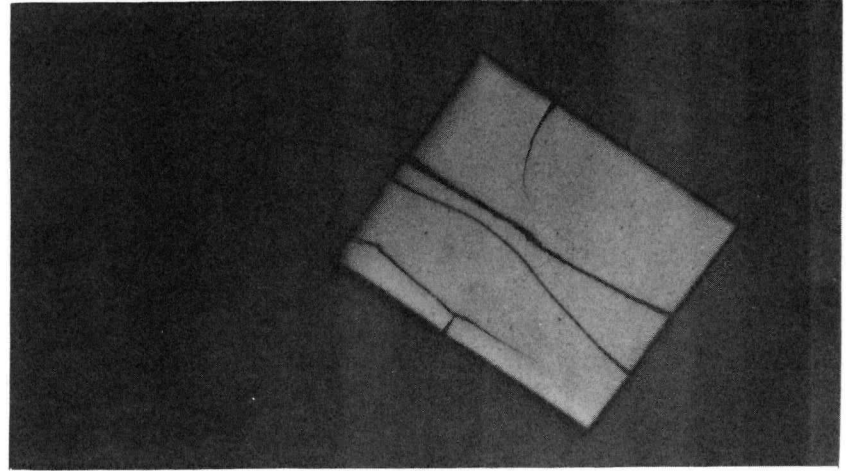
HC32388



100X

c. Typical

HC32387

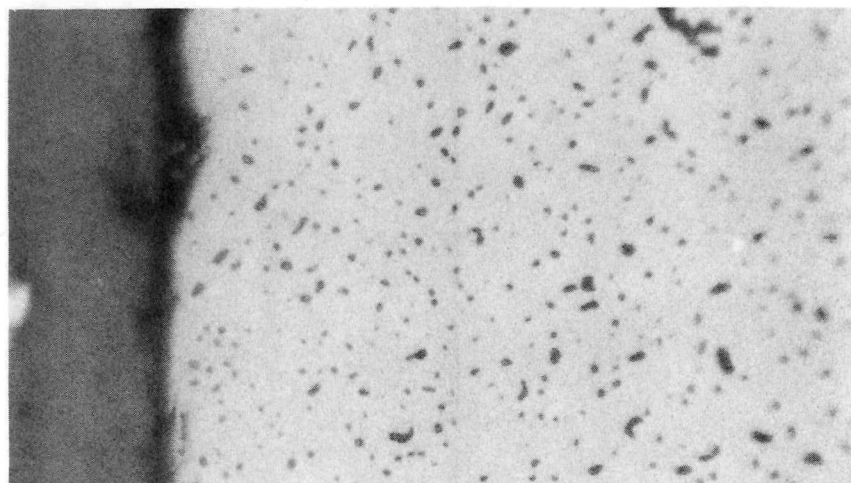


3.5X

d. Macro

HC32361

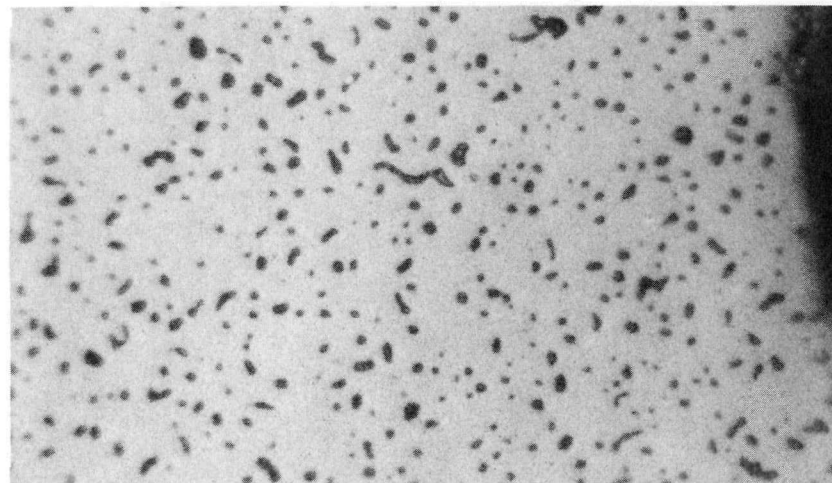
FIGURE 33. NEPTUNIUM TARGET ROD 2 AS-POLISHED METALLOGRAPHIC SAMPLE 6 FROM SECTION C



500X

HC32380

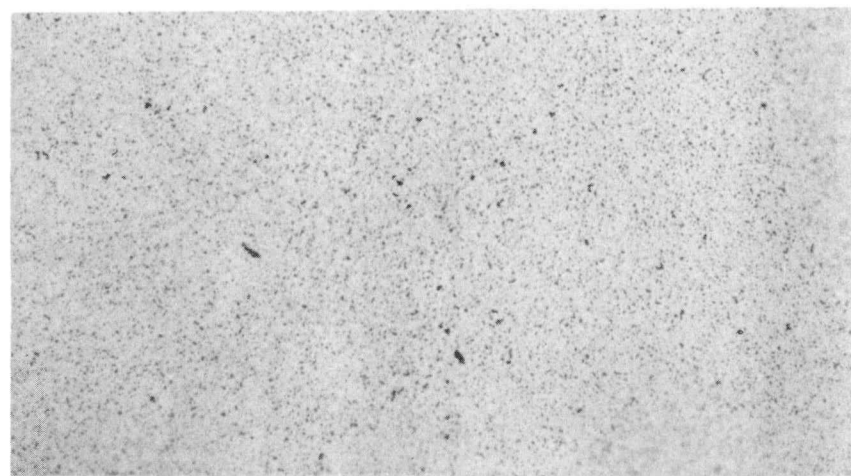
a. Edge



500X

HC32381

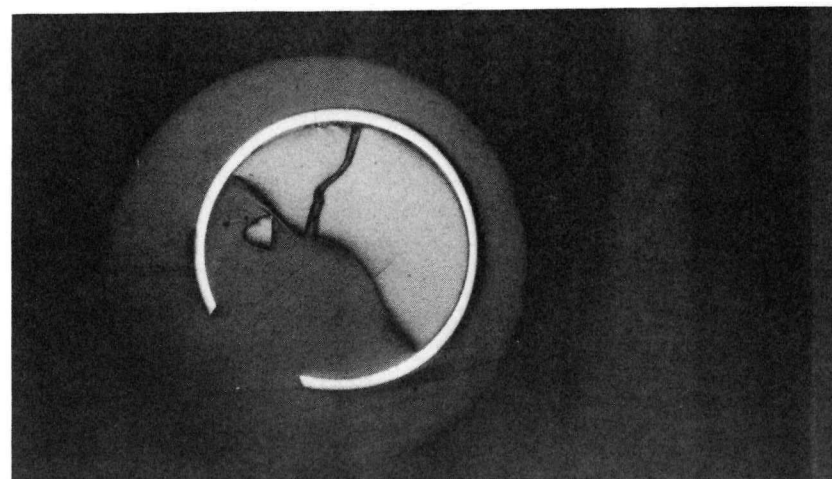
b. Center



100X

HC32376

c. Typical

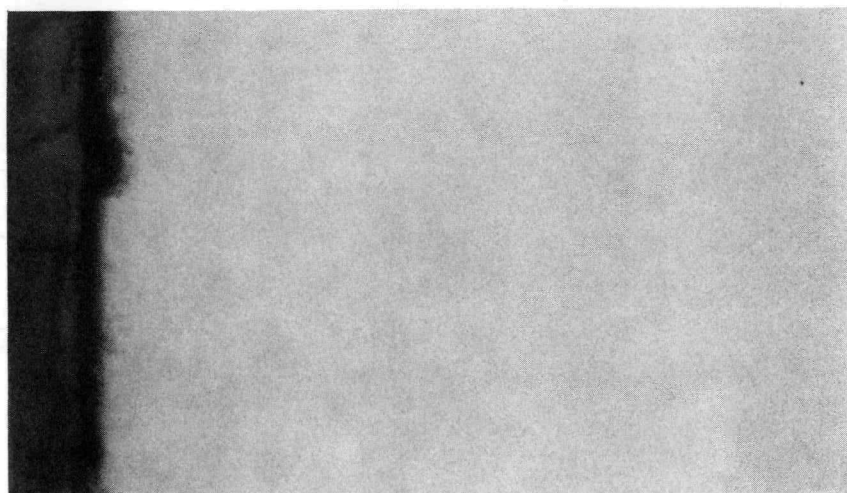


3.5X

HC32360

d. Macro

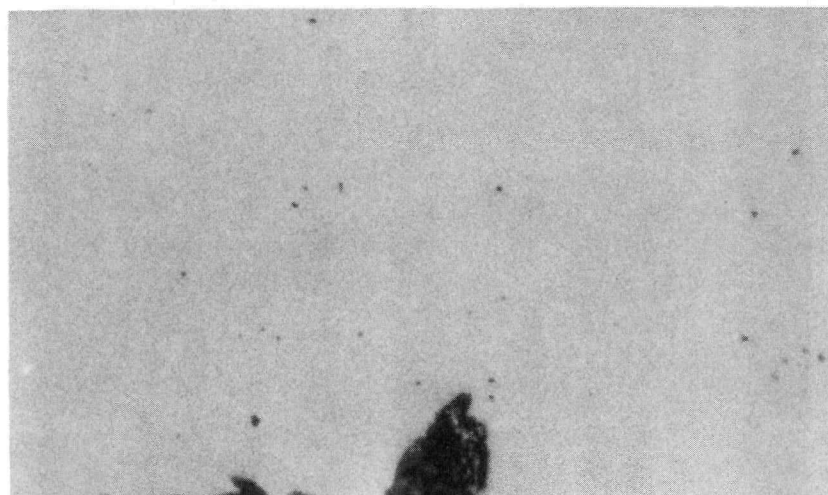
FIGURE 34. NEPTUNIUM TARGET ROD 2 AS-POLISHED METALLOGRAPHIC SAMPLE 8 FROM SECTION B



500X

a. Edge

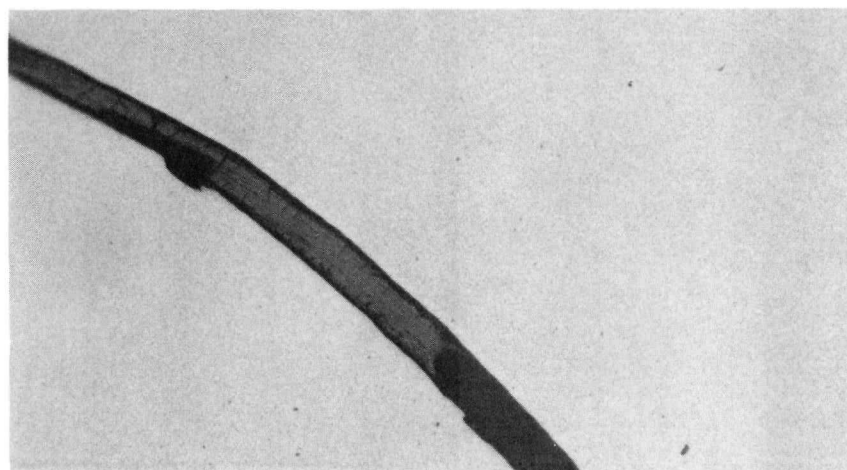
HC32371



500X

b. Center

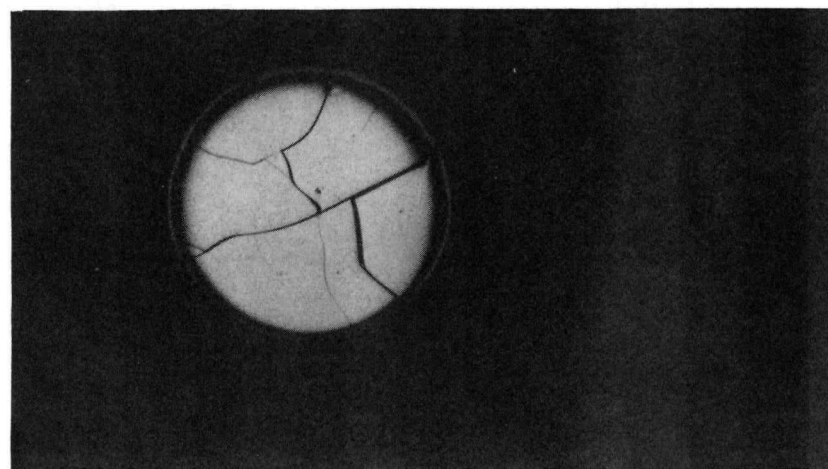
HC32372



100X

c. Typical

HC32367



3.5X

d. Macro

HC32359

FIGURE 35. NEPTUNIUM TARGET ROD 2 AS-POLISHED METALLOGRAPHIC SAMPLE 11 FROM SECTION A

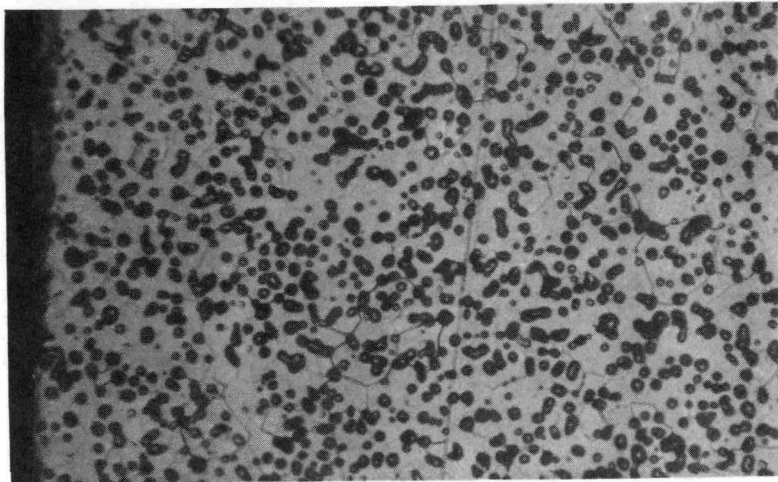
Under metallographic examination in the etched condition, there appears to be no incompatibility between the cladding and fuel, and other than cracking of the fuel there are no detectable defects.

Etching of the target material was accomplished by immersion in a solution of 75 parts HCl/75 parts HBr, and 2 parts HF for 60 minutes. Etched microstructures, as shown in Figures 36 through 41, appear essentially identical to the preirradiation structures. Note that consistent with the modest irradiation temperatures and heat generation rates, the grain size is uniform over the entire cross section. It should be pointed out that the etchant tended to enlarge the pores so that the pores in the etched condition appear to be larger than in the as-polished condition. Also, the microstructure of the irradiated cladding is very similar to microstructure of the unirradiated cladding. Of particular interest is the absence of any indication of intergranular attack in the irradiated stainless steel claddings. The intergranular attack observed during out-of-pile compatibility tests occurred at high temperatures (500 C). The results of the irradiation tests show that there is no compatibility problem at the lower irradiation temperature (~315 C).

Postirradiation Chemical Analyses

Six pellets were selected from target Rod Number 2 for analysis of neptunium and plutonium, ppm Pu-236 in Pu-238, and plutonium isotopic composition. To obtain a representative sample, the entire pellet was pulverized to -60 mesh in a Diamond-Plattner type crusher. The samples were then ground to -200 mesh with a remote motorized mortar and pestle. Extreme care was taken in both the crushing and grinding operations to avoid impurity contamination and sample cross-contamination.

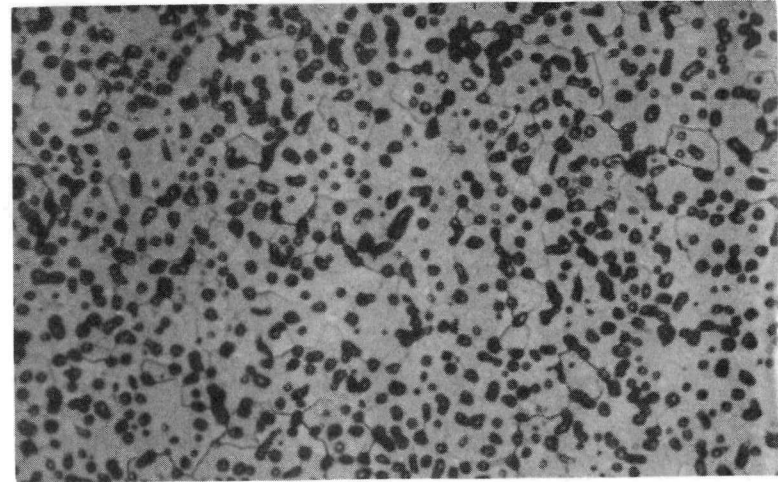
Approximately one gram samples, weighed to ± 0.0001 gram, were transferred to the chemistry cell for dissolution in preparation for the neptunium and plutonium analyses. They were initially reacted in a 6N HCl-1N HF solution containing a small amount of H_2O_2 . Final dissolution was achieved by fuming in H_2SO_4 . The samples were subsequently diluted to 100 ml and aliquots analyzed for total plutonium and neptunium by controlled-potential coulometry. Results are shown in Table 20.



500X

HC34857

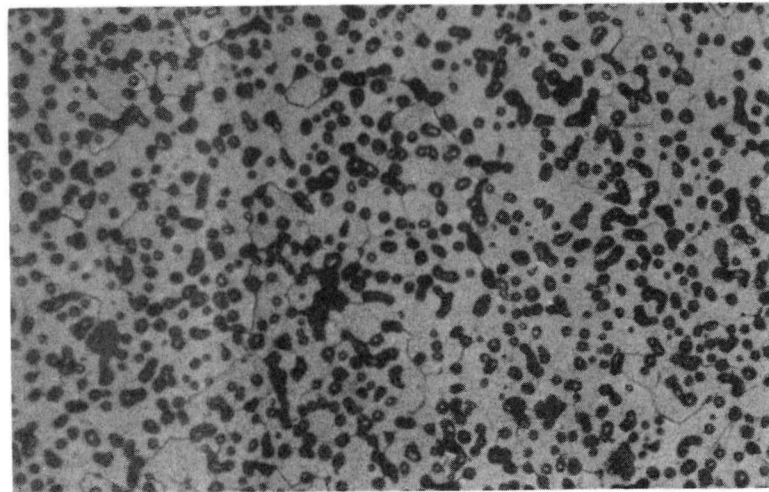
a. Edge



500X

HC34858

b. 1/2 Radius

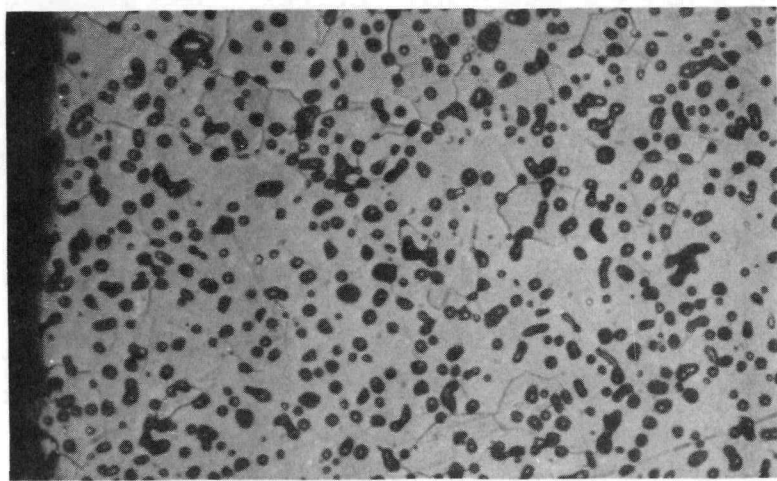


500X

HC34859

c. Center

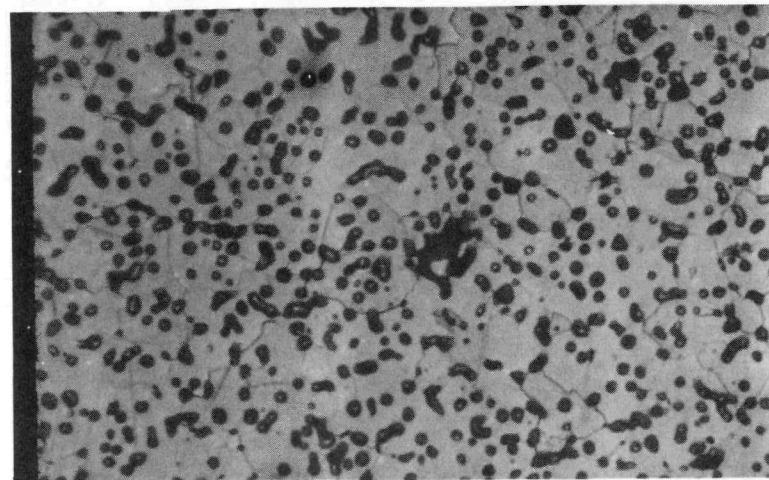
FIGURE 36. IRRADIATED NpO_2 TARGET METALLOGRAPHIC SAMPLE D-1, ETCHED CONDITION



500X

HC34851

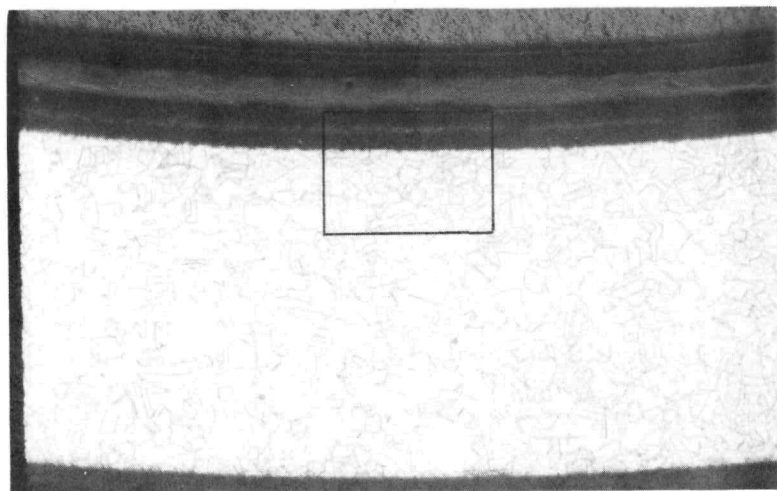
a. Edge



500X

HC34853

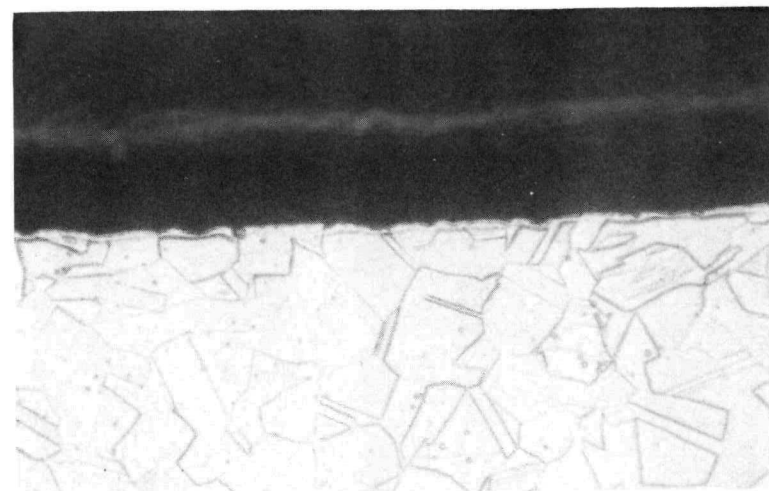
b. Center



100X

HC34860

c. Clad

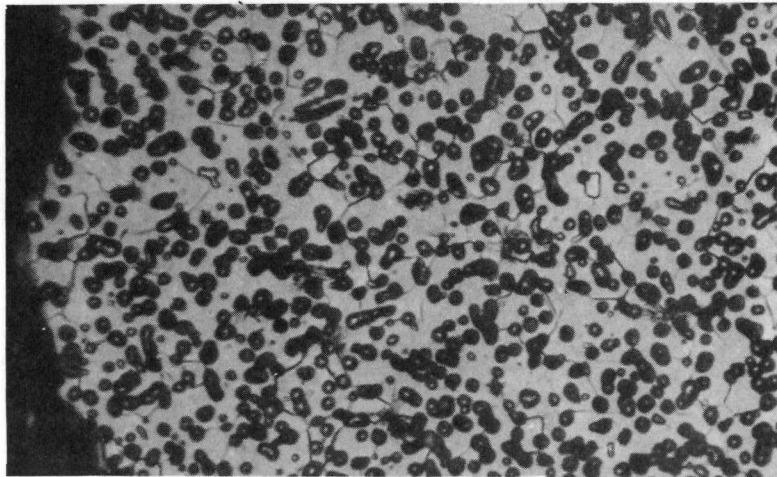


500X

HC34861

d. Clad I. D.

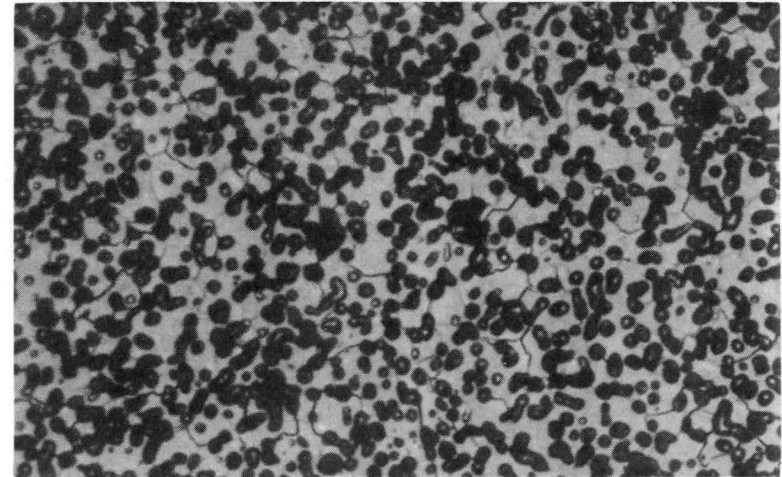
FIGURE 37. IRRADIATED NpO_2 TARGET AND CLAD METALLOGRAPHIC SAMPLE D-3, ETCHED



500X

HC34845

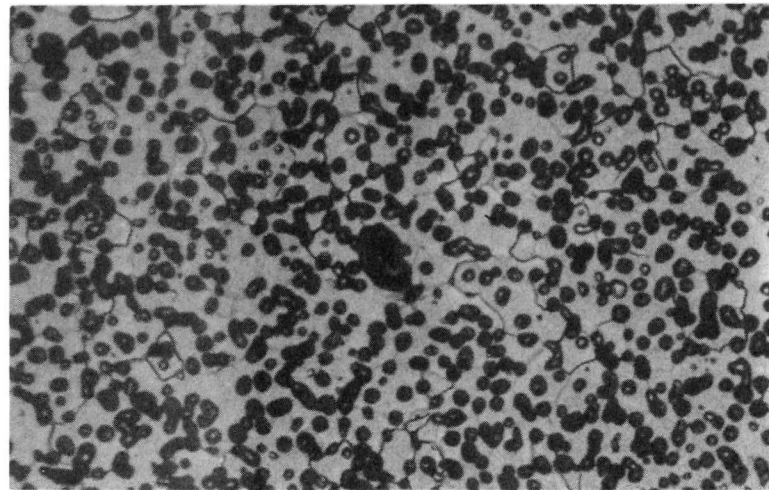
a. Edge



500X

HC34846

b. 1/2 Radius

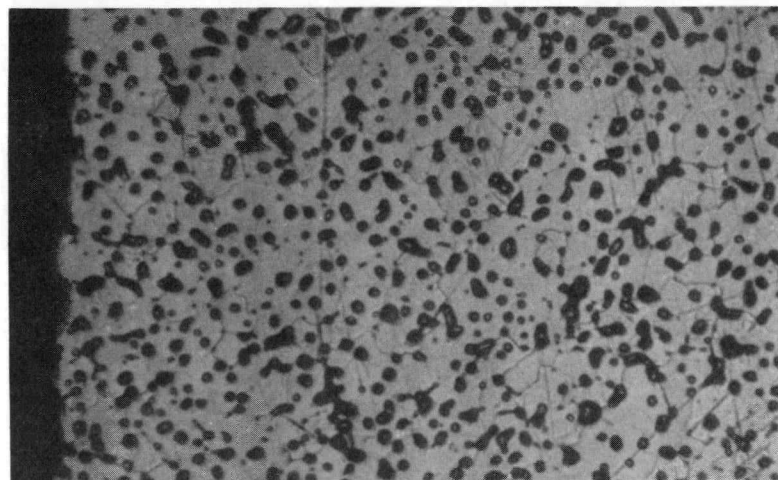


500X

HC34847

c. Center

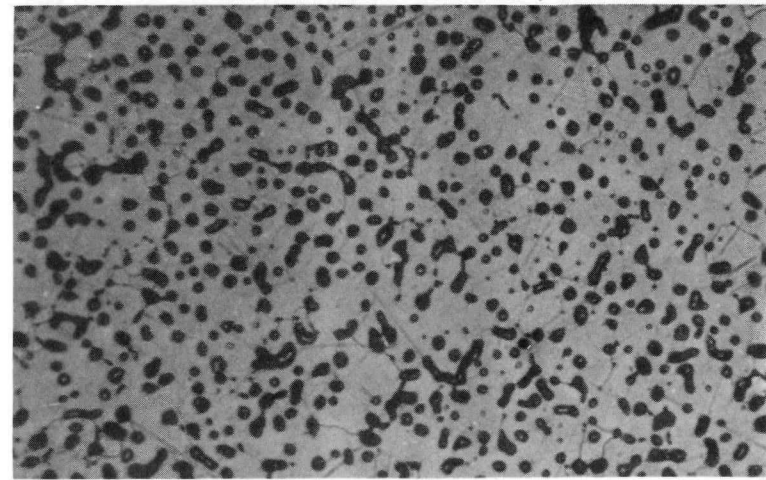
FIGURE 38. IRRADIATED NpO_2 TARGET METALLOGRAPHIC SAMPLE D-4, ETCHED



500X

a. Edge

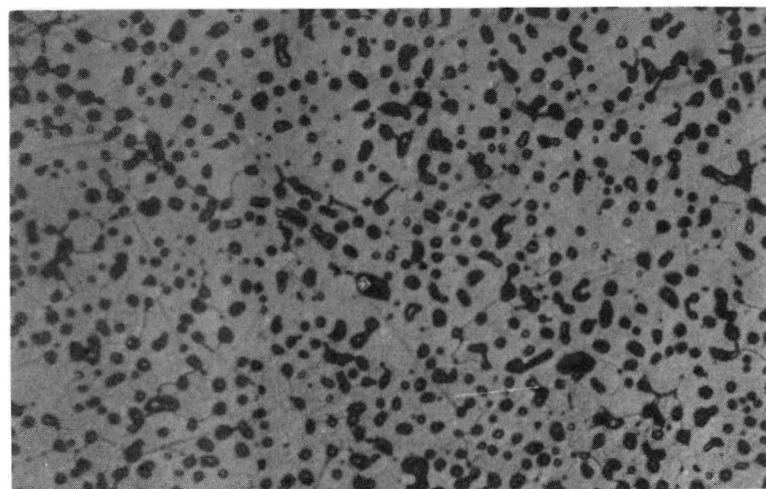
HC34854



500X

b. 1/2 Radius

HC34855

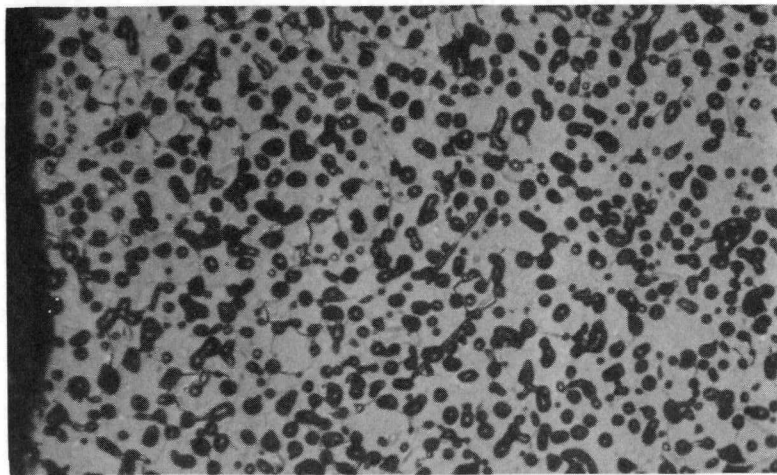


500X

c. Center

HC34856

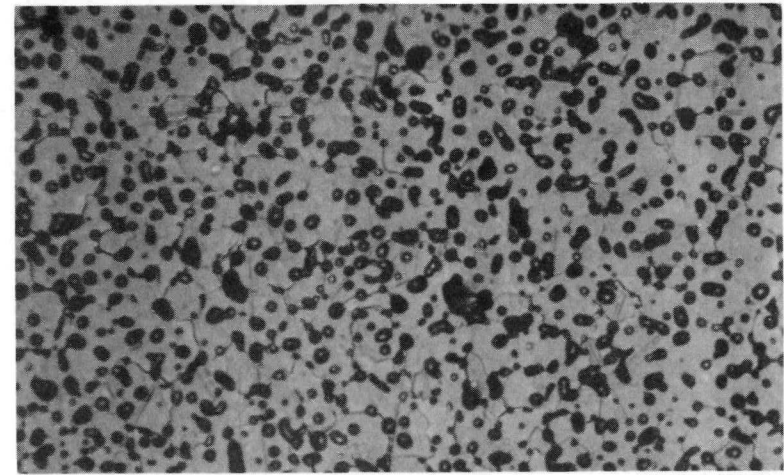
FIGURE 39. IRRADIATED NpO_2 TARGET METALLOGRAPHIC SAMPLE C-6, ETCHED



500X

HC34848

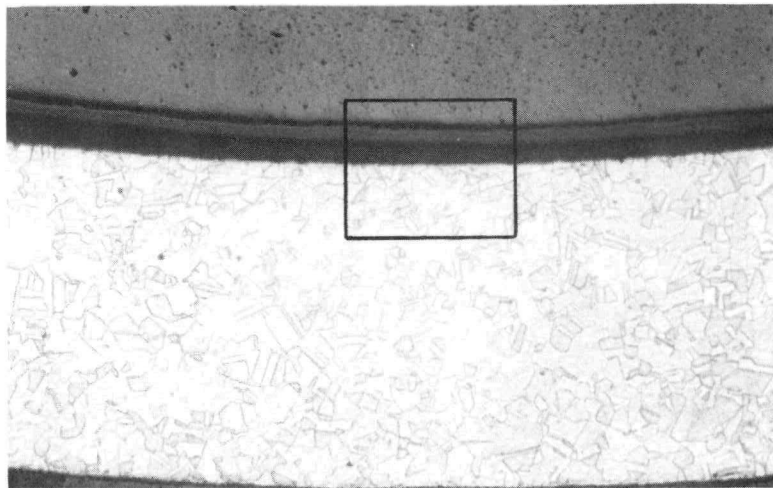
a. Edge



500X

HC34850

b. Center



100X

HC34843

c. Clad

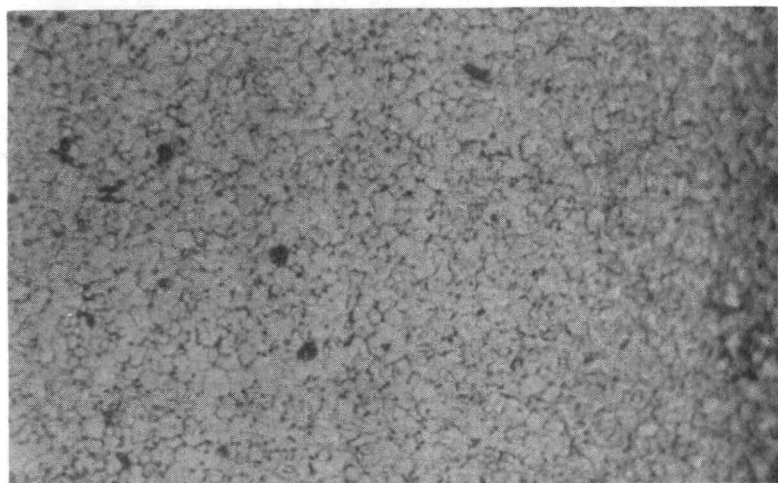


500X

HC34844

d. Clad I. D.

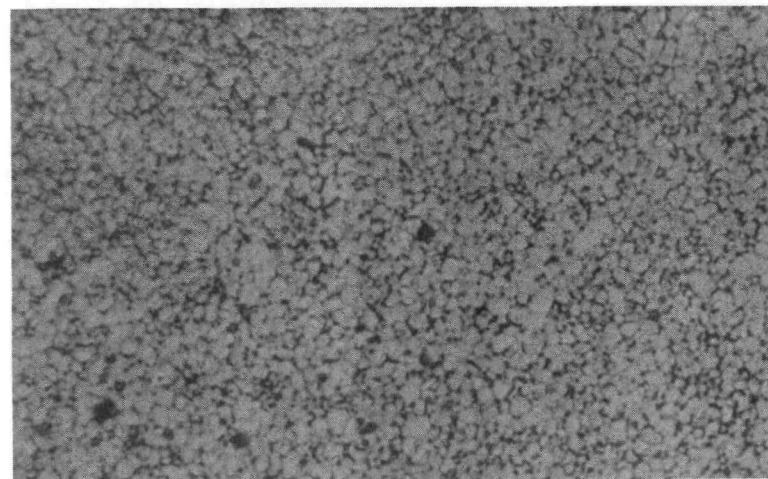
FIGURE 40. IRRADIATED NpO_2 TARGET AND CLAD METALLOGRAPHIC SAMPLE B-8, ETCHED



500X

a. Edge

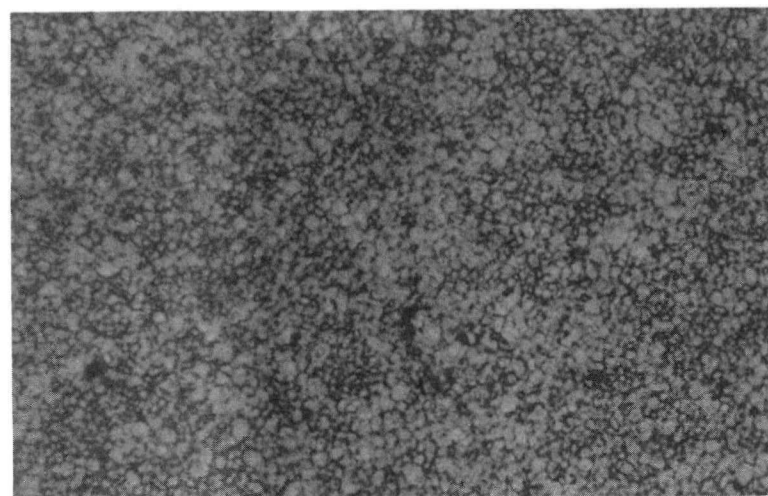
HC34947



500X

b. 1/2 Radius

HC34946



500X

c. Center

HC34945

FIGURE 41. IRRADIATED NpO_2 TARGET METALLOGRAPHIC SAMPLE A-11, ETCHED

TABLE 20. RESULTS OF BCL CHEMICAL ANALYSES OF IRRADIATED NpO_2 TARGETS⁽¹⁾

Sample No.	Specimen Type	Inches From Top of Assembly	Sample Weight, g	Np, g		Np Transmuted, %	Plutonium		
				Before	After		g	%	% Np
1	D	17.6	0.9961	0.1284	0.1052	18.1	0.0212	2.13	16.5
2	D	28.6	0.9824	0.1267	0.0927	26.8	0.0238	2.42	18.8
4	D	53.6	0.8998	0.1161	0.0846	27.1	0.0260	2.89	22.4
7	C	82.4	0.9503	0.2136	0.1482	30.6	0.0347	3.65	16.2
9	B	93.1	0.8549	0.3349	0.2741	18.2	0.0447	5.23	13.3
11	A	99.4	0.8415	0.5315	0.4288	19.3	0.0484	5.75	9.11

(1) Preirradiation analysis: D = 14.65% NpO_2

C = 25.53 "

B = 44.47 "

A = 71.69 "

Aliquots of the solutions were diluted 200-fold in 8N HNO₃ for the Pu-236 concentration and plutonium isotopic analyses. Two- to three-milliliter aliquots were taken from these solutions under identical conditions for shipment to SRL and Mound Laboratory (MLM). These two laboratories performed the analyses for Pu-236 content in the Pu-238 by high resolution alpha spectrometry on purified sample fractions. The analytical results from SRL and MLM were in excellent agreement (see Table 21). The plutonium isotopic analysis was obtained at SRL by surface ionization mass spectrometry on the solution samples while independent powder samples were analyzed by Los Alamos Scientific Laboratory (LASL). The results of the isotopic analyses are presented in Table 22.

Total plutonium analyses on the diluted solutions were determined at SRL by total alpha counting adjusted for plutonium isotopic abundance. At LASL, total plutonium content was determined by isotope dilution mass spectrometry. Neptunium was analyzed by alpha counting after separation from the plutonium by anion exchange. These data are presented in Table 23. All plutonium and neptunium analytical results are summarized in Table 23. The analytical results for plutonium are in good concurrence for the three laboratories, but about 30 to 60 percent lower than the predicted values. For neptunium, the LASL and BCL analytical values are in good agreement at the lower NpO₂ concentration in the target material, but in relatively poor agreement at the higher concentrations. In this instance the predicted values are in good agreement with the BCL values throughout the range of target concentrations. Considering these facts, it seems reasonable to assume that some factor in the theoretical analysis for plutonium formation may be in error.

Electron Microprobe Analysis

Electron microprobe analysis was performed on four irradiated pellets to: (1) determine relative Pu/Np/Zr ratios, (2) establish the magnitude of the flux depression, and (3) integrate the Pu/Np ratio over the pellet area as an independent method of determining total Pu. A Materials Analysis Corporation (MAC) Model 450 shielded electron microprobe was used for these analyses.

TABLE 21. RESULTS OF ANALYSIS FOR Pu²³⁶ CONTENT IN THE Pu²³⁸

Sample Number	Pu ²³⁶ in Pu ²³⁸ , ppm		SNE ⁽¹⁾
	SRL	MLM	
D-1	8.9 ± 0.3	9.5 $\begin{smallmatrix} + 7 \\ - 10 \end{smallmatrix}$ %	9.54
D-2	8.9 ± 0.3	8.5 $\begin{smallmatrix} + 7 \\ - 10 \end{smallmatrix}$ %	9.35
D-4	8.8 ± 0.2	8.7 $\begin{smallmatrix} + 7 \\ - 10 \end{smallmatrix}$ %	9.17
C-7	10.6 ± 0.1	11.0 $\begin{smallmatrix} + 6 \\ - 9 \end{smallmatrix}$ %	10.60
B-9	13.9 ± 0.2	12.6 $\begin{smallmatrix} + 6 \\ - 8 \end{smallmatrix}$ %	12.59
A-11	20.2 ± 0.2	20.7 $\begin{smallmatrix} + 4 \\ - 7 \end{smallmatrix}$ %	17.60

(1) Predicted by SNE⁽⁹⁾ using branching ratio of 0.57 and revised cross sections for Np²³⁷.

TABLE 22. RESULTS OF PLUTONIUM ISOTOPIIC ANALYSES

Sample Number	Pu Isotopic Concentration, atom percent														
	238			239			240			241			242		
	SRL	LASL	SNE ⁽¹⁾	SRL	LASL	SNE ⁽¹⁾	SRL	LASL	SNE ⁽¹⁾	SRL	LASL	SNE ⁽¹⁾	SRL	LASL	SNE ⁽¹⁾
D-1	92.91	92.57	92.70	6.27	6.54	6.42	0.611	0.665	0.676	0.199	0.210	0.201	0.013	0.014	0.012
D-2	91.39	91.07	90.46	7.38	7.65	8.00	0.861	0.913	1.075	0.338	0.345	0.428	0.027	0.027	0.033
D-4	90.71	90.65	89.30	7.85	7.94	8.74	0.983	0.984	1.31	0.417	0.390	0.602	0.035	0.032	0.057
C-7	91.61	92.41	90.23	7.20	6.62	7.91	0.829	0.691	1.22	0.334	0.264	0.586	0.025	0.019	0.058
B-9	93.18	93.81	92.29	6.01	5.52	6.28	0.579	0.485	0.954	0.221	0.176	0.454	0.013	0.010	0.027
A-11	94.95	94.96	94.68	4.58	4.57	4.34	0.346	0.340	0.643	0.120	0.115	0.30	<0.01	0.012	0.028

(1) Predicted values.

TABLE 23. SUMMARY OF CHEMICAL ANALYSIS OF NEPTUNIA TARGET RODS

Sample Number	Location ⁽¹⁾	Plutonium, w/o				Neptunium, w/o		
		BCL	LASL	SRL	SNE ⁽²⁾	BCL	LASL	SNE
D-1	17.6	2.13	2.11	1.95	2.54-2.60	10.6	10.8	10.41
D-2	28.6	2.42	2.59	2.28	3.19-3.32	9.44	10.5	9.5
D-4	53.6	2.89	2.71	2.60	3.57-3.69	9.40	10.2	9.17
C-7	70.0	3.65	3.63	3.35	5.41-5.89	15.6	21.4	16.85
B-9	93.1	5.23	4.88	5.12	7.71-8.45	32.1	25.0	31.10
A-11	99.4	5.75	6.16	5.40	8.72-9.37	51.0	58.6	54.11

(1) Inches from top of assembly.

(2) Predicted values.

Prior to scanning the irradiated samples, four unirradiated pellets were scanned to establish optimum conditions and to calibrate the system. Since three elements or X-ray emissions can be observed simultaneously, the neptunium M_{α} , zirconium L_{α} , and calcium K_{α} (from CaO stabilizer in ZrO_2) X-ray intensities were characterized over the pellet diameters. Standard curves were established for the four NpO_2 compositions, and compared with a 100 percent plutonium metal standard for future reference ($^{94}Pu M_{\alpha}$ X-ray efficiency would be very close to that of $^{93}Np M_{\alpha}$). Excellent results were obtained for the standard curve of neptunium M_{α} X-ray intensity versus w/o NpO_2 (see Figure 42). The microprobe scans across the four unirradiated samples produced flat intensity profiles which indicated that the target material was homogeneous. Only a few NpO_2 - or ZrO_2 -rich areas were noted (see Figures 43 and 44). Figure 43 shows a ZrO_2 -rich area approximately 15 microns across as indicated by a calcium and zirconium X-ray intensity increase and a neptunium X-ray intensity decrease. Figure 44 is the reverse case and shows a NpO_2 -rich area approximately 60 microns across, which was the largest particle seen in any of the other unirradiated or irradiated pellets. This illustrates a "worst case" situation since it was an unirradiated sample of poor consistency.

After all parameters were characterized on the unirradiated samples, the four irradiated specimens were traversed as shown in Figures 45 through 48. Resultant typical X-ray intensity profiles are illustrated in Figures 49 through 52. Figure 49 shows the sensitivity of the microprobe and illustrates the difference between a pore and a depletion area. In this case all profiles show a dip indicating a pore (~ 10 microns). The resolution of the microprobe (minimum particle size detectable) is 5 microns under the conditions of the experiment. Figure 50 illustrates a Np-Pu depleted area. From the eight samples scanned, approximately 95 percent had particle sizes of less than 10 microns.

Plutonium diametral X-ray intensity scans clearly demonstrate the flux depression (edge to center) variance from 13.0 to 44.8 percent over the range 14.65 to 71.69 w/o NpO_2 fuel (Figures 53 through 56). Conversely, neptunium X-ray intensities showed edge-to-center percentage increases from

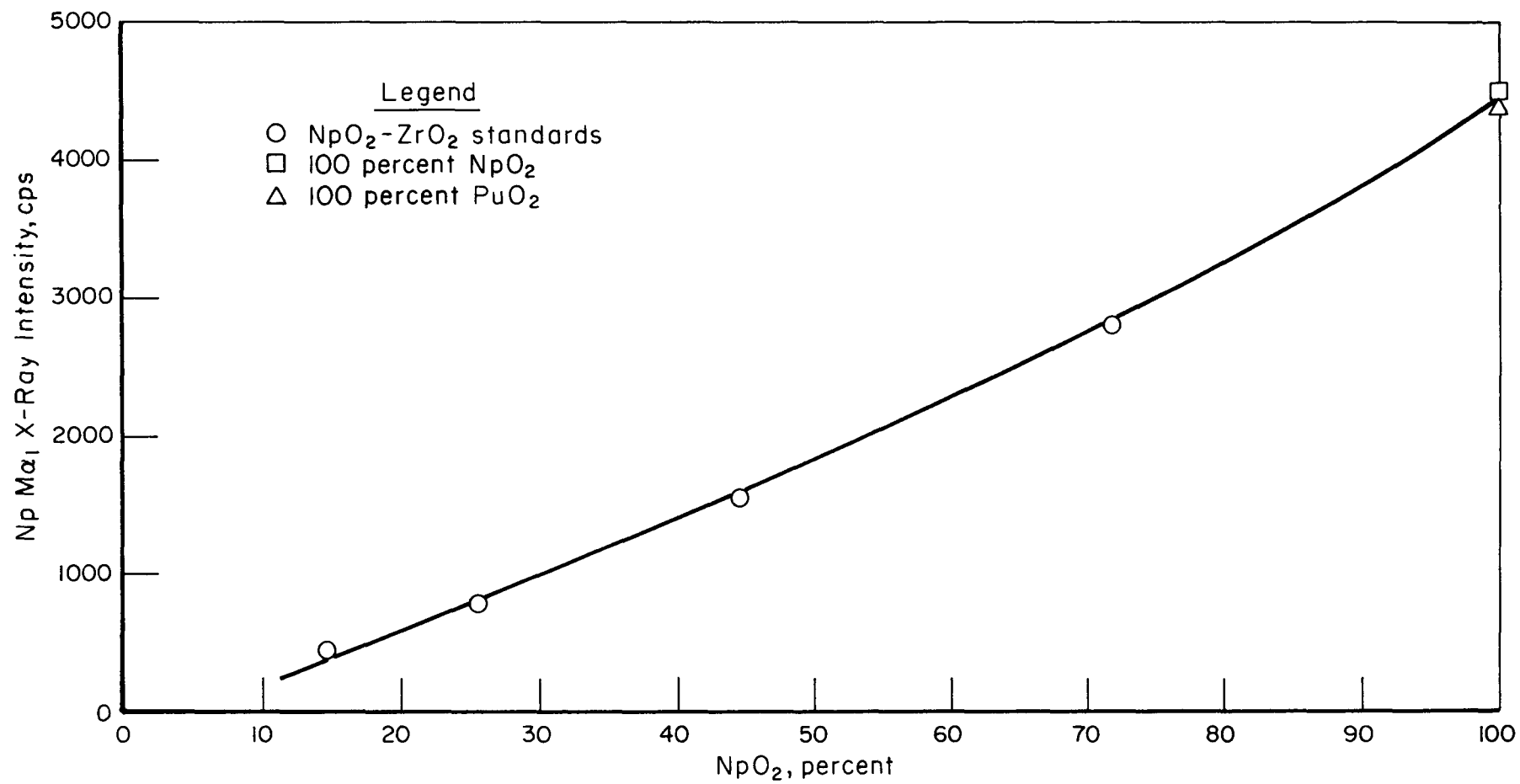


FIGURE 42. NEPTUNIUM Ma_1 X-RAY INTENSITY VERSUS PERCENT NpO_2

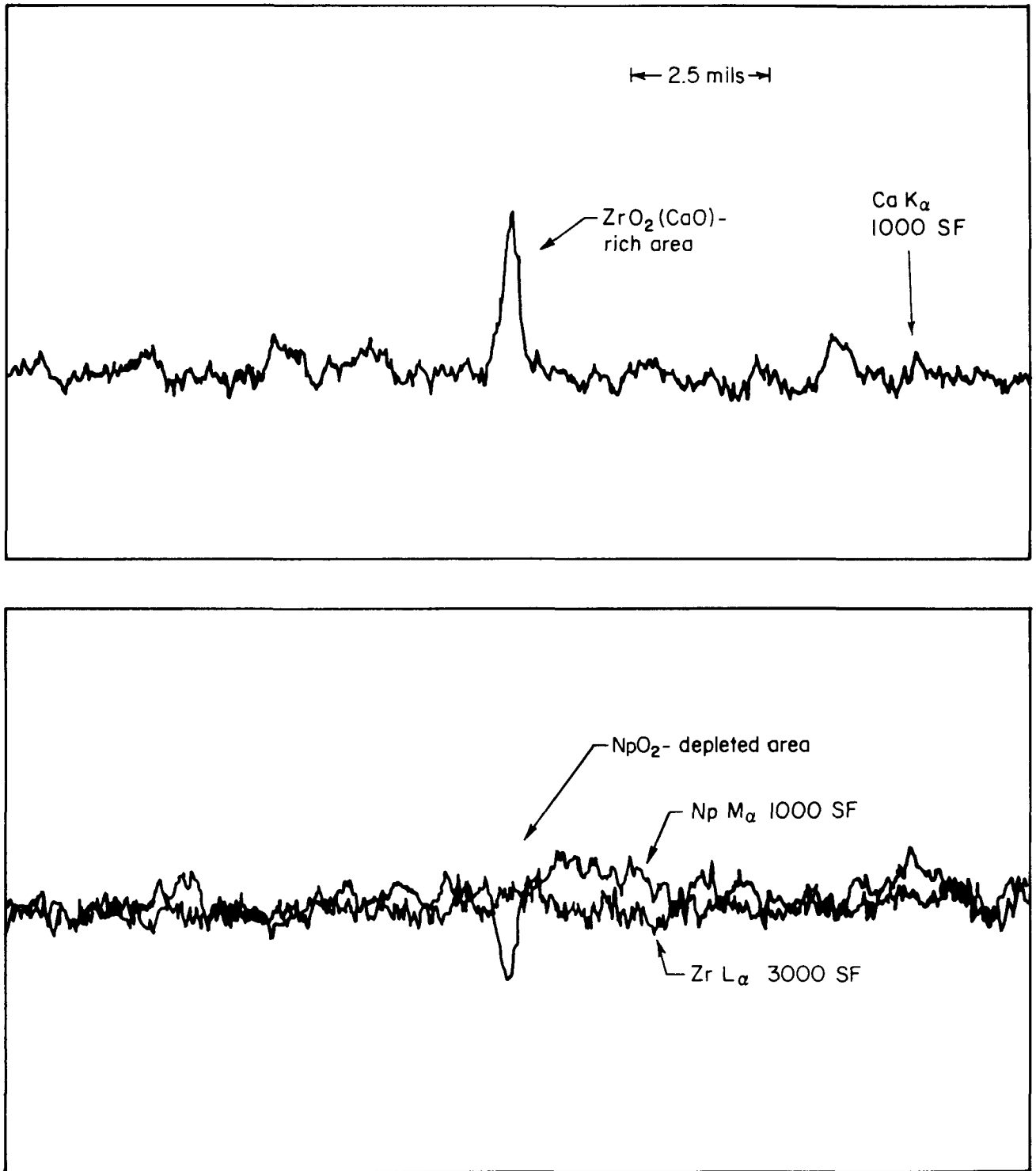


FIGURE 43. UNIRRADIATED STANDARD 2D-35 MICROPROBE SCAN SHOWING ZrO₂-RICH AREA

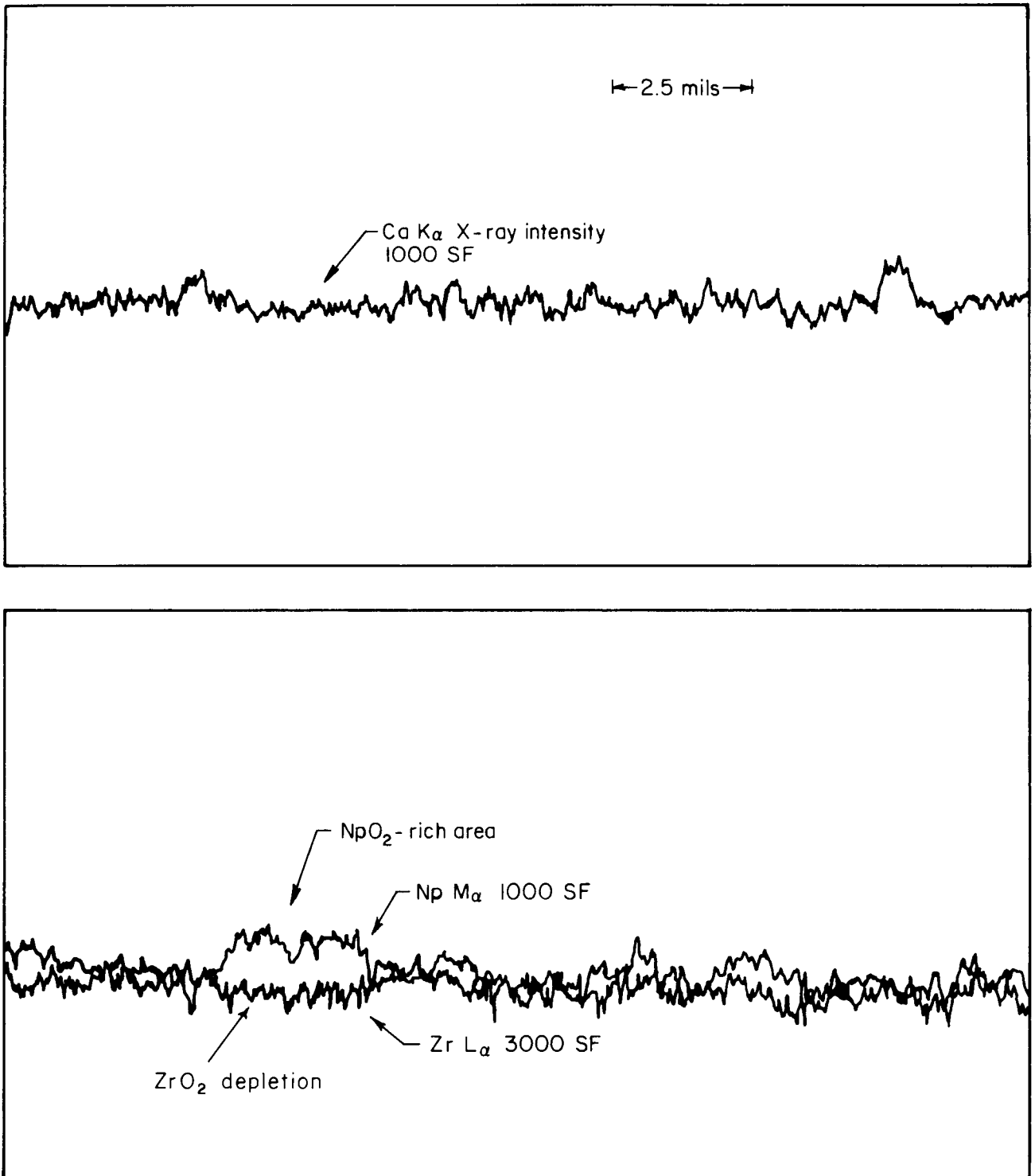


FIGURE 44. UNIRRADIATED STANDARD 2D-35 MICROPROBE SCAN SHOWING NpO $_2$ -RICH AREA

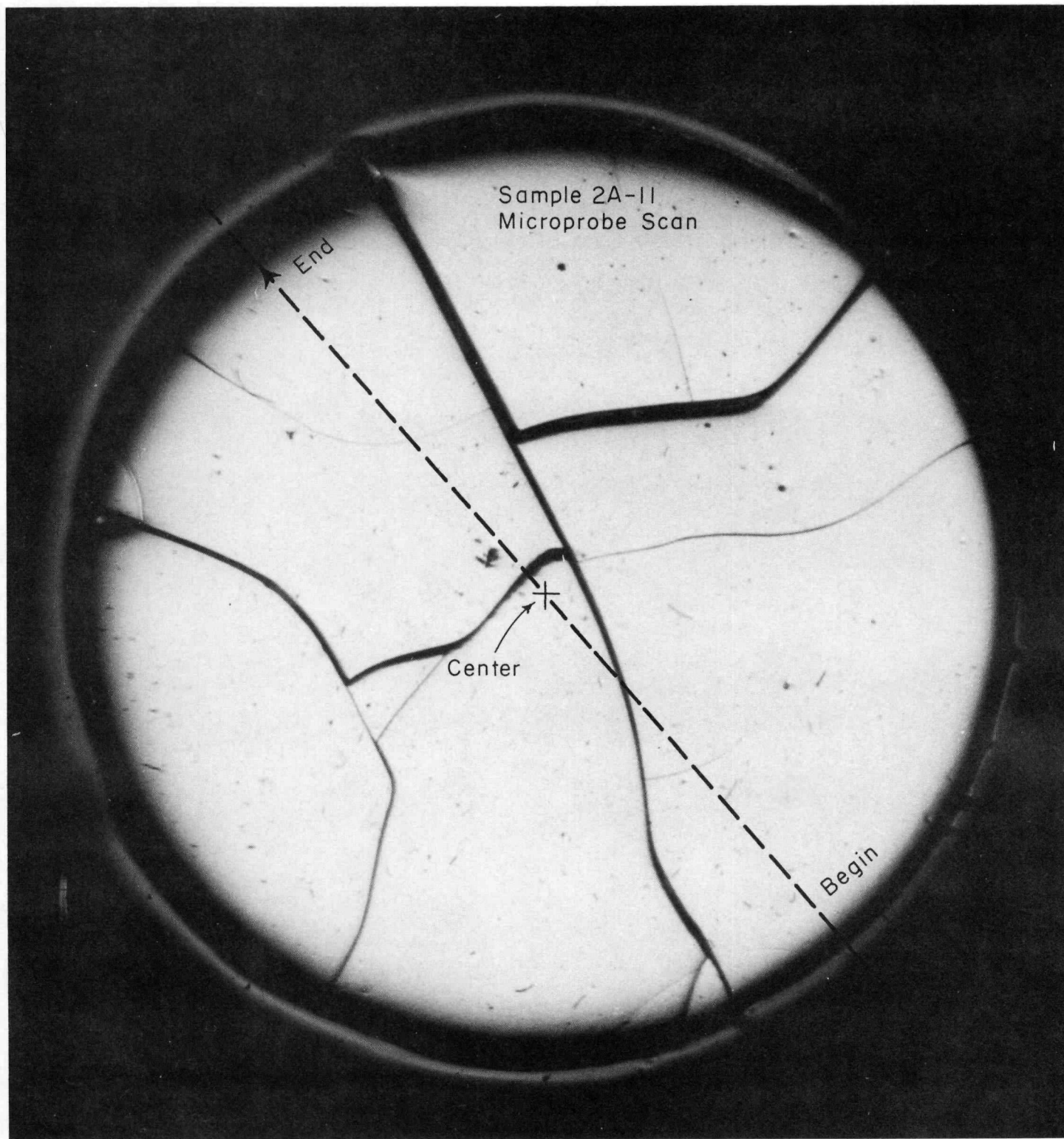


FIGURE 45. SAMPLE 2A-11 MICROPROBE SCAN

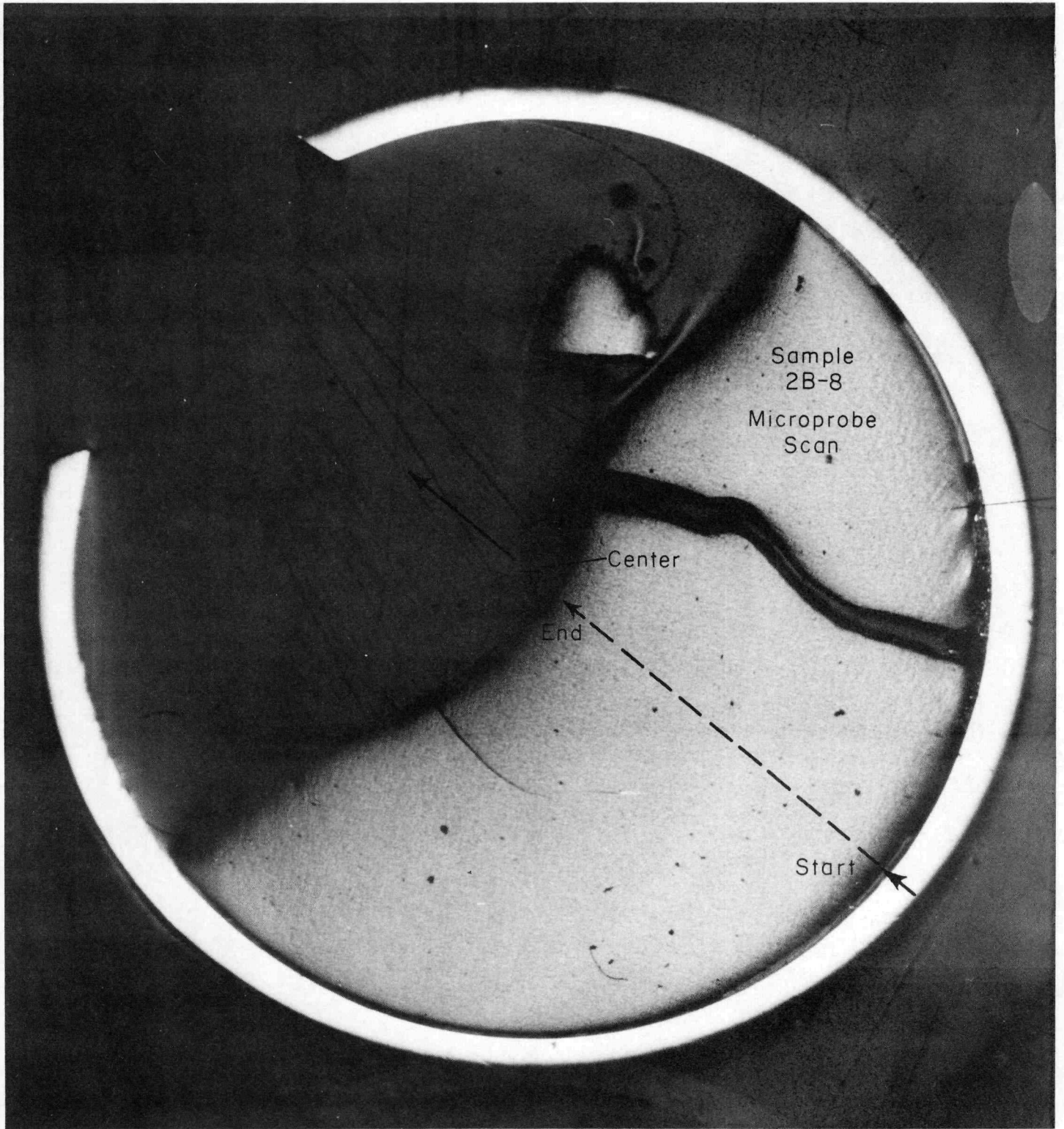


FIGURE 46. SAMPLE 2B-8 MICROPROBE SCAN

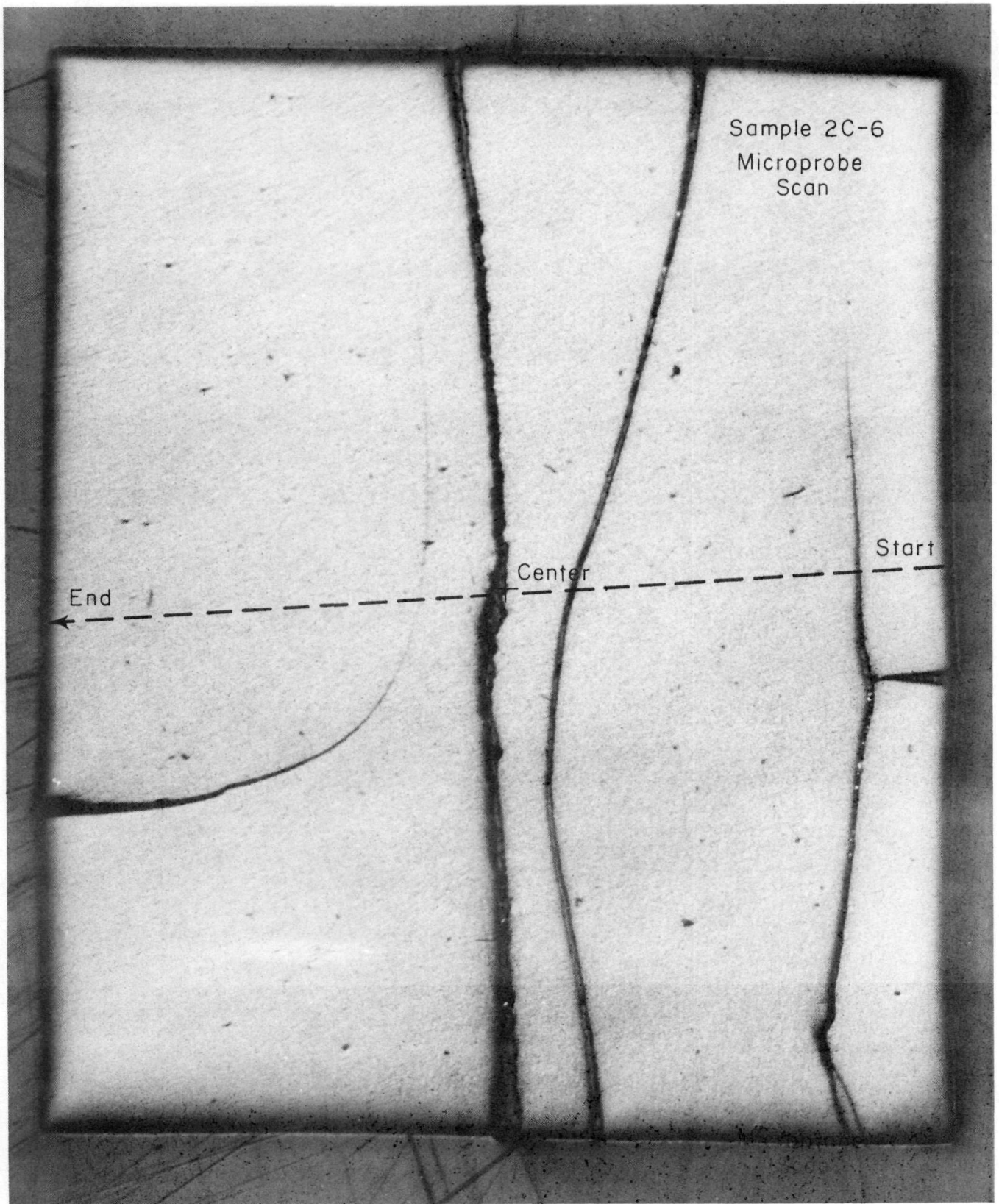


FIGURE 47. SAMPLE 2C-6 MICROPROBE SCAN

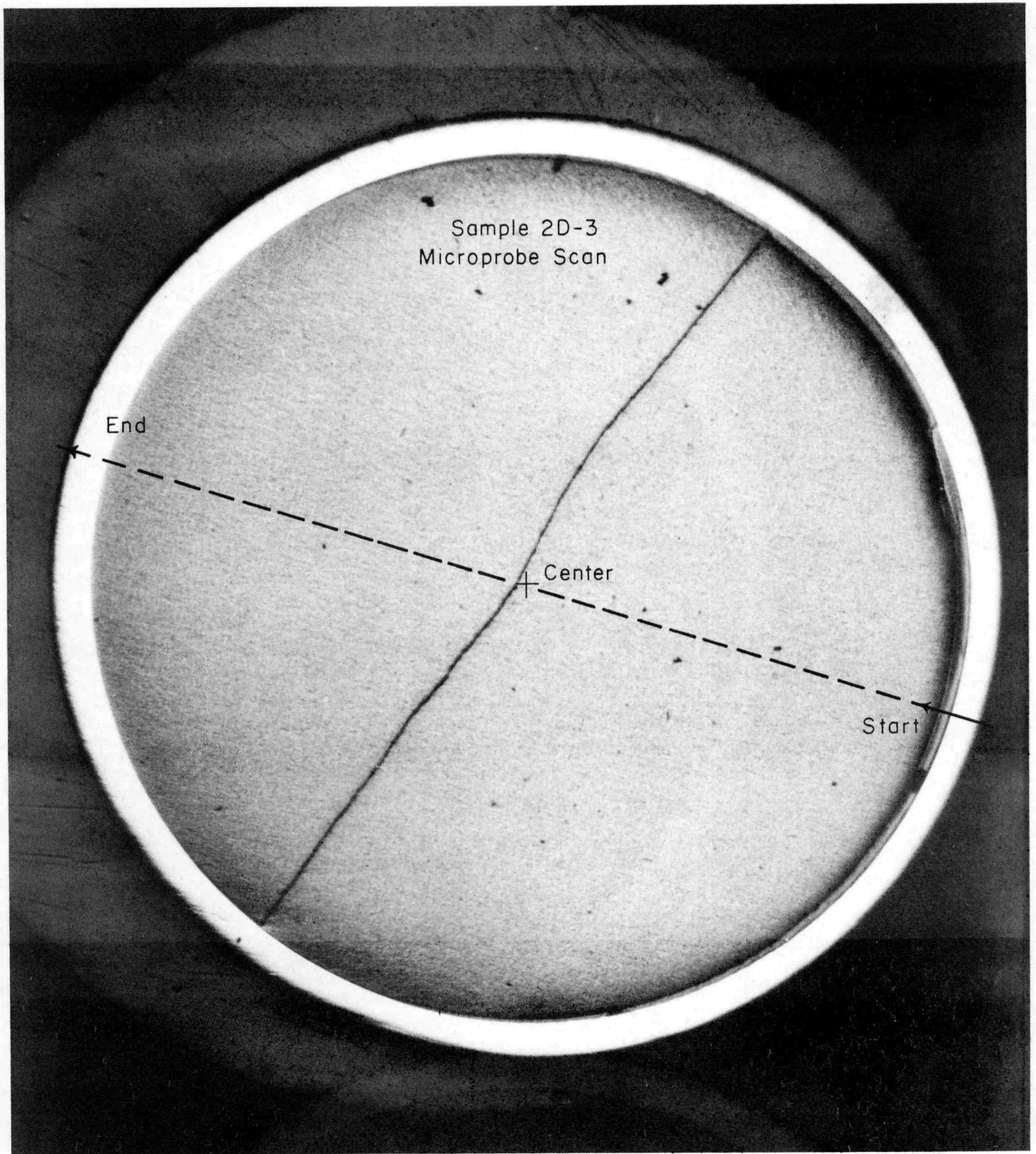


FIGURE 48. SAMPLE 2D-3 MICROPROBE SCAN

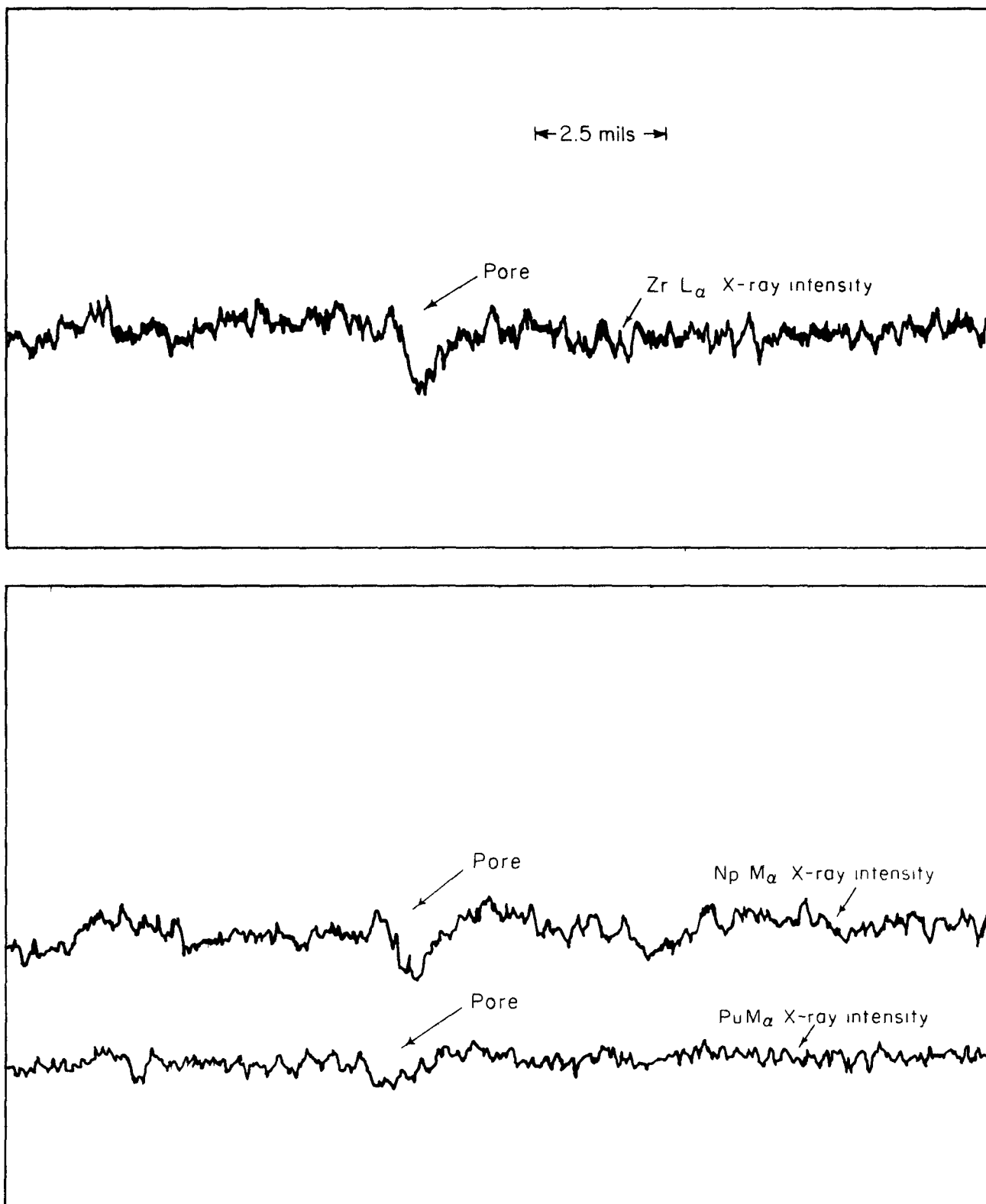


FIGURE 49. IRRADIATED SAMPLE 2D-3 MICROPROBE SCAN

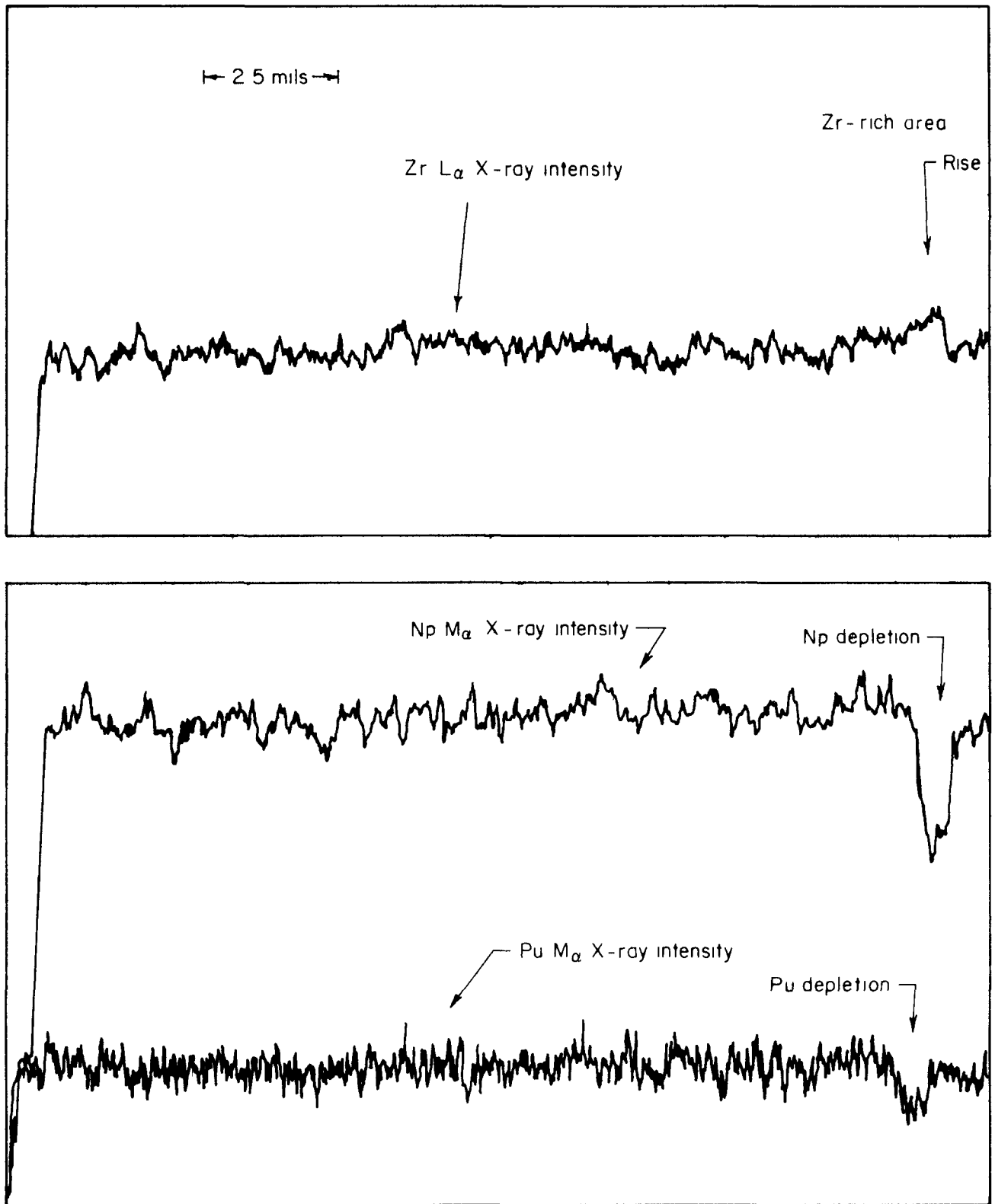


FIGURE 50. IRRADIATED SAMPLE 2C-6 MICROPROBE SCAN

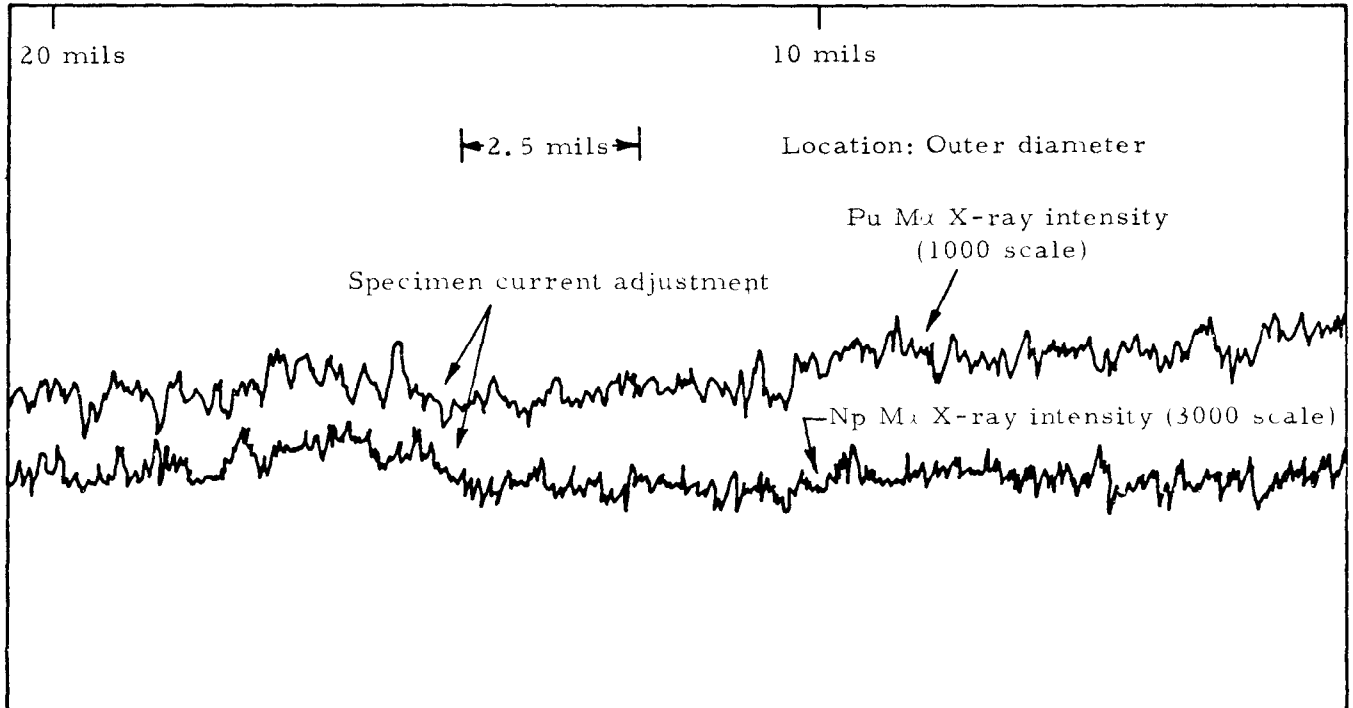
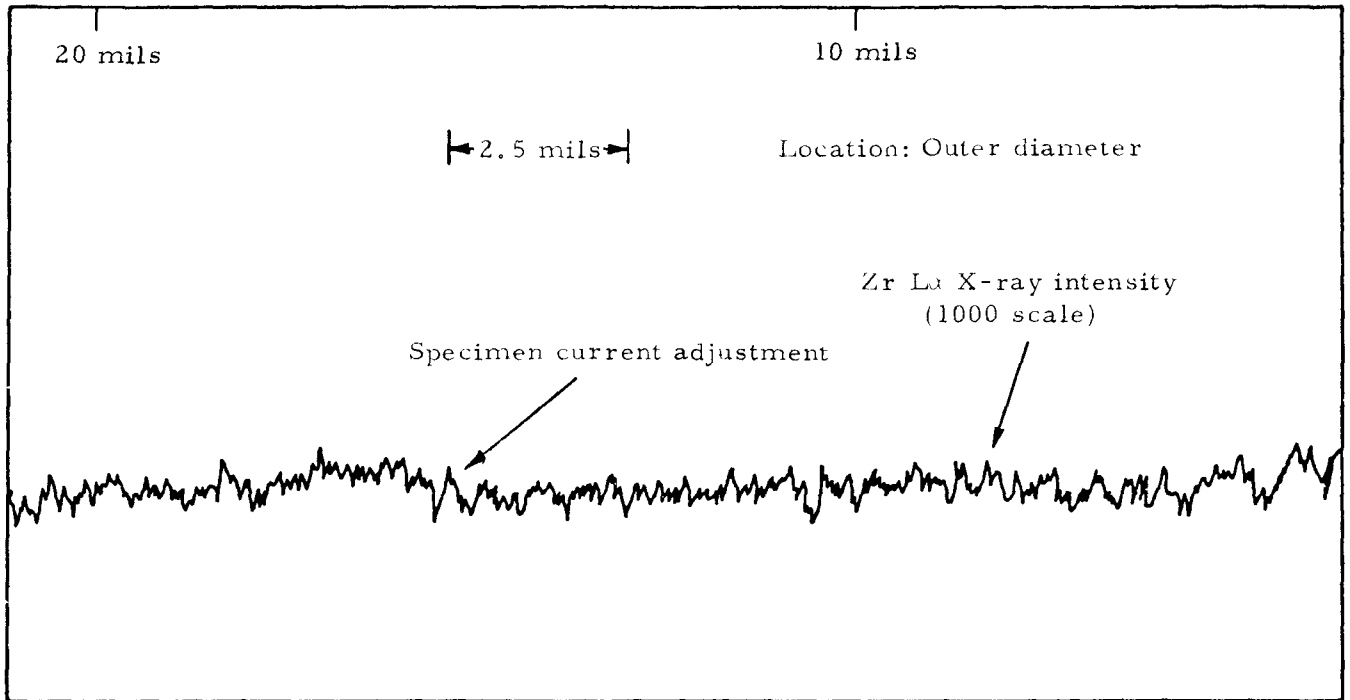


FIGURE 51. IRRADIATED SAMPLE B-8 MICROPROBE SCAN

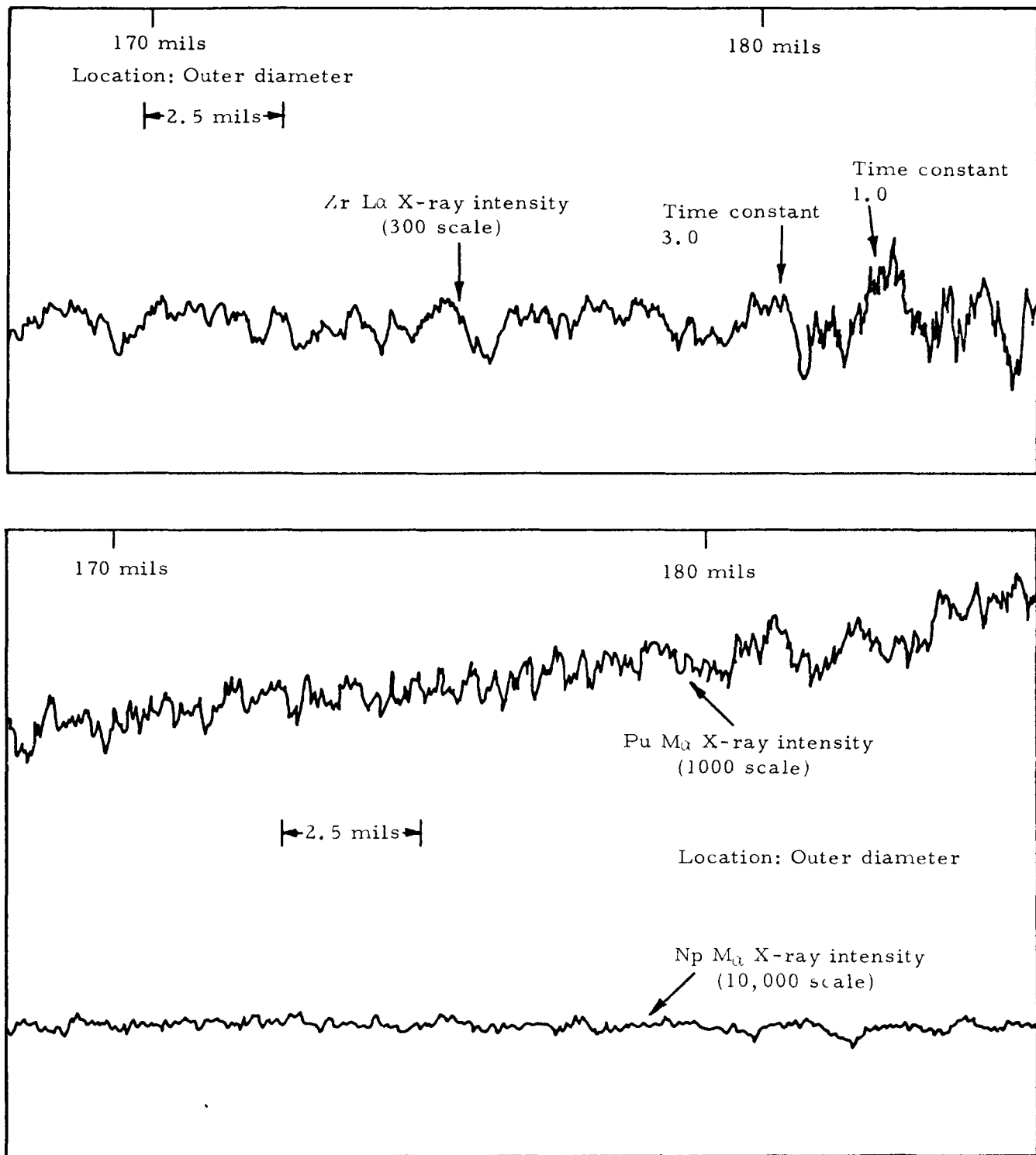


FIGURE 52. IRRADIATED SAMPLE A-11 MICROPROBE SCAN

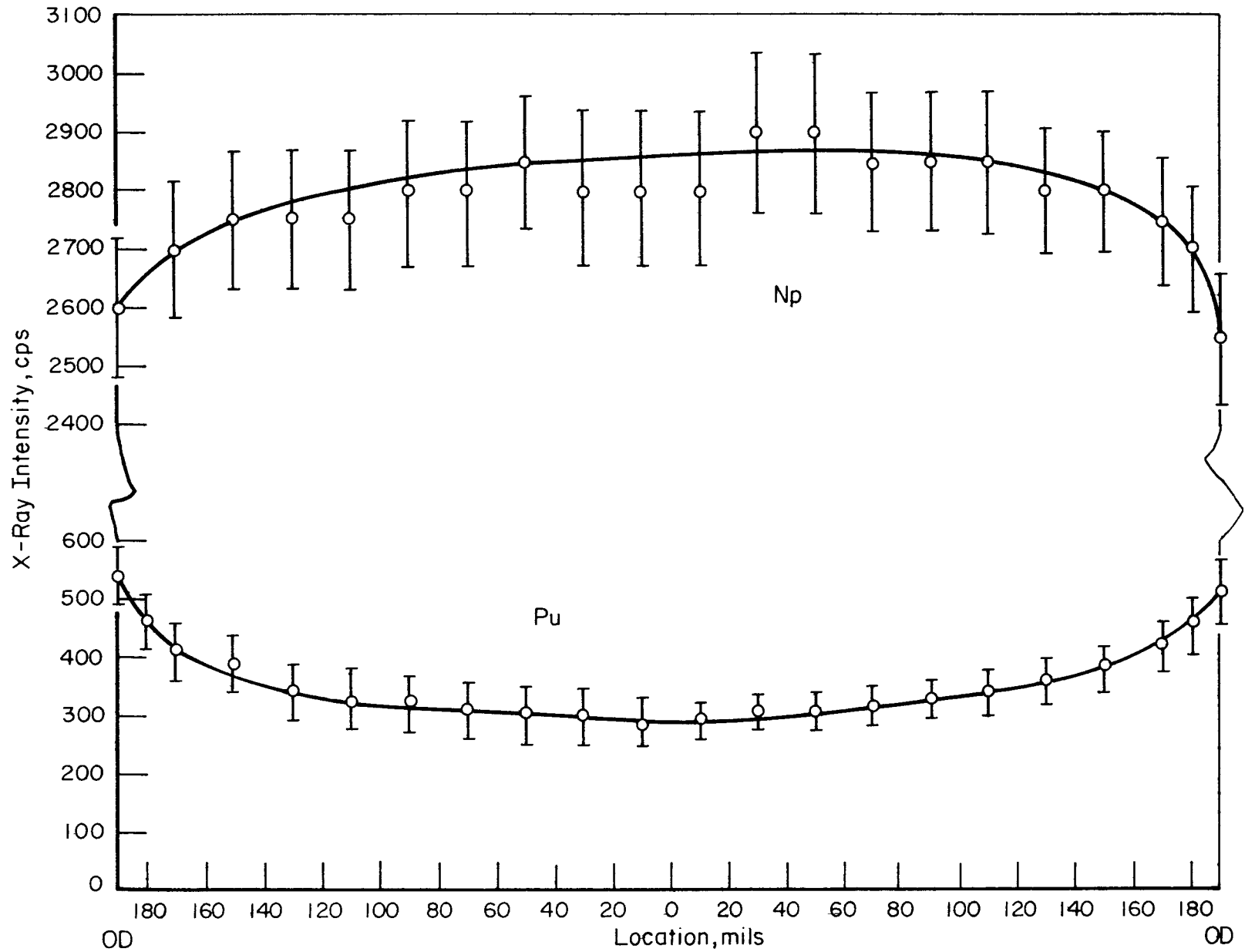


FIGURE 53. SAMPLE 2A-11 Np AND Pu X-RAY-INTENSITY DIAMETRAL PROFILE

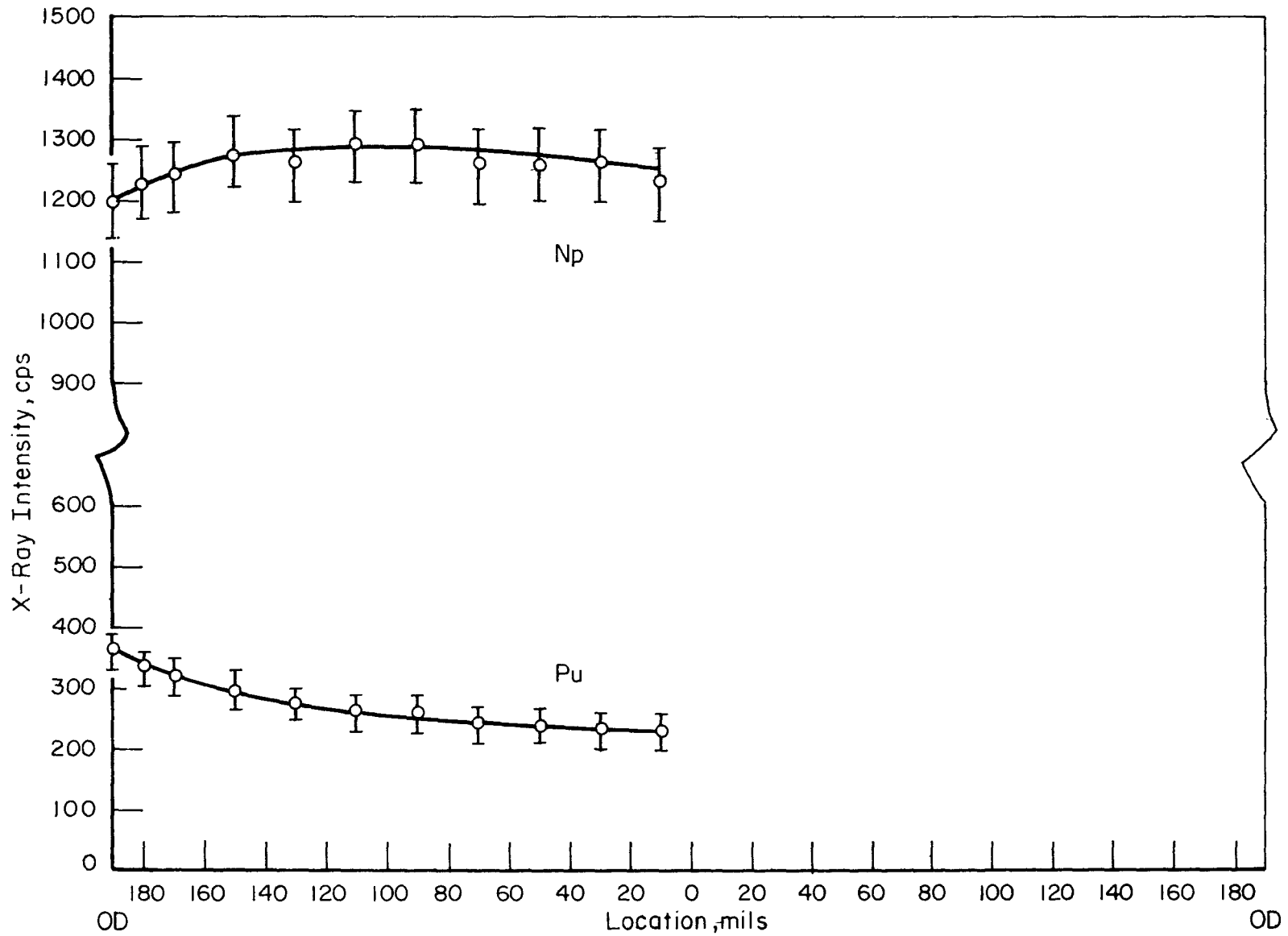


FIGURE 54. SAMPLE 2B-8 Np AND Pu X-RAY-INTENSITY DIAMETRAL PROFILE

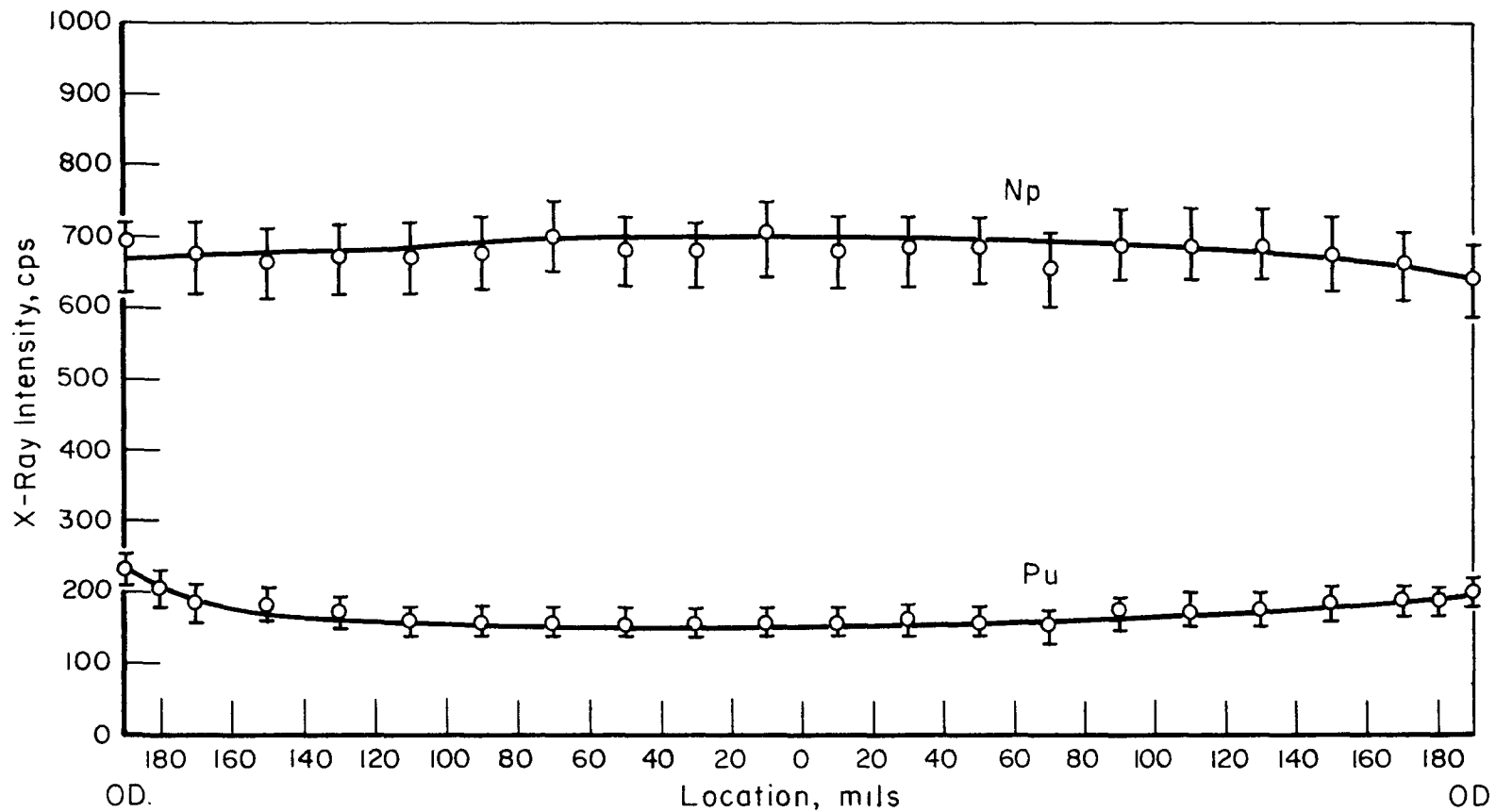


FIGURE 55. SAMPLE 2C-6 Np AND Pu X-RAY-INTENSITY DIAMETRAL PROFILE

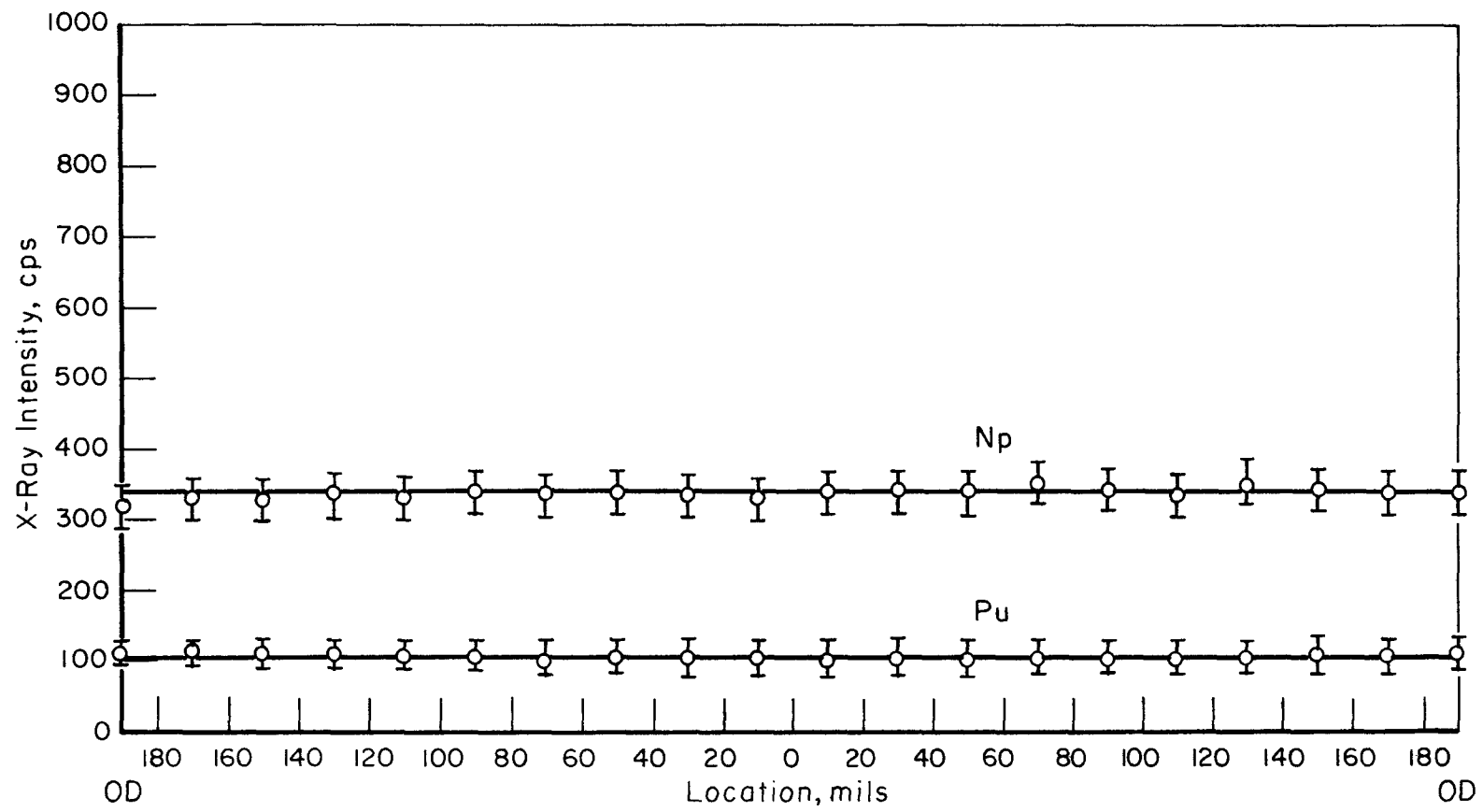


FIGURE 56. SAMPLE 2D-3 Np AND Pu X-RAY-INTENSITY DIAMETRICAL PROFILE

3.0 to 12 percent over the same range. The lowest flux depression, 13.0 percent, and highest percentage conversion (22.4 percent) of Np-237 to Pu-238 were observed in Section D (14.65 w/o NpO₂).

Since plutonium concentrations determined by wet chemistry were significantly lower than predicted in Sections A, B, and C, weighted Pu/Np ratios were determined over the pellet areas and compared with values determined by wet chemistry (see Table 24). Figure 57 shows the Pu/Np diametral profiles. Good agreement was obtained on the D section; values in the A, B, and C sections were 16 to 42 percent higher. Compared with predicted values the probe results agreed well on the sample from Section B, with samples from Sections D, C, and A being 20, 18, and 16 percent low, respectively. No obvious explanation for these differences in analytical values is apparent. It should be noted, however, that greatest concurrence of results occurs in the D section, which is the most likely range of NpO₂ concentration for a production system.

Dosimetry Results

Six cladding samples D-1, D-2, D-4, C-7, B-8, and A-11, as shown in the Figure 29 sectioning diagram, were cut, ultrasonically cleaned and removed from the high level cell for analysis. The original 1/8- to 3/16-in.-wide "wedding bands" were found to be at too high a radiation level (8-10 r/hr) for laboratory operations. Calculations showed that smaller portions would provide sufficient activity for analysis so that ~3/16 in. lengths were cut from the above rings for transferral to the radiochemical laboratory. The samples were again ultrasonically cleaned until smears showed count rates <100 dpm. They were then weighed to ± 0.0001 gram and dissolved in concentrated hydrochloric acid. Suitable aliquots of the original solutions were taken in duplicate for purification and analysis.

The cobalt and manganese were separated from the iron, nickel, and chromium impurities by anion exchange. Carrier techniques were utilized to determine chemical yields; Co was recovered by electroplating the element and Mn was precipitated as MnNH₄PO₄·H₂O. The Co-60 (1.33 MeV) and Mn-54 (0.84 MeV)

TABLE 24. SUMMARY OF MICROPROBE ANALYSES ON IRRADIATED NpO₂ TARGETS

Sample Location	Inches From Top of Assembly	Flux ⁽⁴⁾ Depression, %	Electron Microprobe (EMP) Pu/Np ⁽²⁾	Sample Location	Inches From Top of Assembly	Pu/Np		Calculated Analysis	Calculated ⁽³⁾ EMP
						BCL Analysis	SNE Calculated		
A-11	99.4	44.8	0.139	A-11	99.4	0.113	0.161	1.43	1.16
B-8 ⁽¹⁾	93.1	35.7	0.232	B-9	94.1	0.163	0.248	1.52	1.07
C-6	66.6	27.3	0.271	C-7	69.0	0.234	0.321	1.37	1.18
D-3	33.9	13.0	0.323	D-4	53.6	0.307	0.389	1.26	1.20

(1) Only one-half of a pellet was analyzed. Np value may be low (see curve).

(2) Determined by weighting the Pu/Np values over the pellet cross-sectional area. It was assumed that the X-ray intensities represent constant concentrations over the length of the pellet. Accuracies are approximately ± 10 percent.

(3) No adjustments made for axial location differences.

(4) Based on relative Pu intensities, edge to center.

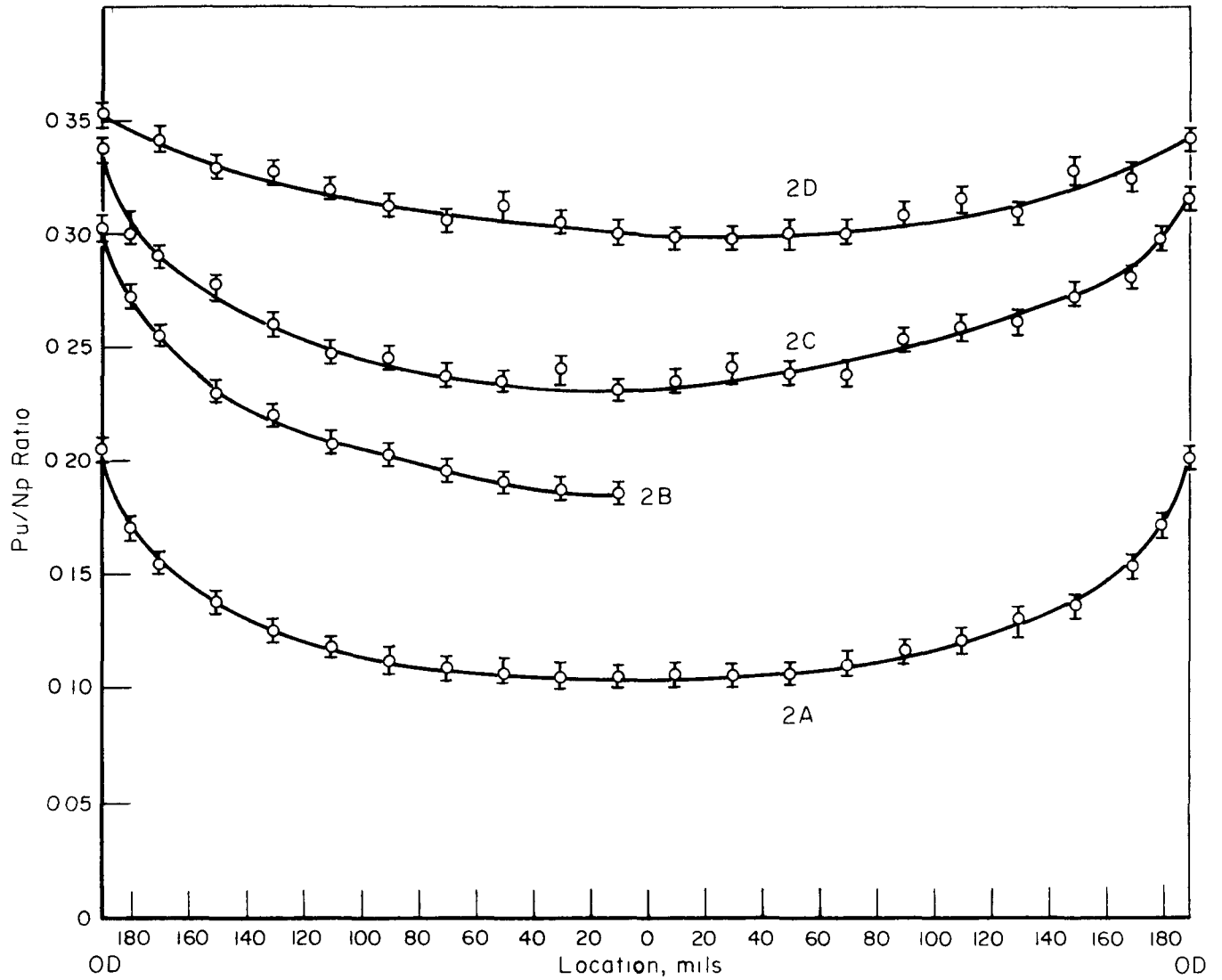


FIGURE 57. Pu/Np DIAMETRAL PROFILES FOR 4 NpO₂ COMPOSITIONS

gamma rays were counted using a high resolution NaI(Tl) scintillation crystal in conjunction with a TMC Model 401D 400 Channel analyzer. Disintegration rates were obtained by direct comparison with NBS standards. ASTM procedures E-261⁽¹⁰⁾, E-262⁽¹¹⁾, and E-263⁽¹²⁾ were used as guidelines in interpretation and reporting of the results.

Thermal and fast fluxes and fluences are shown in Table 25 and illustrated in Figure 58. For a better comparison in relating thermal and fast profiles, the fluxes are normalized to sample D-1 and shown, along with relative gamma scan intensities (also normalized), in Figure 59. A summary of the reactions and constants utilized are given in Table 26. The maximum flux in both cases is seen to be at the sample D-4 location. For all practical purposes the fast flux curve levels off at 9.2×10^{13} n/cm²-sec. However, the thermal flux shows a significant depression in Section C, but a general decrease is seen from 2.3×10^{13} n/cm²-sec at location D-4 to 1.7×10^{13} n/cm²-sec at location A-11. Thermal and fast fluences at D-4 were 7.1×10^{20} and 2.9×10^{21} n/cm², respectively. It appears that the C-7 section value (29 percent lower than D-4) is definitely lower than normal and deviates from the gradually decreasing curve. Experimental errors, including chemical separations and counting, are ± 10 percent so that it appears that the low value is due to (1) cobalt inhomogeneity in the clad, or (2) true flux depression due to a grid spacer in the reactor.

Concerning the actual flux values, some differences may occur due to different conventions used in dosimetry calculations. As stated earlier, ASTM procedures (Part 30, General Test Methods, July, 1973) were used in this report where ϕ_{th} covers the energy range 0-0.5 eV and ϕ_F the number of neutrons/cm²-sec above 0.1 MeV. No corrections were made for: (1) the epithermal energy range 0.5 eV - 0.1 MeV, (2) the cadmium ratio factor $R-1/R$ where $R = \frac{\text{bare Co saturation activity}}{\text{cadmium covered Co saturation activity}}$, (3) neutron energy distribution (a fission spectrum was assumed), (4) Co-60 or Mn-54 burnup (since thermal flux values were below 10^{14}), or (5) flux depression or self-shielding in the 0.016-in. wall Type 304 stainless steel clad.

TABLE 25. THERMAL AND FAST DOSIMETRY RESULTS

Rod Section	Sample No.	Thermal Flux, ϕ_{th} (n/cm ² -sec)	Thermal Fluence, nvt (n/cm ²)	Fast Flux, ϕ_F (n/cm ² -sec)	Fast Fluence, ϕt_F (n/cm ²)
D	1	1.41×10^{13}	4.39×10^{20}	6.48×10^{13}	2.02×10^{21}
D	2	2.06×10^{13}	6.43×10^{20}	8.68×10^{13}	2.72×10^{21}
D	4	2.27×10^{13}	7.11×10^{20}	9.41×10^{13}	2.94×10^{21}
C	7	1.62×10^{13}	5.08×10^{20}	9.02×10^{13}	2.82×10^{21}
B	8	1.88×10^{13}	5.87×10^{20}	9.17×10^{13}	2.87×10^{21}
A	11	1.65×10^{13}	5.19×10^{20}	9.11×10^{13}	2.85×10^{21}

TABLE 26. CONSTANTS AND PARAMETERS USED IN FLUX CALCULATIONS

	Thermal (Co ⁶⁰)	Fast (Mn ⁵⁴)
Dosimeter material	304 SS clad	304 SS clad
% Element of Interest	0.070% Co in D, 0.075% in A, B, C	$69.7 \pm 2\%$ Fe
% Isotopic Abundance	100% Co ⁵⁹	5.82% Fe ⁵⁴
σ , barns	37.1 (at 2200 m/s = 0.025 eV)	0.075 ($\bar{\sigma}^F$)
Flux Energy Range	0 - 0.50 eV	>0.1 MeV
Product γ -ray Energy, MeV	1.17, 1.33	0.84
Product Half Life	5.26 years	314 days
Time of Irradiation Eq FPD	361.64	361.64
Reactor Shutdown	6/9/72	6/9/72

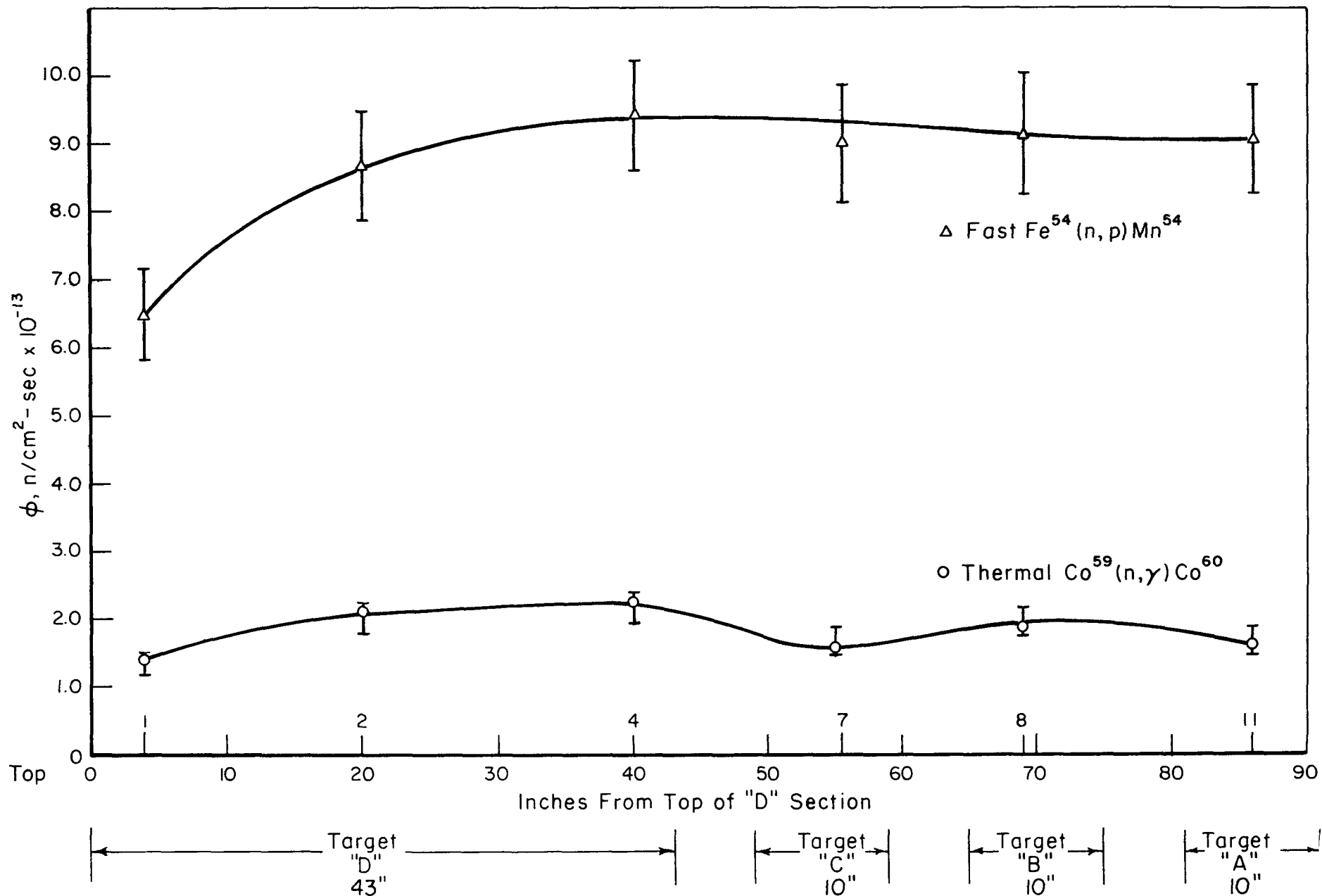


FIGURE 58. NEPTUNIUM ROD NO. 2 THERMAL AND FAST-FLUX PROFILES

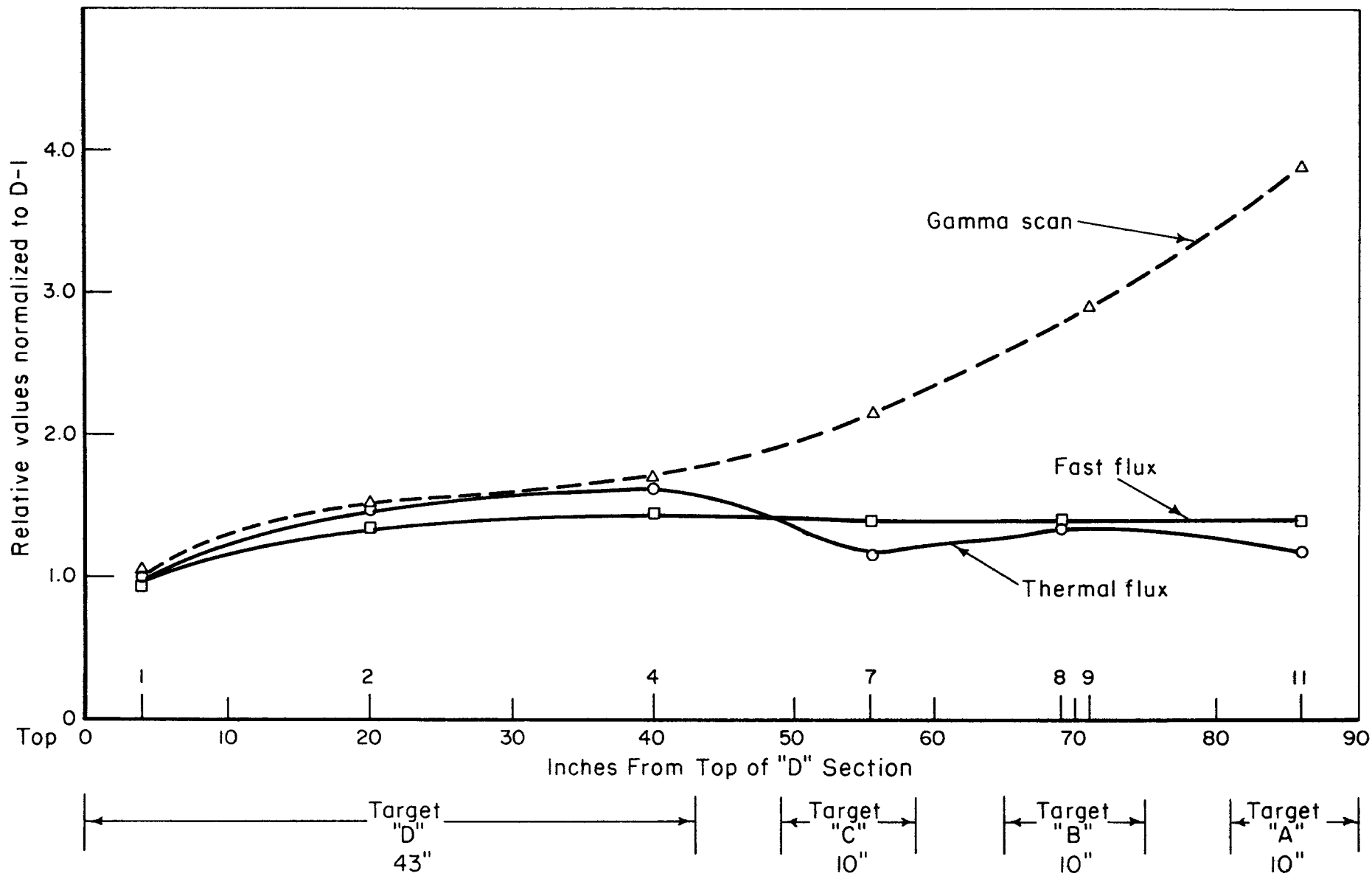


FIGURE 59. NEPTUNIUM ROD NO. 2 NORMALIZED FLUX AND GAMMA SCAN PROFILES

The thermal flux may be somewhat high since there were no cadmium-covered samples available for determining resonance neutron corrections. Theoretically, $\phi_{th} = \phi_{obs} (R-1/R)$ (for $R = 4$, $R-1/R = 0.75$). The fast flux values are probably quite reasonable based on the fission spectrum assumption. They would be directly affected by the ratio

$$\frac{\int_{E > 1 \text{ MeV}}^{\infty} \phi_f(E) dE}{\int_{E=0}^{\infty} \phi_f(E) dE} = 0.69 \quad .$$

If the actual neutron spectrum were "softer" and had fewer neutrons >1 MeV, the fast flux measurement would be lowered proportionately according to the above equation.

For future considerations it is recommended: (1) that dosimeter materials be included in the experiment according to ASTM specifications, i.e., high-purity Al-0.5% Co wires (both bare and cadmium covered) and high-purity Fe wires be used for accurate thermal and fast dosimetry, respectively, and (2) that a cadmium-covered Np fuel section be used as an internal flux monitor according to a tentative ASTM procedure utilizing the fission reaction Np-237 (n, f) Cs-137. Np-237 has a threshold value of 0.4 MeV, and fast fission from Np-238 and Pu-238 would be negligible for fast neutron fluxes $>10^{12}$ n/cm²-sec. Thermal fission from Pu-239 and U-235 is considered negligible due to absorption of thermal neutrons by the cadmium covering.

Conclusions

The mechanical and physical performance of all four target sections was excellent but less fuel pellet cracking was observed in the D section. Compatibility of clad and target material was also excellent, with no evidence of corrosion or interaction. Since flux depression was minimal and neptunium-237 to plutonium-238 conversion was highest in the D section, the lowest

concentration target of 14.65 w/o NpO_2 was the most efficient for plutonium-238 production. The conversion was experimentally measured to be 22.4 percent. In addition, the lowest concentration of Pu-236 contaminant was produced in this target section.

Although disagreement between the total amounts of plutonium predicted and analyzed was noted, particularly in the higher concentration NpO_2 targets, the implications with respect to the goal of establishing feasibility of production of Pu^{238} in commercial reactors is inconsequential. Agreement is excellent among the various methods of analysis and not too far off the calculated value with respect to the D target, which is in the NpO_2 concentration range most likely to be used. Future experiments and more data points will resolve any discrepancies.

IV. PROCESSING STUDIES

Had it been possible to use the Al-NpO₂ composite developed at SRL as target material for this program, there would have been no necessity for processing studies. The technology for recovery of Pu²³⁸ from this material has become a state-of-the-art process over the past decade.⁽¹³⁻¹⁶⁾ The brief time available at the inception of the program for selection, development, and fabrication of the target rods, however, left little or no time for exploration and experimentation with a diluent material. Accordingly, ZrO₂ was selected as diluent, based not only on its excellent nuclear characteristics, but particularly on its anticipated excellent stability over a wide range of solution compositions with NpO₂ under reactor irradiation. Because of this factor, approval was granted readily for the experimental irradiation in an operating commercial reactor.

The results of the postirradiation examination, reported in the previous section, substantiate the validity of this selection of diluent material for an initial, critical experimental irradiation. Difficulty in dissolving the target material for analysis, however, raised questions concerning its utility from the viewpoint of processing for recovery of plutonium and neptunium. The studies reported below bear on this problem.

Dissolution

Discussion with personnel at Idaho Falls (IF), Battelle's Pacific Northwest Laboratories (BNW), Savannah River (SRL), and the Oak Ridge National Laboratory (ORNL) verified our conclusion that the HCl-HF solution which was used to dissolve analytical specimens would be highly unsatisfactory as a solvent in a recovery process. Accordingly, an experimental search was carried out for an effective solvent which would provide a practical base for the anion exchange recovery process.

Since the glove boxes in the plutonium laboratory provided insufficient shielding, the irradiated pellets could not be used directly for the dissolution experiments. Therefore, simulant pellets were fabricated of 16 w/o NpO₂-4 w/o PuO₂-80 w/o ZrO₂ (CaO). Blended powder containing the above

constituents was cold pressed at 20,000 psi into seven pellets, each 0.438-inch in diameter. The green pellets were subsequently sintered at 1650 C for 4 hours in flowing pure nitrogen. Geometric densities obtained on the pellets ranged from 5.1 to 5.3 g/cm³ or about 82 to 85 percent of theoretical. These pellets were used in subsequent dissolution experiments. Their neptunium and plutonium contents are presented in Table 27.

TABLE 27. ANALYSIS OF $ZrO_2(CaO)-NpO_2-PuO_2$ SAMPLE PELLETS

Sample weight, g	0.8776
Np, mg, aliquot 1 ^(a)	5.947
, aliquot 2 ^(a)	5.987
average	5.967±0.020
Pu, mg, aliquot 1 ^(b)	2.947
, aliquot 2 ^(b)	2.968
average	2.958±0.010
NpO_2 , percent	15.5
PuO_2 , percent	3.83

(a) 5 ml from 100.

(b) 10 ml from 100.

The experiments involved an evaluation of dissolution by the following approaches: (1) nitric acid containing 0.1M HF, (2) aqua regia, (3) 20M HF, (4) pretreatment with HCl or CCl_4 vapor, and (5) H_2SO_4 fuming. Each of these dissolution approaches was aimed at achieving one of the following goals.

- (1) Verification of incapability to dissolve material in nitric acid
- (2) Verification of capability to dissolve material in HF following Idaho Falls' procedures⁽¹⁷⁾

- (3) Evaluation of pretreatment to enable ultimate dissolution in nitric acid.

Experimental Procedure

Most of the experiments were done on samples of material from pellets ground up to -200 mesh particle size. Some experiments were carried out using pellet chunks of about 1/8 inch in diameter in order to evaluate the effect of particle size on dissolution rate. The specific procedures were as follows:

Nitric Acid Studies

- (1) Measure 0.3 to 0.5 g portions into four 15 ml centrifuge tubes.
- (2) Add excess HNO_3 acid: 8M, 10M, 12M, and 15M, respectively, to each tube. Make 0.1M in HF.
- (3) Heat in boiling water for 8 hours.
- (4) Filter. Collect filtrate and washings in volumetric flask.
- (5) Dry precipitate and weigh. If significant weight change has occurred, analyze filtrate for Np and Pu.

Aqua Regia (3HCl:HNO₃) Studies

- (1) Measure two 0.3 to 0.5 g portions into Teflon centrifuge tubes.
- (2) Add excess aqua regia and heat in boiling water for 8 hours.
- (3) Centrifuge and collect filtrate and washings in volumetric flask.
- (4) Dry precipitate, if any, and weigh.
- (5) Analyze filtrate for Np and Pu if significant weight change has occurred in precipitate.

HF Studies

- (1) Measure two 0.3 to 0.5 g portions into Teflon centrifuge tubes.
- (2) Add excess 20M HF and heat in boiling water for 8 hours.
- (3) Centrifuge and pour off filtrate. Save filtrate and washings in volumetric flask.
- (4) Add excess 6M HNO₃ to residue in centrifuge tube.
- (5) Heat in boiling water for 8 hours.
- (6) Filter. Collect filtrate and washings in volumetric flask.
- (7) Dry precipitate, if any, and weigh.
- (8) Analyze filtrate for Np and Pu.

Pretreatment Studies

- (1) Weigh 0.3 to 0.5 g portions into porcelain boat.
- (2) Heat at 300 C for 2 hours while passing dry HCl or CCl₄ through tube. Use inert carrier gas, if necessary. Pass exit vapors through NaOH trap.
- (3) Cool and weigh.
- (4) Transfer residue to 15 ml centrifuge tube and add excess 8M HNO₃
- (5) Heat in boiling water bath for 8 hours.
- (6) Filter into volumetric. Analyze for Np and Pu.
- (7) Repeat entire procedure, but chlorinating at 400 C and at 500 C.

H₂SO₄ Studies

- (1) Weigh 0.3 to 0.5 g portions into porcelain dish.
- (2) Add concentrated H₂SO₄ to wet powder sample.
- (3) Fume to dryness.
- (4) Dissolve residue in hot 8N HNO₃.

(5) Filter into volumetric. Analyze for Np and Pu.

Results

The results of the dissolution experiments are summarized in Table 28 below. In the nitric acid cases, the residual material after treatment with nitric acid ranged from 3/4 to 2/3 of the original sample weight. This included the results of treatment with aqua regia. One may conclude, therefore, that nitric acid, aided by low concentrations of HF catalyst, and aqua regia solvent systems, appear capable of dissolving about 1/3 of the contained NpO_2 and PuO_2 .

The Idaho Falls process, using 20M HF followed by 6M HNO_3 , dissolves virtually all of the NpO_2 and PuO_2 . More Pu than one would care to lose reports to the HF solution, but this amount could no doubt be reduced by adjustment of process parameters.

The chloride pretreatment studies were carried out using CCl_4 as the chlorinating agent. Up to 500 C in the gas-phase treatment, no weight change was observed in the sample material. Treatment of this residue with 8M HNO_3 resulted in a weight loss of about 25 to 50 percent. At 600 C, however, about 55 percent weight loss occurred during the gas-phase treatment. (A solid condensate, fitting the description of ZrCl_4 , was deposited on the exit tube.) After the HNO_3 treatment of this residue, a slight amount of solid (about 1 percent of the original weight) remained.

The key to success in the chlorination treatment appears to be finding the proper temperature. No material was vaporized until the chlorination temperature reached 600 C. Sixty-five percent of the NpO_2 and 75 percent of the PuO_2 were found in the nitric acid solution of the essentially completely dissolved residue. This result leads to the conclusion that some of the Np and Pu were volatilized during the chlorination. Proper adjustment of the process parameters seems likely to lead to full recovery of the Np and Pu. A qualitative test for chlorine in the nitric acid solution from the residue after 300, 400, and 500 C chlorination treatments shows a small amount of chlorine in the first two and about three times as much in the third.

TABLE 28. RESULTS OF DISSOLUTION EXPERIMENTS

Dissolvent	Sample Weight, g	Residue Weight, g	Dissolved, percent of original sample	
			NpO ₂	PuO ₂
8M HNO ₃	0.3100	0.2249	N.A. (c)	N.A.
10M HNO ₃	0.3345	0.2269	N.A.	N.A.
12M HNO ₃	0.3211	0.2006	5.15 (33) (b)	1.41 (37) (b)
15M HNO ₃	0.3144	-- (a)	--	--
Aqua Regia	0.3230	0.2151	5.08 (33)	1.35 (35)
20M HF	0.3275	0.1435	0.222 (1.4)	0.34 (8.9)
+6M HNO ₃			15.2 (98)	3.42 (89)
CCl ₄ -300 C	0.3087	0.3115		
+HNO ₃		0.1532	N.A.	N.A.
400 C	0.3205	0.3180		
+HNO ₃		0.2501	N.A.	N.A.
500 C	0.3232	0.3250		
+HNO ₃		0.2481	N.A.	N.A.
600 C	0.3400	0.1550		
+HNO ₃		0.0035	10.1 (65)	2.88 (75)
Fuming H ₂ SO ₄	0.3061	0.0037	14.7 (95)	3.45 (90)

(a) Sample lost when test tube ruptured.

(b) Value in parenthesis is percent of total NpO₂ or PuO₂ in sample which was dissolved.

(c) N.A.--Not analyzed.

The fuming sulfuric acid-nitric acid solution treatment shows excellent recovery of the Np and Pu from the sample pellet material, 95 and 90 percent, respectively. Considering the preliminary nature of these experiments, the possibility of approaching 100 percent recovery by proper adjustment of parameters seems quite promising.

Based on the above results, there appeared to be several options for reprocessing of the ZrO_2 diluted target materials. Firstly, the applicability of the Idaho Falls' process was verified. Secondly, either a chlorination pretreatment or fuming with H_2SO_4 appeared capable of leading to a nitric acid soluble product and nitric acid feed solutions amenable to reprocessing by well-established ion exchange or solvent extraction processes.

Several additional experiments were carried out to complete the dissolution studies and to provide feed solutions for the subsequent recovery studies. These experiments were carried out to evaluate the rate of dissolution of small chunks of NpO_2 - PuO_2 - ZrO_2 pellets as compared with the rate for powder. The size of the chunks was $\sim 1/8$ inch. The fourth experiment was aimed at providing a clear nitric acid feed solution for reference in the recovery studies. The results of these experiments are presented below.

Experiment No. 1

1.0400 g of the chunks was fumed with H_2SO_4 for 8 hours with no reaction. 8N HNO_3 was added and the mixture simmered for 8 hours with no reaction. There was no color in the solution.

Experiment No. 2

1.0430 g of the chunks was fumed with H_2SO_4 for 8 hours with no reaction. The sample was washed and ground to -200 mesh. An 0.8200 g portion of the powder was fumed for 8 hours with H_2SO_4 then taken up in hot 8N HNO_3 which dissolved it completely.

Experiment No. 3

1.0055 g of the chunks was chlorinated in a stream of CCl_4 at 660 C. There was no apparent reaction. The temperature was taken up to 700 C with still no apparent reaction and just a trace of condensable vapors. One chunk of the above material was simmered in 8N HNO_3 with no apparent reaction. The remainder of the chunks was ground to -200 mesh. 0.8662 g of powder was chlorinated at 620 C for 2-1/2 hours with considerable vaporization occurring. After an additional 2-1/2 hours at 630 C, the residue was 0.3640 g. This residue dissolved readily in 100 ml of hot 8N HNO_3 . A trace of chloride ion was measured in a 20-ml aliquot of the solution.

Experiment No. 4

A 1.0440-g sample was ground and dissolved in hot HNO_3 -HCl with HF and H_2O_2 additions. After dissolution, the solution was fumed in HNO_3 several times to drive off the HCl and HF. The final solution was made 8N in HNO_3 .

These results establish the practical infeasibility of dissolving the ZrO_2 - NpO_2 - PuO_2 material in pellets or chunks by any means other than the proven Idaho Falls' technique. On the other hand, there are several expedients for dissolving this target material when it is ground to -200 mesh. This is in accordance, of course, with well-known dissolution technology. The solutions from these experiments were used in the recovery studies described below.

Recovery

The solutions from the dissolution experiments were processed through a recovery procedure similar to the anion exchange process used at BNW. The procedure was as follows:

- (1) The feed solutions were made 8 molar in nitric acid, 0.1 molar in ferrous sulfamate, and heated to 55 C.

- (2) After passing the feed through a column of Dowex-1-X4 resin, the column was washed with 8M HNO_3 -0.005M HF solution.
- (3) The plutonium was eluted with 5.7M HNO_3 -0.05M N_2H_4 -0.05M $\text{Fe}(\text{SO}_3 \cdot \text{NH}_2)_2$ solution.
- (4) The neptunium was eluted with 0.35M HNO_3 solution.
- (5) The plutonium eluate was made 8M in HNO_3 , passed through a second column, and washed with 8M HNO_3 -0.005M HF solution.
- (6) Plutonium was eluted from the second column with 0.35M HNO_3 solution.

Results of the analyses of the neptunium and plutonium product solutions are presented in Table 29 below.

TABLE 29. RESULTS OF ANION EXCHANGE RECOVERY PROCEDURE

Feed Solution	PuO ₂ Recovered,		NpO ₂ Recovered,	
	percent		percent	
	Total Sample	Total PuO ₂	Total Sample	Total NpO ₂
Experiment No. 1 H ₂ SO ₄ /chunks	0.15	4	0.58	4
Experiment No. 2 H ₂ SO ₄ /powder	2.17	57	13.5	87
Experiment No. 3 Cl volatilized	1.67	44	6.5	42
Experiment No. 4 HCl/HNO ₃	2.18	57	14.3	92

The results from the Experiment No. 1 solution reinforce the conclusion expressed previously: little or no dissolution is effected on chunk-size particles. In the remaining cases, complete dissolution of the powder samples

was accomplished; therefore, the lack of complete recovery must be ascribed to deficiencies in the process. Yet the results are quite encouraging. Taking the Experiment No. 4 solution as a standard (since essentially all the HCl was removed by repeated HNO_3 fuming), the H_2SO_4 fuming process (Experiment No. 2) yielded an equivalent degree of recovery. In the case of the chloride volatilization (Experiment No. 3), it seems quite likely that some of the Pu and Np were lost with the volatiles. As pointed out earlier, volatilization conditions need to be optimized to reduce losses for the sample fumed with sulfuric acid.

The most likely reason for the incomplete recovery from Experiment No. 2 and Experiment No. 4 solutions is the nature of the resin. No special effort was made to duplicate resin particle size distribution or degree of crosslinking used by the previous experimentalists. Undoubtedly, some Pu reported in the neptunium fraction and vice versa, but no analyses were carried out to confirm this. Complete recovery and separation should be readily attainable with slight process adjustments and improved process controls. No time was available for this ultimate proof of process on this program.

Although recovery was not 100 percent in this first run, it was of about the same magnitude as that found for the reference nitric acid solution. This procedure shows considerable promise for reprocessing the irradiated $\text{NpO}_2\text{-ZrO}_2$ (CaO) targets. Based on these results, the H_2SO_4 fuming process is recommended for further study. A process flow sheet is shown in Figure 60.

Alternate Diluents

Concurrently with the above studies, a review was made of potential alternate diluents to the ZrO_2 . Although not the only consideration, major emphasis was placed on capability to dissolve and reprocess the target material. Table 30 presents those materials screened for final consideration.

Considering all the factors, $\text{NpO}_2\text{-MgO}$ emerged as the most desirable target material. A survey of the literature was made for data relating to MgO in combination with the oxides of U, Np, and Pu. In general, very little information exists. No information was found on composites of $\text{NpO}_2\text{-MgO}$.

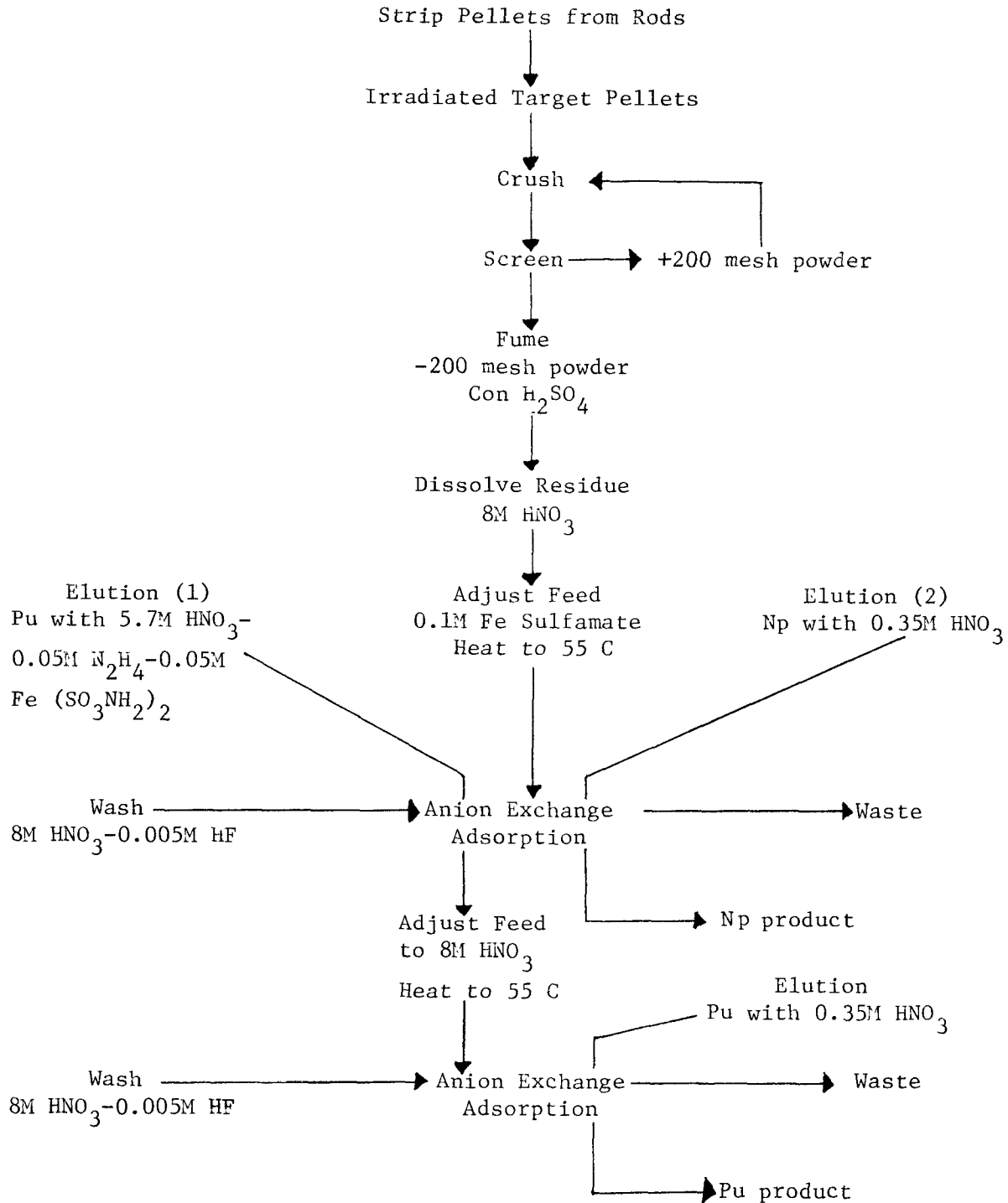


FIGURE 60. FLOW SCHEMATIC FOR RECOVERY OF NEPTUNIUM AND PLUTONIUM FROM IRRADIATED NpO_2 - ZrO_2 TARGET RODS

TABLE 30. ALTERNATE MATERIALS FOR TARGET DILUENT

Cladding	Target Material	Reprocessing	Neutron Economy
Stainless Steel	$\text{NpO}_2\text{-CaO-ZrO}_2$	Dissolution problem	OK
	$\text{NpO}_2\text{-MgO}$	Should be soluble in HNO_3 . Amenable to ion exchange process	OK
	$\text{NpO}_2\text{-SS}$	Electrolytic dissolution	Poor High Pu-236
	$\text{NpO}_2\text{-Al}_2\text{O}_3$	Dissolution questionable	OK
Zircaloy	$\text{NpO}_2\text{-Al}$	Shear-leach. Then dissolve	

Studies of $\text{UO}_2\text{-MgO}$ and $\text{PuO}_2\text{-MgO}$ fuels have been associated primarily with fuel development for the UK Zenith zero-energy reactor-physics experiment⁽¹⁸⁾ and the PRTR⁽¹⁹⁾, respectively. In the Zenith experiment, the fuel compacts composed of 71 w/o MgO and 29 w/o UO_2 were fabricated with a density of only 75 percent of theoretical. Fission-gas retention was good up to about 500 C, but above this temperature there was a sharp increase in gas release. This behavior is understandable in view of the low density of the fuel.

The $\text{PuO}_2\text{-MgO}$ pellets fabricated at Hanford had two different compositions; one containing 2.71 w/o PuO_2 and the other with 12.95 w/o PuO_2 . These pellets attained densities of 86 to 92 percent of theoretical. The higher PuO_2 composition was irradiated to a maximum burnup of 0.96×10^{20} fissions/cm³, which produced a maximum center temperature of 1700 C. Satisfactory irradiation performance was demonstrated; however, one of the reports⁽¹⁹⁾ suggested that MgO may have limited application because of its reaction with water. This implication resulted from a failure of one of the $\text{PuO}_2\text{-MgO}$ capsules during irradiation in PRTR⁽²⁰⁻²²⁾. Fission products were spread throughout the primary cooling chambers and considerable effort was needed to decontaminate the system.

Other references generally verified the stability of pure MgO under irradiation⁽²³⁻²⁵⁾. Most of the damage is annealed out during irradiation at temperatures of 600 C and above⁽²³⁾.

With regard to phase behavior, both PuO₂ and UO₂ appear to form eutectic systems with MgO⁽²⁶⁻²⁹⁾. The eutectic temperature for both systems is high, approximately 2280 C for UO₂-MgO and 2260 C for PuO₂-MgO. Solubilities of PuO₂ in MgO and MgO in PuO₂ are ≤ 0.5 w/o. The NpO₂-MgO system should be similar. Properties of these types of dispersion materials have been reviewed by Livey⁽³⁰⁾. Studies at Battelle⁽³¹⁻³²⁾ have shown that PuO₂ and MgO mixtures do not react appreciably when held at temperatures below 1500 C for a period of 96 hours. These data strongly suggest that there will be no problems in the fabrication of NpO₂-MgO pellets other than those related to achievement of high densities. Sintering temperatures are not expected to exceed 1650 C and the short period of time of several hours required for densification should be of no consequence.

Based on the above review, one cannot categorically decide whether or not NpO₂-MgO targets have promise. The reaction of MgO with water is cause for concern, but the reaction rate would undoubtedly be related to the temperature and the sintering parameters utilized for fabrication of the targets. In the case of the PuO₂-MgO, fuel center temperatures were about 1300 C above that expected in the NpO₂ targets. The relatively low temperatures of the targets during irradiation compared with high sintering temperatures may well result in a product that is inert to the reactor environment. The way to resolve this question is to carry out a study of the reaction rate of NpO₂-PuO₂-MgO pellets with water at elevated temperatures to determine whether or not magnesia can be utilized as a diluent for future target irradiations.

Two other concepts are suggested for study as alternate to the ZrO₂ diluent. The first utilizes alumina as a diluent, but, in this case, sintering would be carried out at a relatively low temperature. Alumina has been rejected as a diluent until now because dissolution of high-fired material was expected to be difficult. But recent results with the pulverized zirconia targets suggest that properly treated alumina could have characteristics required for target irradiation and yet be soluble in nitric acid. If dissolution of the neptunia-alumina pellets is achieved, the anion exchange processing scheme presently employed by SRL could be used for target reprocessing without modification.

The second approach involves fabrication of a two-component pellet where a thin layer on one end contains the neptunia in undiluted form and the remainder of the pellet is composed of calcia-stabilized zirconia or alumina; either diluent will be satisfactory for this concept. Calculations suggest that a layer of neptunia approximately 1000 microns in thickness would produce a flux depression of 5 to 10 percent. This depression would result in a corresponding increase in the Pu-236 content over that normally produced in the target rods. We estimate that the Pu-236 content of a rod containing 20 w/o neptunia overall in a wafer array would be increased by only 1 ppm over the amount present in a fully diluted pellet. This penalty appears to be tolerable.

Fabricated pellets would have dimensions of about 0.125 inch thick by 0.375 inch in diameter, where about 0.025 inch of one end would be composed entirely of neptunia. Much thicker pellets with alternate layers could be fabricated in production by use of specialized die filling techniques. Problems anticipated with this approach center around possible differences in shrinkage characteristics which could lead to crack or fissure formation. Work thus far with the calcia-stabilized zirconia, however, indicates that there is an excellent chance that good pellets can be fabricated. Dissolution of the neptunia and plutonia by nitric acid must be demonstrated in order for this concept to be viable. Another aspect of the wafer approach which must be investigated is the diffusion of pure NpO_2 into the zirconia or alumina component.

Analytical measurements on sintered wafer pellets should provide adequate proof of dissolution and recovery of neptunium and plutonium. With the relatively low temperatures generated in the irradiation, diffusion of neptunium or plutonium would be expected to be negligible. Therefore, results obtained on the sintered pellets should be representative of behavior for irradiated targets.

The Production Cycle

In the foregoing sections of this report, the technical aspects of the BCL effort to develop a target rod material for production of Pu^{238} from irradiation of Np^{237} in commercial reactors have been presented. The results

of this effort indicate that, although some additional development effort is necessary, a technology exists for this process. To SNS, the significant question now becomes: what is the cost of the Pu²³⁸ product likely to be, and is there a facility or group of facilities available and capable to carry out the production process? The former question and part of the latter question have been treated by NUS and their results are reported in Reference (9). This section of the report deals with BCL's evaluation of the availability and capability of facilities to complete the entire production cycle. The complete cycle for Pu-238 production is

- (1) Recovery of Np-237 from spent fuel
- (2) Fabrication of Np-237 targets for irradiation
- (3) Irradiation in a commercial reactor
- (4) Reprocessing of irradiated targets to recover Np-237 and Pu-238
- (5) Recycle of recovered Np-237 to Step (2)
- (6) Fabrication of Pu-238 into heat sources
- (7) Recycle of used heat sources to Step (4) to recover Pu-238.

At this time, Items (6) and (7) are not really pertinent to the production cycle of interest. Facilities, both Government and industrial, for fabrication of Pu-238 into heat sources are in existence and operational. Recycle of heat sources is not an immediate problem, and, besides, it could probably be accomplished in a side loop of the reprocessing facility.

In Reference (9), NUS treats the remainder of the above production cycle. In discussions with the commercial fuel reprocessors, they established that Np-237 could be recovered from waste streams at a reasonable cost. Although not planning to do so routinely, the process modifications to accomplish this are available and will be activated at customer's request. No discussions were held with target fabricators, but it was assumed that anyone with capability to produce plutonium fuels could fabricate the neptunia target rods. Costs were estimated based on this assumption. This seems a reasonable assumption, particularly since this is a small volume operation; considerations at BCL indicate that even a fuel research facility such as ours could fabricate the target rods at nearly the desired production rate.

Although the response was not universally positive, several utilities indicated a willingness to allow target assemblies in their reactors. Again the characteristically small volume operation does not require too many reactors to achieve the full production rate considered (120 kg Pu-238 per year).

The major difficulty in establishing a complete production cycle lies in the lack of reprocessing facilities for the irradiated targets. Discussions with commercial reprocessors led to the conclusion that they would not use their currently planned production facilities for anything but the reprocessing of light-water reactor fuels. These facilities are dedicated to this purpose, and reprocessing industry management seems disinclined to consider any diversion. A survey was made, therefore, of several national laboratory facilities in order to evaluate their interest in and capability to reprocess the irradiated NpO_2 target rods. A summary of BCL's findings and conclusions in this regard are presented below.

Savannah River Laboratory

SRL, of course, is the current basic producer of Pu-238 for the USAEC. They will work in this plant only on nitric acid systems. (The targets are insoluble in HNO_3 .) Even if the targets were nitric acid soluble, SRL is capacity limited, particularly for the full-scale production. It would be necessary to build and staff a completely new and separate plant with capability to handle either HF or the H_2SO_4 fuming process.

Oak Ridge National Laboratory

ORNL has facilities primarily for HNO_3 dissolution, although they have used aqua regia and HCl, but not HF. They do not want to use HF in their facilities. Also, their facilities are pretty well committed. They would entertain a development program to work up a suitable flow sheet for the current target material, but the facility for full-scale processing would still be questionable. Thus, an extensive development program plus new plant and staff would also be required here.

Idaho Falls

Based on work with UO_2 - ZrO_2 - CaO systems, IF has technology to reprocess using HF dissolution. Plant is throughput limited and, though 100 rods could be handled in about a 2-month campaign, it could handle full production only when new dissolvers are installed. (There is question of efficiency of new Hastelloy C dissolvers.) Other problems are commitment of plant to current customer and inadequate alpha-handling facilities. It would be necessary to modify existing facilities for handling of Pu-238 and convince IF customer to yield priority. Idle cell facilities at this plant could probably be modified for target processing at a cost considerably less than that needed to achieve the same capability elsewhere. Key items of equipment, such as the large electrolytic dissolver for removal of the cladding, make these facilities extremely attractive for treatment of the target rods. Recently, however, IF has been committed to the reprocessing of HTGR fuels and, consequently, its facility and staff would not be available for Pu-238 recovery.

Battelle's Pacific Northwest Laboratories

BNW has hot cells well prepared for ion exchange extraction processing. In addition, they have access to engineering hot cells for full-scale production. Facilities are available, capability has been demonstrated, and management has expressed a willingness to attempt to implement the fuming sulfuric acid process. Appendix D presents an informal proposal to this end. Based on the BNW estimated costs, the Pu-238 recovered from a 5-rod campaign would cost \$125 per gram for recovery; the product from a 100-rod campaign would cost \$50 per gram. Although no estimates are given for the 1,000- or 3,000-rod campaigns, we would extrapolate these costs to the twenties and tens. Considering the basic experimental nature of these facilities, these extrapolated costs appear to correlate well with the cost estimates summarized in Reference 9.

V. RECOMMENDATIONS

The results of this study have established that a stable neptunia-containing target material can be fabricated and irradiated in commercial nuclear power reactors with no perturbation of reactor operation other than neutron consumption. Pu-238 is produced in these targets in sufficient concentration to project a reasonable cost for the recovered product. These conclusions have been reinforced by the theoretical analyses, cost analysis, and engineering studies performed by NUS in this program.

In the course of the study, it became apparent that lack of a reprocessing capability might prevent the closing of the production cycle for Pu-238 by this scheme. This conclusion stemmed from the lack of a reprocessing facility as well as the lack of a process technology for the ZrO_2-NpO_2 target material. Toward the end of the program, both these deficiencies were resolved; the fuming sulfuric acid dissolution process was demonstrated, and BNW proposed to provide a fully adequate facility and staff for even a 120 kg per year Pu-238 production rate based on the process. Thus, a completely viable production cycle to produce Pu-238 by irradiation in commercial nuclear power reactors can be envisioned.

Assuming that the SNS need for lower cost Pu-238 still stands, it is recommended that this program be reactivated with the major emphasis being on a demonstration of the complete fuel cycle using ZrO_2-NpO_2 target material. The scope of the program would be built around either a 5- or a 100-rod irradiation, or some intermediate number, depending on available funds. A program of this scope would enable exercise of all elements of the cycle: fuel fabrication, irradiation, and reprocessing, on a scale sufficient to confirm cost prognoses for the full-scale production effort. Favorable results would provide the groundwork for expansion to full-scale production in the next phase of the study.

Some additional supportive development effort would be required for the above program. This would entail further delineation of the fabrication parameters, and a firming up of the conditions for the reprocessing. It is also recommended that development of an alternative target material, soluble in nitric acid, be carried out as a backup to the ZrO_2-NpO_2 material. Existence of such an alternative would permit greater leeway in choice of reprocessing technology, and open up potential participation in the reprocessing operation to a larger number of operators.

VI. REFERENCES

- (1) Roach, K.E., Turner, S.E., and Maxwell, W.A., "The Production of ^{238}Pu in Commercial Light Water Reactors", USAEC Report SNE-53 (December, 1969).
- (2) Roach, K.E., et al., "Plutonium-238 Production in Commercial Water Reactors Experimental Program - Project Definition Phase", Report SNE-69 (September, 1970).
- (3) Roach, K.E., Mullett, W.L., Brown, G.M., Maxwell, W.A., Turner, S.E., and Mitchell III, W., "Plutonium-238 Production in Commercial Water Reactors Experimental and Analytical Program", Report SNE-101 (July, 1971).
- (4) Ackermann, R.J., Faircloth, R.L., Rauh, E.G., and Thorn, R.J., "The Evaporation Behavior of Neptunium D. Oxide", *J. Inorg. Nucl. Chem.*, 28, 111-18 (1966).
- (5) Myrick, R.E., and Folger, R.L., "Fabrication of Targets for Neutron Irradiation of Neptunium Dioxide", *Ind. Eng. Chem. Process Design Development*, 3-(4), 309-13 (1964).
- (6) Caldwell, C.S., Puechl, K.A., Fisher, F.D., and Roth, J., "Preparation of $\text{UO}_2\text{-PuO}_2\text{-ZrO}_2$ Fuels", Third International Conference on Plutonium, Plutonium 1965, held in London, November 22-6, 1965, published by Barnes & Noble, New York.
- (7) Wright, T.R., Kizer, D.E., and Keller, D.L., "Studies in the $\text{UO}_2\text{-ZrO}_2$ System", BMI-1689 (1964).
- (8) Deem, H.W., "Fabrication, Characterization, and Thermal-Property Measurements of ZrO_2 -Base Fuels", BMI-1775 (1966).
- (9) Roach, K.E., Turner, S.E., Mitchell III, W., and Gurley, M.D., "Plutonium-238 Production in Commercial Water Reactors Experimental and Analytical Program", NUS-1277, (September, 1974).
- (10) E261-70 Neutron Flux by Radioactivation Techniques, Measuring, ASTM Standards, Part 30, General Test Methods, (July, 1973).
- (11) E262-70 Thermal Neutron Flux by Radioactivation Techniques, Measuring, ASTM Standards, Part 30, General Test Methods, (July, 1973).
- (12) E263-70 Fast Neutron Flux by Radioactivation of Iron, Measuring, ASTM Standards, Part 30 General Test Methods, (July, 1973).
- (13) Burney, G.A., "Ion Exchange Process for the Recovery of Pu-238 from Irradiated Np-237", *Ind. Eng. Chem., Process Design Develop.*, 3, 328 (1964).

- (14) Jenkins, I.L., Shorthold, C.G.C., Streeton, R.J.W., and Wain, A.G., "The Separation of Pu-238 from Irradiated Np-237 and from Fission Products", Part 1. Preliminary Work. Part 2. Processing Runs., AERE-R-5074, (May, 1966).
- (15) Wheelwright, E.J. "Recovery and Purification of Plutonium and Neptunium from Irradiated NpO₂-Al and NpO₂-Graphite Targets", BNWL-B-6, (September, 1970).
- (16) Groh, H.J., and Schlea, C.S., "Plutonium-238 Recovery from Irradiated Np-237 at Savannah River", Progress in Nuclear Energy, Series III, Stevenson, C.E., Mason, E.A., and Greahy, A.T., (Eds), 4, p. 536, Pergamon Press, Inc., New York, (1970).
- (17) Butzman, R.G. and Newly, B.J., "Laboratory Feasibility Studies of Aqueous Reprocessing of Zirconium Dioxide - Uranium Dioxide Fuels", IN-1069, (March, 1967).
- (18) George, D., and Wheatley, C.C.H., J. Nucl. Energy, Parts A & B, 18, 233-239 (1964).
- (19) Freshley, M.D., and Carroll, D.F., Hanford (USA) Report HW-SA-3127 (1963).
- (20) Divine, J.R., Nucl. Tech., 18 (2), 171-176 (1973).
- (21) Perrigo, L.D., Demmitt, T.F., Hayden, K.D., Weed, R.D., and Ayres, J.A., BNWL-SA-636, Battelle-Northwest (1966).
- (22) Ayres, J.A., "Decontamination of Nuclear Reactors and Equipment, Ronald Press, New York (1970).
- (23) Wilks, R.S., J. Nucl. Mater., 26, 137-173 (1968).
- (24) Henderson, B., and Bowen, D.H., J. Phys. C: Solid St., Phys., 4, 1487-1495 (1971).
- (25) Desport, J.A., and Smith, J.A.G., J. Nucl. Mater., 14, 135-140 (1964).
- (26) Hough, A., and Marples, J.A.C., J. Nucl. Mater., 15 (4), 298-309 (1965).
- (27) Carroll, D.F., Hanford (USA) Report HW-76303 (1963).
- (28) Budnikov, P.P., et al., Second Geneva Conference, 1958, 15/P/2193.
- (29) Lambertson, W.A., and Mueller, M. H., J. Amer. Ceram. Soc., 36, 332 (1953).
- (30) Livey, D.T., Trans. Brit. Ceram. Soc., 62 197-220 (1963).

- (31) BMI-1831, "Mid-Year Report on Development Program for Fabrication of Composite Fuel Form of Pu²³⁸O₂", p 32 (1968).
- (32) BMI-1849, "Summary Report on Development Program for Fabrication of Composite Fuel Form of Pu²³⁸O₂", p 4 (1968).

APPENDIX A

BATTELLE-COLUMBUS SPECIFICATION FOR
NEPTUNIA-CALCIA-STABILIZED ZIRCONIA TARGET PELLETS

BATTELLE-COLUMBUS SPECIFICATION FOR
NEPTUNIA-CALCIA-STABILIZED ZIRCONIA TARGET PELLETS

1.0 Scope

1.1 This specification applies to solid cylindrical NpO_2 - (CaO-ZrO_2) target pellets that will be encapsulated and irradiated in the Connecticut Yankee Reactor Core III of the Connecticut Yankee Atomic Power Company (CYAPC).

2.0 Design Requirements

2.1 No change shall be made in the design details or quality of material furnished under this specification without the written approval of Southern Nuclear Engineering (SNE).

3.0 Manufacture

3.1 The pellets shall be prepared from neptunium dioxide (NpO_2) powder supplied by Savannah River and reactor-grade calcia-stabilized (CaO) zirconia (ZrO_2) containing 10 to 12 w/o CaO purchased from ZIRCOA. Standard cold-pressing and sintering techniques will be used for all pellet fabrication. No materials shall be added to the powders except small quantities of organic binders and/or an organic lubricant needed for pelletization.

4.0 Materials Accountability

4.1 Accountability and accounting for the NpO_2 shall be in accordance with AEC Manual Chapter 7400. Battelle-Columbus is an Exempt AEC Contractor operating under the contract cognizance of the Chicago Operations Office. Battelle-Columbus will be responsible to the AEC through the Chicago Office for the receipt, processing, removals and losses of the NpO_2 through established accountability and accounting procedures. At the conclusion of the program, a closed accountability balance of all materials received will be furnished to both SNE and the AEC. Any generated scrap or unused materials will be shipped for reprocessing or burial as instructed by SNE.

5.0 Chemical Characterization and Tests

5.1 Neptunium contents of the pellets for the various target segments will conform to those values specified below, which are based on the information given in SNE Drawing No. 69-646-10.

Segment	Neptunium Density, g per cm ³	Total Volume of Fuel ₃ Segment, cm ³	Total Mass Neptunium, g	Total Mass NpO ₂ , g	NpO ₂ Composition of Target Pellets, w/o
1A 2A	5.44	18.88	102.69	116.55	77.22
1B 2B	2.72	18.88	51.35	58.28	48.76
1C 2C	1.36	18.88	25.67	29.13	28.06
1D 2D	0.68	81.17	55.20	62.65	15.18

5.2 Chemical analysis for neptunium, zirconium, and calcium will be performed in accordance with established procedures for these elements.

5.3 Since the oxygen-to-metal ratio of the pellets is unknown and would be meaningless unless referenced to back-up data on phase relationships and stoichiometry, emphasis for pellet characterization and behavior will be placed in microstructural examinations and prolonged heat treatment of encapsulated pellets. Stoichiometry of the pellets will be that which results from sintering to high temperatures in an atmosphere of high-purity nitrogen and is expected to vary slightly for each composition because of the changes in NpO₂ and ZrO₂ contents.

5.4 Impurities present in the pellets shall not exceed the levels given below:

<u>Impurity Element</u>	<u>Maximum Content, ppm</u>
Silver	0.3
Bismuth	2.0
Boron	1.0
Cadmium	5.0
Chromium	200.0
Copper	25.0
Iron	500.0
Lithium	0.5
Magnesium	300.0
Manganese	150.0
Molybdenum	50.0
Nickel	100.0
Lead	60.0
Silicon	300.0
Tin	40.0
Vanadium	20.0
Zinc	50.0

5.5 Spectrographic analysis will be utilized to determine trace impurities.

- 5.6 The hydrogen content of the pellets shall not exceed 10 ppm, including the amount contributed by water. Hydrogen content shall be determined from mass spectrographic analysis of a gas sample taken during measurements for total gas in Paragraph 5.9, below. It shall be assumed that the ratio of hydrogen to other species found in this gas sample is for all practical purposes the same, and this ratio will be used to calculate the hydrogen content of pellets analyzed for total gas release.
- 5.7 Chlorine content shall not exceed 10 ppm as determined from an analysis of a pellet randomly selected from a batch of pellets containing 15.18 w/o NpO₂.
- 5.8 Total water content shall not exceed 10 ppm. Moisture desorption temperatures employed in the analysis shall be 1000 C.
- 5.9 Total gas release inclusive of water shall not exceed 0.05 cm³ per g of target material at STP. Gas release shall be measured by outgassing for at least 30 min at 1 x 10⁻⁶ mm of mercury at a temperature of 1000 C.
- 5.10 Pellets of each composition will be sectioned and examined metallographically to magnifications of 500 X. This examination shall indicate a minimum of 90 percent solid solution of the NpO₂-calcia-stabilized ZrO₂ powders.
- 5.11 Pellets examined metallographically will be subjected to quantitative alpha autoradiography. The uniformity of the neptunium dispersion shall be such that there are no areas of high NpO₂ concentration exceeding 200 μ.
- 5.12 One pellet of each composition will be encapsulated in a Type 304 stainless steel can and heat treated for 1 month at a temperature of 500 C. The cladding and pellets will be examined for diffusion interaction of the various constituents prior to the loading of the targets into the reactor.

6.0 Physical Properties and Dimensions

- 6.1 Densities of finished pellets shall be in the range specified below for each target composition.

<u>Segment</u>	<u>NpO₂ Composition, w/o</u>	<u>Total Pellet Density, g per cm³</u>
1A 2A	77.22	8.60 ± 0.15
1B 2B	48.76	6.10 ± 0.15
1C 2C	28.06	5.40 ± 0.15
1D 2D	15.18	5.10 ± 0.15

- 6.2 Three pellets shall be selected from the pellets prepared from each batch of material and measured for weight and volume. Geometric densities determined from these measurements shall fall within the range specified in Paragraph 6.1, above.

- 6.3 Pellet dimensions shall conform to those given on SNE Drawing No. 69-646-11. Tolerances on the pellets are 0.380 to 0.385 in. for the diameter and 0.350 to 0.650 in. for the length.
- 6.4 The plane of each pellet end shall not deviate from a plane perpendicular to the center axis by more than 0.08 in. across the pellet diameter.
- 6.5 The pellets shall be subjected to visual inspection for chips and fissures and they shall conform to the following specifications.
- 6.5.1 Chipped pellets shall not have lost more than 10 percent of the area at either end.
- 6.5.2 The sum of the circumferential length and depth of each imperfection on the cylindrical surface shall not exceed 0.20 in. The maximum axial length of any one chip shall not exceed 0.20 in. The sum of the circumferential lengths of all chips and pock marks in any one plane perpendicular to the pellet axis shall not exceed 0.20 in. In cases of "borderline" acceptability, chipped or fissured pellets may be accepted when they are within the weight per unit volume specification and withstand subsequent handling and tube loading without further deterioration.
- 7.0 Test Sampling
- 7.1 Dimensional samples
- 7.1.1 Each pellet shall be inspected visually for chips, fissures, and other imperfections.
- 7.1.2 All pellets shall be inspected for compliance to dimensional tolerances as stated in Paragraph 6.3.
- 7.1.3 For pellet squareness, a portion of the pellets may be randomly sampled. The sampling plan and rejection criteria shall be subject to mutual agreement.
- 7.2 Chemical samples
- 7.2.1 A batch of material shall be defined as the NpO_2 and CaO -stabilized ZrO_2 powders blended initially by wet ball milling in the amounts necessary to obtain the NpO_2 compositions specified in Paragraph 5.1. A batch of pellets shall consist of the compacts pressed and sintered under identical conditions in the same furnace cycle.
- 7.2.2 One pellet prepared from each batch of material shall be selected and stored as an archive sample to be utilized during postirradiation evaluation of the target rods.
- 7.2.3 An analysis is to be performed on one pellet from each batch of material to assure compliance with Section 5.0.

7.2.4 Gas release will be determined using the entire pellet selected at random in Paragraph 7.2.3.

7.2.5 Sections from one pellet from each pellet batch will be examined metallographically and submitted for quantitative autoradiography.

7.2.6 One pellet of each composition will be encapsulated in a Type 304 stainless steel can and heat treated for 1 month at 500 C.

8.0 Test Reports

8.1 Copies of the chemical analyses reported for total neptunium, zirconium, calcium and impurities together with the analyses taken on the cladding and end component material plus reports of physical properties and dimensions shall be submitted to SNE and CYAPC on completion of the program.

9.0 Packaging and Handling

9.1 The pellets shall be packed and handled in a manner that will insure their compliance with the above specification when loaded into the cladding tubes.

9.2 The identity of pellet batches shall be retained throughout the manufacture of finished fuel assemblies.

10.0 Inspection

10.1 The manufacturer shall afford SNE and CYAPC representatives all reasonable facilities, information, and right of inspection to satisfy themselves that the pellets furnished are in accordance with this specification.

10.2 Acceptance of pellets and target rods by SNE or CYAPC shall release Battelle-Columbus of all responsibility for performance of these rods while in the reactor.

11.0 Compliance with Regulations

11.1 The vendor shall have appropriate licenses and clearances required for compliance with all applicable regulations of Federal, State, and Local bodies with respect to receiving, accounting for, processing, storing, and shipping neptunium.

APPENDIX B

SPECIFICATION FOR TYPE 304L STAINLESS STEEL TUBING
FOR NUCLEAR APPLICATION

SPECIFICATION FOR TYPE 304L STAINLESS STEEL TUBING
FOR NUCLEAR APPLICATION

Scope:

This specification defines requirements for Type 304L stainless steel tubing to be used as NpO₂ target rod cladding for production of Pu-238 in commercial power reactors. This specification is based on RDT M3-2T and ASTM A213 specifications for seamless ferritic and austenitic stainless and alloy steel tubes.

Applicable Documents:

ASTM

- A-213 Seamless Ferritic and Austenitic Alloy-Steel Boiler, Superheater, and Heat Exchanger Tubes
- A-450 Specification for General Requirements for Carbon, Ferritic Alloy, and Austenitic Alloy Steel Tubes
- E-3 Standard Methods for Preparation of Metallographic Specimens
- E-45 Recommended Practice for Determining the Inclusion Content of Steel
- E-165 Standard Methods for Liquid Penetrant Inspection
- E-112 Standard Methods for Estimating the Average Grain Size of Metal.
- A-370 Methods and Definitions for Mechanical Testing of Steel Products

RDT

- Md-2T Stainless and Alloy Steel Seamless Tubes
- F3-8 Ultrasonic Examination of Metal Pipe and Tubing for Longitudinal Discontinuities.

Requirements:

1.1 Material. The steel furnished under this specification shall conform to the requirements of the current edition of the "Specification for General Requirements for Carbon, Ferritic Alloy, and Austenitic Alloy Steel Tubes (ASTM A450)"

1.1.1 Chemical Composition

carbon, maximum	0.030 percent
manganese, maximum	2.00 percent
phosphorus, maximum	0.04 percent
sulphur, maximum	0.03 percent
silicon, maximum	0.75 percent
nickel	8.00-13.00 percent
chromium	18.00-20.00 percent
boron, maximum	0.0010 percent
iron	balance

Testing methods and inspection levels are described in the Appendix, Number 1.

1.1.2 Grain Size. The grain size as determined by ASTM E-112 shall be Number 5 or finer. Testing methods and inspection levels are described in the Appendix, Number 2.

1.1.3 Corrosion Resistance. Finished tubing shall be tested for susceptibility to intergranular attack in accordance with ASTM A393 and ASTM E-3. Cracking or intergranular attack shall be cause for rejection. Testing methods and inspection levels are described in the Appendix, Number 3.

1.2 Temper. The tubing shall be cold drawn to finished size without further heat treatment.

1.3 Cleanliness of Tubing

1.3.1 In Process. Lubricants shall be removed prior to heat treatment and use of sulphur and chloride bearing materials shall not be permitted.

1.3.2 Finished Product. Finished tubing shall be free from grease, oil, and other residue. Tubing samples will have a clean white cloth wiped over the surface and through the bore. Residue presence on the cloth is cause for rejection. Testing methods and inspection levels are described in the Appendix, Number 4.

1.4 Mechanical Properties

- 1.4.1 Tensile Properties. TP 304L shall have a minimum tensile strength of 70,000 psi and a minimum yield point of 25,000 psi at room temperature. Testing methods and inspection levels are described in the Appendix, Number 5.
- 1.4.2 Hardness. Tubes shall have a hardness not exceeding Brinell 190 (Rockwell B90).
- 1.4.3 Ductility. Tubing shall conform to the flattening test in ASTM A450. Testing methods and inspection levels are described in the Appendix, Number 6.
- 1.4.4 Flaring. Tubing shall pass the flare test in ASTM-A450. Testing methods and inspection levels are described in the Appendix, Number 7.
- 1.4.5 Hydrostatic Test. Tubing shall be tested for 30 seconds at the mill as prescribed in ASTM A450. Testing shall be conducted subsequent to final drawing or heat treatment. Tubes which exhibit bulges, leaks, cracks, or other defects shall be rejected. Testing methods and inspection levels are described in the Appendix, Number 8.
- 1.4.6 Burst Test - The burst pressure of finished tubing at room temperature shall be equal to or greater than that calculated using the following equation:

$$P = \frac{ST}{IR+0.6T} \quad \text{where,}$$

P = burst pressure, psig

S = 90% minimum specified tensile strength

T = wall thickness, inch

IR = internal radius, inches

Testing methods and inspection levels are described in the Appendix, Number 9.

- 1.4.7 Inclusions. A sample from each tube lot shall be examined as described in ASTM E-45 and using testing and inspection levels in the Appendix, Number 10.

- 1.5 Surface Condition. The finished tubing shall be free from oxide or scale. No surface grinding or belt sanding shall be permitted on the finished tubing. Surfaces should be free of mars and intergranular attack.
- 1.6 Nondestructive Testing
- 1.6.1 Ultrasonic Inspection. Each tube shall be examined for 100 percent of its length and conducted in accordance with RDT F3-8, level S-2. Any tube indicating discontinuities larger than the calibration standard shall be rejected. Testing methods and inspection levels are described in the Appendix, Number 11.
- 1.7 Dimensions and Tolerances
- 1.7.1 Sizes. Finished tubing sizes shall be specified by contract or purchase order.
- 1.7.1.1 Dimensional Tolerance. Variation in the finished tubing inside and outside diameter shall be limited to plus or minus 0.001 inch from specified dimension.
- 1.7.2 Ovality. Ovality shall not exceed 0.002 inch.
- 1.7.3 Eccentricity. The eccentricity shall be the difference between the maximum and minimum wall thickness at any cross section and shall not exceed 5 percent of the wall thickness.
- 1.7.4 Straightness. Tubing shall be free of bends and kinks and the bow shall not exceed 0.010 inch per linear foot with a maximum value of 0.050 inch per finished length as measured on a flat surface.

Preparation for Delivery:

- 2.1 Packaging. Tubes shall be individually protected with cardboard sleeves or by other approved means and packaged in rigid containers constructed in a manner to ensure delivery of clean, straight, undamaged material. Each box shall be legibly and conspicuously marked with the following data:

Purchase order number

Name of manufacturer

Grade

Size

Lot and heat or ingot number
Temper
Number of pieces in container
Number of pieces in lot.

2.2 Identification. Each tube shall be marked or tagged as below:

- (1) Standard No. RDT M3-2 and ASTM A213
- (2) Heat treatment, lot identification, and heat number
- (3) Manufacturer grade and size
- (4) Physical condition (cold drawn, annealed, etc.)

Notes:

3.1 Fabrication Record. Tubing lot records, traceable to feed material lots, showing complete fabrication and sequence of fabrication operations shall be available to the buyer.

APPENDIX

<u>Requirement</u>	<u>Inspection or Test Level</u>	<u>Testing Method</u>
1. Alloy Composition		
a. Heat	Each Heat	One analysis of each heat shall be made by the manufacturer and submitted to the buyer.
b. Tubing	Each Lot	Each lot shall be analyzed by the manufacturer and submitted to the buyer.
2. Grain Size	Each Lot	Each lot of tubing shall be examined as prescribed in ASTM E-112.
3. Corrosion Resistance	Each Lot	Testing shall be in accordance with ASTM-393.
4. Cleanliness	Each Tube	Testing shall be by visual examination and by drawing a clean white cloth through each tube box.
5. Mechanical Properties	Each Lot	Tensile properties shall be determined by ASTM A370.
6. Ductility and Soundness	Each Lot	Tubing shall be tested according to the flattening test prescribed in ASTM A450.
7. Flaring	Each tube	A one-inch sample shall be cut from each tube and subjected to the flare test in ASTM A-450.
8. Hydrostatic	Each tube	As per ASTM A-450
9. Burst Test	Each Lot	Test shall be conducted on representative 12-inch tubing samples.

APPENDIX

(continued)

<u>Requirement</u>	<u>Inspection or Test Level</u>	<u>Testing Method</u>
10. Inclusions	Each Lot	Inclusions shall be determined as described in ASTM E-45
11. Ultrasonic Test	Each Tube	Each tube shall be examined in accordance with RDT F3-8. Test results will accompany tube shipment.

APPENDIX C

GENERAL SPECIFICATIONS FOR
NEPTUNIA TARGET PELLETS

GENERAL SPECIFICATIONS FOR
NEPTUNIA TARGET PELLETS

Scope:

This specification applies to solid right circular cylinder target pellets for encapsulation in stainless steel cladding and subsequent irradiation in a selected LWR(s).

Fabrication (General):

The pellets shall be prepared from neptunium dioxide (NpO_2) powder supplied by Savannah River or a commercial vendor. This powder will be combined with an approved reactor-grade diluent. Standard cold pressing and sintering techniques will be used for pellet fabrication. No binder materials shall be added to the powders to aid pelletization unless previous studies confirm no harmful effects during irradiation of the aforementioned pellets, or that evidence is presented which assures no harmful residue remains in the pellet after the sintering cycle.

Powder Characterization:

Neptunia powder received for pellet fabrication shall be assayed for the following components: thorium, uranium, plutonium (weight percent), plutonium-238 (ppm) and total neptunium content. The weight loss at 800 C shall be determined for accountability purposes. In the event that good analytical data are available, the above requirements can be waived if agreeable with the purchaser and supplier.

Pellet Characterization:

Chemical Analysis. Duplicate analyses will be performed to determine neptunia contents of pellets selected at random with a history traceable to a specific powder batch*. Pellets not meeting design requirements subject that powder batch to rejection. Limits for neptunia content will be specified prior to powder blending.

* A powder batch shall be defined as a given amount of powder having the same composition, blending, and cominution history.

Spectrographic Analysis. Impurity elements present in the pellets shall not exceed the levels given below.

<u>Impurity Element</u>	<u>Maximum Limit, ppm</u>
Aluminum	400
Boron	20
Cadmium	10
Chromium	300
Copper	50
Iron	500
Potassium	200
Magnesium	300
Manganese	150
Molybdenum	100
Nickel	200
Lead	50
Silicon	300
Tin	100
Vanadium	100
Zinc	200
Carbon	200

The total impurity content must not exceed 2000 ppm. In the event that the above impurity levels cannot be achieved due to inherent impurities in the constituent powders, or more stringent requirements are desired, new limits may be negotiated between supplier and purchaser.

Metallography. Pellets from a pellet batch* will be sectioned and examined metallographically to a magnification of 500X. Specimens will be examined in both the as-polished and the etched conditions. A polished surface of a transverse section from a pellet shall show that the porosity is evenly distributed. No second phase will be evident in the microstructure aside from the limits for neptunia given in Autoradiography.

* A pellet batch shall be defined as those pellets pressed from the same powder batch and sintered in the same furnace cycle.

Autoradiography. The metallographically prepared pellets will be subjected to autoradiographic analysis to determine the NpO_2 dispersion. The acceptable requirements are shown below.

<u>Concentration</u>	<u>Agglomerate Size, μ</u>
100 w/o NpO_2	< 100
90 w/o NpO_2	< 500
50 w/o NpO_2	< 250

The dispersion of neptunia as evaluated by means of α -autoradiography shall be homogeneous within the limits shown above.

Microprobe examination. In lieu of autoradiography, pellets may be examined with an electron microprobe with suitable resolution to distinguish the particle size of neptunia agglomerates. Sufficient scans must be made to provide for a statistical evaluation of the specimen surface to satisfy particle size limits given in Autoradiography.

Gas Analysis. A pellet selected at random shall be examined for total gas release which will not exceed $0.05 \text{ cm}^3/\text{g}$ of target material at STP. Gas release shall be measured by out-gassing at 1×10^{-6} torr at 1000 C for 30 minutes. Other gas specifications are listed below.

Total H_2O	- 20 ppm max
Hydrogen	- 10 ppm max (only for pellets to be loaded in zircalloy cladding)
Chlorine	- 25 ppm max
Fluorine	- 25 ppm max

The gas content shall be determined by mass spectrographic analyses of evolved species at 1000 C.

Pellet Density and Dimensions:

Density. Pellets from each pellet lot shall be dimensionally characterized upon removal from the furnace to ascertain whether pellets have sintered to acceptable densities. Pellets shall have a density exceeding 85 percent of theoretical, which shall be specified by purchaser prior to initiation of pellet fabrication operations. Density tolerance shall be ± 2 percent absolute. The theoretical density of the dispersion or solid solution shall

be calculated from the theoretical densities of the component materials and this evaluation shall be based on a weight percent basis.

Dimensions. All pellets will be 100 percent dimensionally characterized before loading into target rods. The pellet diameter will be specified by the purchaser. Tolerance on the pellet diameter is $0.xxx \pm .001$, whereas the length may vary from 0.350 to 0.650 inch.

The flat ends of the right circular cylinder pellets shall not deviate from a plane perpendicular to the center axis by more than 0.060 inch across the pellet diameter.

Integrity. All pellets will be 100 percent visually examined and will conform to the specifications in Table 1.

Sampling:

The sampling plan shall be negotiated between supplier and purchaser. A typical plan for a batch of approximately 300 pellets is given below for guidance.

<u>Attribute</u>	<u>Inspection Frequency</u>
Chemical analysis	2 pellets/pellet batch min
Spectrographic analysis	1 pellet/pellet batch min
Metallography	2 pellets/pellet batch min
Autoradiography	as metallography
Gas analysis	1 pellet/pellet batch min
Density	2 pellets/pellet batch min
Dimensions	Military standards 414- (sampling)

Storage and Identification:

The pellet containers will be color-coded to ensure no batch mixing and identity will be maintained upon loading into target rods. Pellets will be stored in a condition that precludes moisture and gas pickup from the time the gas analyses are performed until the pellets are encapsulated

in the cladding. An alternative is to out-gas the pellets at 500 C to 10^{-3} torr just prior to loading and encapsulation.

Inspection:

The fuel supplier shall afford AEC and SNE representatives all reasonable right of inspection to satisfy that the pellets are in accordance with the above specification.

TABLE 1. PELLET INTEGRITY SPECIFICATIONS

Attribute	Frequency, Percent	Method of Measurement	Specification
Radial Crack	100	Visual	0.150 inch length, max
Circumferential Crack	100	Visual	180 degrees length, max
Axial Crack	100	Visual	0.200 inch length, max
End Chip	100	Visual	10 percent of area, max, and 0.015 inch depth, max, provided that not more than 50 percent of each shoulder is missing
Circumferential Chip	100	Visual	10 percent of area, max, and 0.015 inch depth, max
Appearance	100	Visual	No discolorings, blis- ters, or foreign inclu- sions are acceptable on the surface

APPENDIX D

INFORMAL REPROCESSING PROPOSAL

January 27, 1975

Mr. M. Pobereskin
Battelle Memorial Institute
509 King Avenue
Columbus, Ohio 43201

Dear Mike,

We have reviewed our capabilities for processing irradiated neptunium targets, and conclude that we do have the capability for processing appreciable numbers of target rods. The maximum number we can process will depend on the availability of the hot cell at the time the processing is done. If we are to process 3,000 rods (a total of about 120 kg Pu), a total of over a year of operation will be required. However, an operation of this magnitude is not out of the question.

Our estimate of capability and cost is based on flowsheet information developed at BCL and supplied to us by telephone or personal visit. We understand that the target rods will contain neptunium oxide in a zirconia matrix, with each rod containing about 800 g of zirconia and, after irradiation, about 120 g of neptunium and 40 g of plutonium. The dissolution process consists of fuming with sulfuric acid and dissolving the sulfate in nitric acid. We assume that the dissolution will proceed smoothly, and that the dissolver solution will be suitable for processing by anion exchange to recover neptunium and plutonium. We have extensive experience with the anion exchange process, and see no problems if the dissolver solution is suitable.

Work would be performed in the High Level Radiochemistry Facility (325 Building), which consists of three hot cells with four feet of high density concrete shielding. Two of the cells are about 6' x 7', and the third is 6' x 14'. The cells are equipped with double HEPA filtration, but do not have charcoal filters or other provisions for iodine removal. Therefore, the irradiated targets will have to be cooled so that ^{131}I is no problem. Both solid and liquid wastes are transferred to Atlantic Richfield Hanford Company (ARHCO) for disposal, and we assume no changes in our procedures for waste handling.

The first processing to be done will be five rods with a total weight of about 5 kg, and containing about 600 g of neptunium and 200 g of plutonium. This effort will involve equipment development and flowsheet demonstration. A total time of about 5 months will be required for the program, and an estimated cost of \$25,000. This assumes that the flowsheet works as expected, and allows for design, fabrication, installation, and testing of small-scale equipment.

Mr. M. Poberskin
January 27, 1975
Page 2

The second processing will consist of 100 rods containing about 12 kg of neptunium and 4 kg of plutonium. Since this is mostly ^{238}Pu , there will be no serious problem with criticality, but an appreciable amount of heat generation. This work is estimated to require 8 months total time and about \$200,000. It includes design, fabrication, installation, and testing of large-scale equipment.

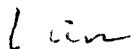
Subsequent processing will be either 1,000 or 3,000 rods. At present, it appears that we will be able to handle this level of effort, but the cost and time estimates would be quite speculative until we do at least the five rod batch.

A major consideration is other demands on hot-cell time. The campaigns of 5 and 100 rods can be accommodated easily by minor rescheduling of other activities. Larger-scale runs will require extended dedication of one or more cells to this program, and could impact schedules for isotope production activities or Division of Waste Management and Transportation programs. However, the work could be done in our facility if sufficient ERDA priority were obtained.

We will need at least three months notice to schedule the first processing batch, and when this work is completed, we can provide more meaningful data for the larger-scale batches. Cost estimates are rough at present since we have not tested all of the flowsheet in our facilities, and unforeseen problems could arise. Our estimates are based on somewhat similar past jobs, and are in FY 1975 dollars. No provision was made for escalation since we are not sure when the work will be performed.

We would appreciate a copy of your report on development of dissolution procedures. This will be valuable to us when we start equipment development.

Sincerely yours,



H. H. Van Tuyl, Manager
Applied Chemistry Section

HHVT:lm